AN ABSTRACT OF THE THESIS OF

Gary J. Huftile for the degree of Doctor of Philosophy in Geology presented on May 21, 1992. Title: Convergence Rates Across the Ventura Basin, California

Abstract approved: Signature redacted for privacy.

Robert S. Yeats

Four cross sections are balanced and retrodeformed to 250±50 ka and 975±75 ka to yield crustal shortening amounts and rates for the western Transverse Ranges of California. The cross sections compare the shortening that occurs along a transfer zone in which displacement is transferred eastward from a surface reverse fault (Red Mountain fault) to a blind thrust, to a combination of both a surface reverse fault (San Cayetano fault) and the blind thrust, and to a surface reverse fault (Modelo lobe segment of the San Cayetano fault). Deformation can be separated into three phases: (1) pre-Vaqueros (pre-late Oligocene-early Miocene) tilting in the hanging-wall block of the Oak Ridge fault that is coincident with normal faulting farther south at Big Mountain and to the east in the east Ventura basin, (2) Pliocene reverse faulting and folding, and (3) Quaternary deformation. Crustal shortening rates have increased through time. For the four cross sections, crustal shortening rates were 4±4 mm/y, 5±2 mm/y, 6±5 mm/y, and 14±6 mm/y for the interval between 250 ka and 975 ka. Since 250±50 ka, crustal shortening rates increased to 23±12 mm/y, 29±7 mm/y, 27±11 mm/y, and 25±11 mm/y. But

crustal convergence rates determined by Global Positioning System (GPS) surveys, taken over an interval of 2.7 years, indicate a shortening rate of only 7±2 mm/y across the basin. The discrepancy between a rate of strain over a short, recent time period of little seismic activity, and a faster rate determined by the offset of bedrock horizons over several hundred thousand years indicates that much of the present crustal movement is being stored as elastic strain that could result in the release of energy in damaging earthquakes.

Convergence Rates Across the Ventura Basin, California

by

Gary J. Huftile

A THESIS

submitted to

Oregon State University

in partial fulfillment of
the requirements for the
degree of

Doctor of Philosophy

Completed May 21, 1992

Commencement June 1993

TABLE OF CONTENTS

CHAPTER 1: Thin-skinned Tectonics of the Upper Ojai Valley and Sulphur Mountain Area, Ventura Basin, California 1
Acknowledgements 1
Abstract 2
Introduction and Geologic Setting 4
Stratigraphy 14
Structure 31
Horizontal Shortening and Convergence Rates 47
Oil Accumulation 51
Conclusions 54
Discussion 56
CHAPTER 2: Cenozoic Structure of the Piru 7½-minute Quadrangle, California 57
Abstract 57
Introduction 59
Stratigraphy 66
Structure 80
Conclusions 89
Seismic Hazard 91
Acknowledgements 93
CHAPTER 3: Convergence Rates Across a Displacement Transfer Zone in the Western Transverse Ranges near Ventura, California 94
Abstract 94
Introduction 96
Stratigraphy 110
Cross Sections 113
Residual Gravity Modeling 148
Discussion 158
Conclusions 159
Appendix 160
CHAPTER 4: Crustal Convergence Across the Modelo Lobe Segment of the San Cayetano Fault: Implications for Crustal Kinematic Models of Southern California 164
Abstract 164
Introduction 166
Stratigraphy 175
Structure 183
Balanced Cross Section 190
Residual Gravity Modeling 197
Conclusions 202
BIBLIOGRAPHY 203

LIST OF FIGURES

Figure		Page
1-1	Location map of the Upper Ojai Valley (UOV) study area in the western Transverse Ranges	5
1-2	Geologic map of the Upper Ojai Valley area and locations of cross sections	9
1-3	Map showing locations of wells, cross sections, and oil-producing areas	11
1-4	Generalized stratigraphic section showing age and relative competence of strata	13
1-5	Cross sections A-A' through D-D'	15
1-6	Subcrop geologic map showing Lion Mountain anticline, Reeves syncline	21
1-7	Area-balanced cross section	25
1-8	Schematic illustration of unroofing of the uplifted area north of the San Cayetano fault, depositing clasts of progressively older formations in progressively younger deposits	27
1-9	Structure-contour map of San Cayetano and Sisar faults	33
1-10	Schematic cross sections illustrating the development of the Sulphur Mountain anticlinorium	37
1-11	Structure-contour map of the Lion and Big Canyon faults	39
2-1	Index map showing the major structural features of the Ventura basin and surrounding areas and the location of the Piru quadrangle	60
2-2	Sources used in map compilation	62
3-1	Index map showing the surface traces of western Transverse Ranges faults and major folds, and cross-section locations of Figures 2-4	97
3-2	Cross section A-A'	100
3-3	Cross section B-B'	104
3-4	Cross section C-C'	107
3-5	Profile 2, recorrelated and unmigrated Vibroseis seismic reflection line	121
3-6	Map showing seismicity related to the Red Mountain fault from 1980-1985	124
3-7	Map showing the distribution of sandstones (shaded) in the Fernando Formation at the surface using mapping by Dibblee [1988] and Yeats [unpublished mapping]	126
3-8	Map and cross section showing different eastward projections of Pleistocene stratain the Carpinteria basin, the only occurrence of Pleistocene strata in the hanging-	

wall block of the Red Mountain fault, into the line of section in Figure 2 129
3-9 Map showing residual gravity over the study area from A. Griscom [written communication, 1991] that was used to model the structural cross sections 149
3-10 Residual gravity models of structural cross sections, Figures 3-2, 3-3, 3-4 151
4-1 Index map showing the locations of folds and faults in the study area, cross section A-A' (Figure 4-3), areas of Figures 4-2 and 4-4a 167
4-2 Geologic map of the east Ventura basin and the Modelo lobe area 169
4-3 Present-day structure of the Modelo lobe segment of the San Cayetano fault and Oak Ridge fault 171
4-4a Residual gravity map over the study area, located on Figure 4-1 (A. Griscom, written communication) 198
4-4b Residual gravity model over Figure 4-3 showing agreement of an independent data set, residual gravity, with the structural model 199

LIST OF TABLES

1-1	List of wells cited in text and figures	8
1-2	Comparison of depth to brittle-ductile transition and original bed length	50
3-1	Estimates of lateral separation on the Santa Ynez fault	114
3-2	Ranges of horizontal shortening	135
3-3	Summary of horizontal shortening and shortening rates	136
3-4	Densities used in modeling of residual gravity anomalies	155
4-1	Ranges of shortening on cross section A-A'	196

LIST OF PLATES

I Geologic map of the Piru 7½-minute quadrangle, Ventura County, California

II Explanation of plates

III Well and cross section locations

IV Cross sections, Piru 7½-minute quadrangle

V Structure-contour map of the San Cayetano fault and subcrop map of the strata in the hanging-wall block of the San Cayetano fault

VI Structure-contour map of the top of the Repetto Member of the Fernando Formation

Convergence Rates Across Ventura Basin, California

Chapter 1:

Thin-skinned Tectonics of the Upper Ojai Valley and Sulphur Mountain Area, Ventura Basin, California

Gary J. Huftile
Department of Geosciences
Oregon State University
Corvallis OR 97331-5506

ACKNOWLEDGEMENTS

This work was funded by Grant 14-08-0001-G1372 from the Earthquake Hazards Reduction Program of the U. S. Geological Survey. Additional funding was provided by the Southern California Fault Studies project at Oregon State University funded by the petroleum industry, Sun Exploration and Production Company, and Amoco Production Company. The author received a fellowship from Chevron USA, Inc. Data were provided by Arco Oil and Gas, Chevron USA, Inc., UNOCAL, Sun Exploration and Production Company, Ted Off, and Howard Stark. Discussions with Bob Yeats, Ed Hall, Gregg Blake, Steve Hart, Glenn Gregory, and Ted Off were helpful in working out the geology. The illustrations were drafted by Paula Pitts and Jaimie Bradbury.

ABSTRACT

By integrating surface mapping with subsurface well data and drawing cross sections and subsurface maps, the geometry of shallow structures and their geologic history of the Upper Ojai Valley of California can be reconstructed. The geometry of shallow structures, the geologic history, and the location of earthquake foci then offer constraints on the deep structure of this complex area.

The Upper Ojai Valley is a tectonic depression between opposing reverse faults. Its northern border is formed by the active, north-dipping San Cayetano fault which has 6.0 km of stratigraphic separation in the Silverthread area of the Ojai oil field and 2.6 km of stratigraphic separation west of Sisar Creek. The fault dies out farther west in Ojai Valley, where the south-vergent shortening is transferred to a blind thrust. The southern border of the Upper Ojai Valley is formed by the Quaternary Lion fault set (Sisar, Big Canyon, and Lion faults), which dip south and merge into the Sisar decollement within the south-dipping, ductile, lower Miocene Rincon Formation. Folds with north-dipping axial planes, including the Lion Mountain anticline and Reeves syncline, are middle Pleistocene or older and are related to movement on an unnamed fault in the footwall block of the San Cayetano fault and on the San Cayetano fault, respectively. By middle Pleistocene time, the Sulphur Mountain anticlinorium and the Big Canyon syncline began forming as a fault-propagation fold; the fault-propagation fold is rooted in the Sisar decollement,

a passive backthrust rising from a blind thrust at depth. The formation of the Sulphur Mountain anticlinorium was followed closely by the ramping of the south-dipping Lion fault set to the surface over the nonmarine upper Pleistocene Saugus Formation. To the east, the San Cayetano fault overrides and folds the Lion fault set near the surface. Area-balancing of the deformation shows shortening of 15.5 km, and suggests a 17 km depth to the brittle-ductile transition.

INTRODUCTION AND GEOLOGIC SETTING

The Upper Ojai Valley is part of the east-trending central Ventura basin in the Transverse Ranges province of California (Figure 1-1). The central Ventura basin is bordered by opposing reverse faults: on the north by the moderately north-dipping San Cayetano and Red Mountain faults and on the south by the steeply south-dipping Oak Ridge fault. The San Cayetano and Red Mountain faults in part comprise the northern boundary of the Ventura basin except at the easternmost end of the San Cayetano fault. The Ventura basin contains at least 6100 m of Plio-Pleistocene strata, the thickest section of this age in the world (Jennings and Troxel, 1954; Yeats, 1977). The strata are composed of trough turbidites grading upward to shallow-marine and nonmarine strata. The basin began forming in latest Miocene to early Pliocene time.

The Upper Ojai Valley is also bordered by opposing reverse faults, on the north by the north-dipping San Cayetano fault and on the south by the south-dipping Lion fault set (Figure 1-1). The San Cayetano fault has brought Eocene rocks over sediments as young as Holocene (Rockwell, 1988).

Eocene and Oligocene strata are primarily sandstone, forming a sequence of competent strata at least 3500 m thick. Upper Oligocene to lower Pliocene mudstone and shale vary in thickness from 1130 m to 1280 m and are less competent than the underlying rocks. Lower Pliocene and younger strata are thinner in the Upper Ojai Valley than they are in the main axis of the

Figure 1-1: Location map of the Upper Ojai Valley (UOV) study area in the western Transverse Ranges. WC, Wheeler Canyon; SC, Sespe Creek; SPC, Santa Paula Creek.

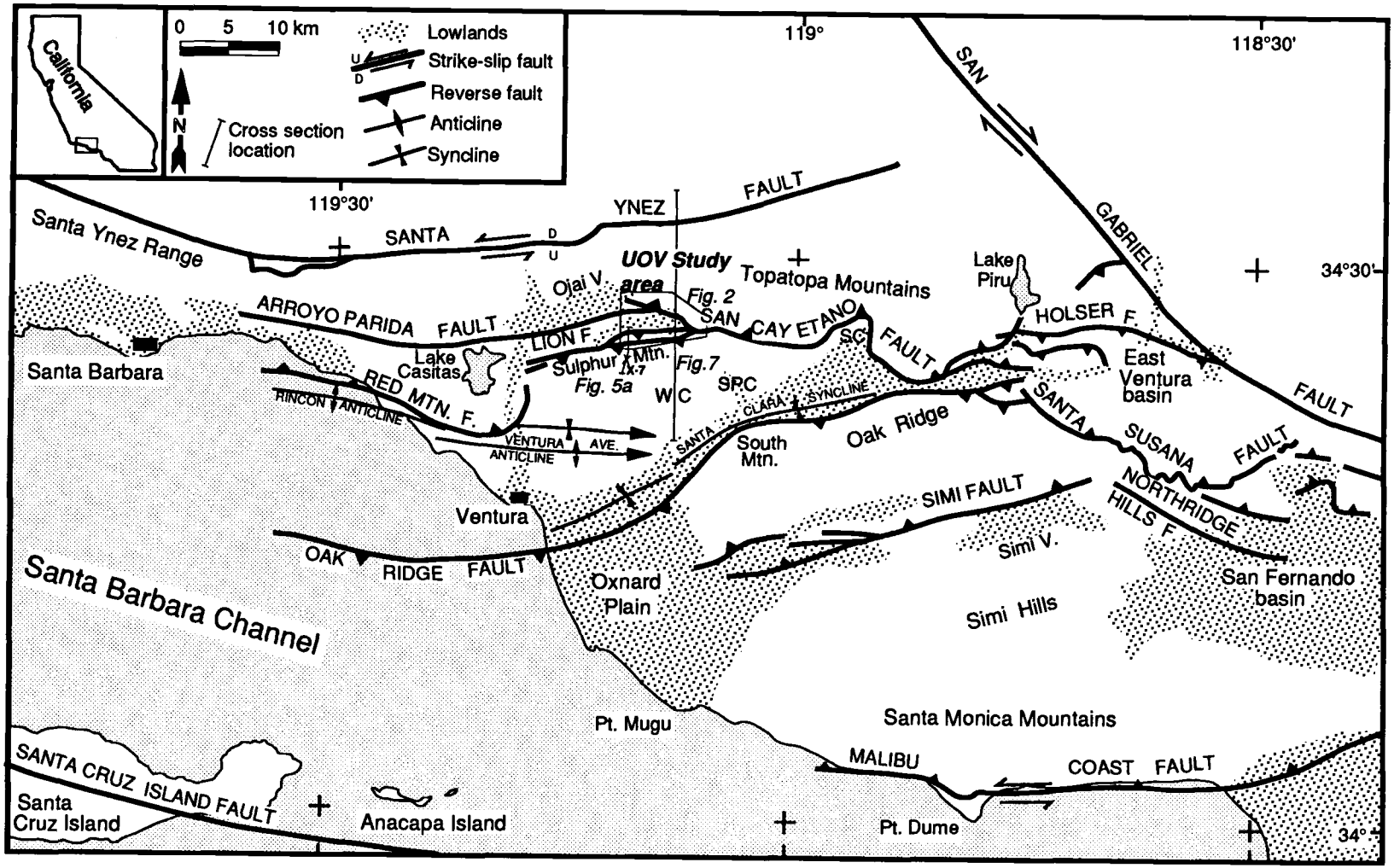
California
0 5 10 km
N
Cross section location
Lowlands
Strike-slip fault
Reverse fault
Anticline
Syncline
119°
118°30'
119°30'
34°30'
34°
SAN GABRIEL FAULT
YNEZ FAULT
SANTA
Santa Ynez Range
UOV Study area
Fig. 2
Topatopa Mountains
Ojai V.
Lake Piru
ARROYO PARIDA FAULT
LION F.
SAN CAY ETANO FAULT
SC
HOLSER F.
Lake Casitas
Sulphur Mtn.
Fig. 5a
Ix-7
Fig. 7
WC
SRC
East Ventura basin
Santa Barbara
RED MTN. F.
RINCON ANTICLINE
CLARA SYNCLINE
VENTURA AVE. ANTICLINE
SANTA SUSANA FAULT
South Mtn.
Oak Ridge
SIMI FAULT
NORTHRIDGE HILLS F.
Ventura
OAK RIDGE FAULT
Simi V.
Oxnard Plain
San Fernando basin
Simi Hills
Santa Barbara Channel
Pt. Mugu
Santa Monica Mountains
MALIBU COAST FAULT
SANTA CRUZ ISLAND FAULT
Santa Cruz Island
Anacapa Island
Pt. Dume

Figure 1-1

Ventura basin in the Santa Clara Valley to the south. The nonmarine upper Pleistocene Saugus Formation lies unconformably over folded Pliocene and older strata, separated from the main Plio-Pleistocene Ventura basin by the Sulphur Mountain faulted anticlinorium which has upper Miocene Monterey Formation at the surface (Figure 1-2).

Surface geology (Figure 1-2) was mapped by Putnam (1942), Fine (1954), Bush (1956), Schlueter (1976), Dibblee (1982; 1987a), and Rockwell (1983). The geologic map was compiled from these maps and field-checked in 1986 and 1987. The Upper Ojai Valley includes the Sulphur Mountain, North Sulphur Mountain, Sulphur Crest, Sisar, Bear Canyon, and Silverthread areas of the Ojai oil field (Figure 1-3). Subsurface data from 372 oil wells (Figures 1-1, 1-3, 1-4, Table 1-1; Huftile, 1988a) were integrated with the surface data to reconstruct the geologic history and arrive at conclusions about the deep structure of the structurally complex oil-producing area. Large-scale maps, cross-sections, and a list of all wells used are available at cost from the author.

Table 1-1

List of wells cited in text and figures

Map Symbol	Company	Well Name	TD[ft(m)	Section-Township-Range
N3	Argo	Nesbitt 3	5703(1738)	8-4N-21W
			5966(1818)rd	
HL3	Argo	Hillside 3	9062(2762)	8-4N-21W
			9221(2811)rd	
H2	Argo	Harth 2	7721(2353)	8-4N-21W
BF2	Argo	Barker-Ferndale 2	7246(2209)	16-4N-21W
VF107	Argo	Valex-Ferndale 107	8275(2522)	16-4N-21W
313	Argo	Valex-Ferndale 313	8540(2603)	16-4N-21W
F8	Argo	Ferndale 8	10135(3089)	16-4N-21W
			7644(2330)rd	
			3186(971)rd	
18	Santa Fe	Arco 18	6850(2088)	17-4N-21W
19	Santa Fe	Arco 19	6408(1953)	17-4N-21W
20	Santa Fe	Arco 20	7295(2224)	17-4N-21W
			6780(2067)rd	
67	Arco	Ojai 67	7492(2284)	17-4N-21W
			5395(1644)rd	
			3733(1138)rd	
			4102(1250)rd	
24	Argo	Hamp 24	1010(308)	17-4N-21W
34	Argo	Hamp 34	3858(1176)	17-4N-21W
			3770(1149)rd	
			3840(1170)rd	
			4846(1477)rd	
38	Argo	Hamp 38	5678(1731)	17-4N-21W
			5348(1630)rd	
55	Sun	Hamp 55	5236(1596)	17-4N-21W
72	Sun	Hamp 72	6080(1853)	17-4N-21W
28	Santa Fe	Arco 28	6598(2011)	18-4N-21W
S1	Arco	Scott 1	5791(1765)	1-4N-22W
33	Arco	Ojai 33	1380(421)	12-4N-22W
B2	Ojai	B & L 2	2461(750)	12-4N-22W
B3	Ojai	B & L 3	7922(2415)	12-4N-22W
50	Arco	Ojai 50	3842(1171)	13-4N-22W
87	Arco	Ojai 87	4000(1219)	13-4N-22W
101	Arco	Ojai 101	4829(1472)	13-4N-22W
105	Arco	Ojai 105	5126(1562)	13-4N-22W
SC7	Unocal	Sulphur Crest 7	5306(1617)	13-4N-22W
SM	Market	Sulphur Mountain 1	6002(1829)	13-4N-22W
97	Arco	Ojai 97	4540(1384)	14-4N-22W
FR1	Phoenix	Freeman-Rafferty 1	1600(488)	21-4N-22W
FR3	Phoenix	Freeman-Rafferty 3	3000(914)	21-4N-22W
A1	Arco	Freeman 1	3452(1052)	21-4N-22W
S2	Continental	SMP 2	2737(834)	21-4N-22W
S3	Continental	SMP 3	6569(2002)	21-4N-22W
SOC1	Standard	Freeman 1	8686(2647)	21-4N-22W
SC102	Unocal	Sulphur Crest 102	5750(1753)	23-4N-22W
X7	Unocal	Ex-Mission 7	9327(2843)	33-4N-22W

Figure 1-2: Geologic map of the Upper Ojai Valley area and locations of cross sections. The Miocene Monterey Formation, which is both the source and reservoir rock, is shaded. See text for references.

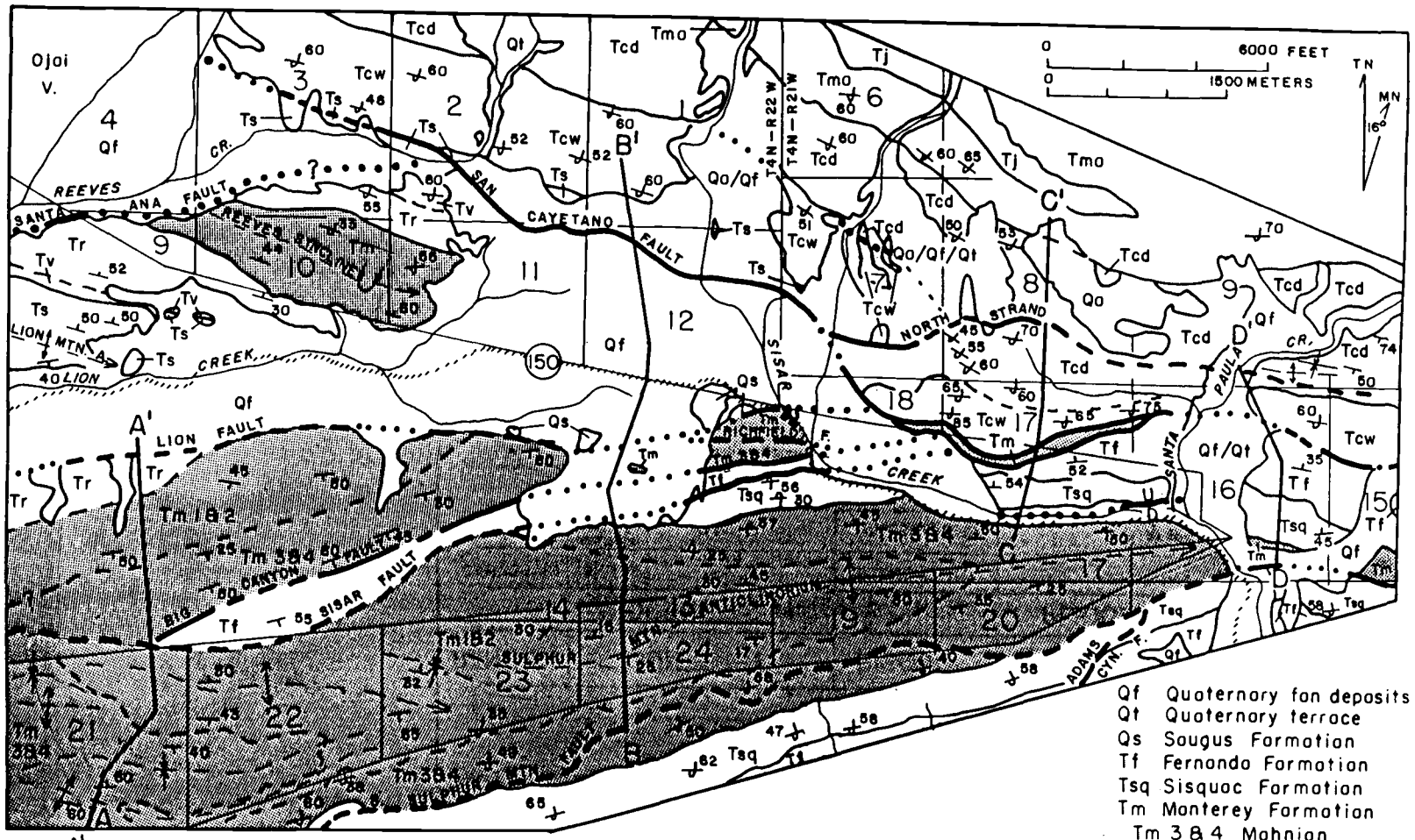
Ojai V.
REEVES
SANTA ANA FAULT
SAN CAYETANO FAULT
NORTH STRAND
LION MTN.
LION CREEK
LION FAULT
SISAR CANYON
SISAR FAULT
SULPHUR MTN.
SANTA PAULA CR.
ADAMS CYN.
T4N — R22W
T4N — R21W
6000 FEET
1500 METERS
TN
MN
16°
A
A'
B
B'
C
C'
D
D'
Qf Quaternary fan deposits
Qt Quaternary terrace
Qs Sougus Formation
Tf Fernando Formation
Tsq Sisquoc Formation
Tm Monterey Formation
Tm 3 & 4 Mohnian
Tm 2 Luisian
Tm 1 Relisian
Tr Rincon Formation
Tv Voqueros Formation
Ts Sespe Formation
Tcw Coldwater Formation
Tcd Cozy Dell Shale
Tmo Matilija Formation
Tj Juncal Formation
A — A' Cross section location
Highway
Oil seep
Strike and dip
Overturned strike and dip
Anticline
Syncline
Overturned syncline
Fault, dashed where inferred dotted where covered
Contact, dashed where inferred dotted where covered

Figure 1-2

Figure 1-3: Map showing locations of wells, cross sections, and oil-producing areas. See Table 1-1 for well symbols. The oil-producing areas of Ojai oil field area are shaded.

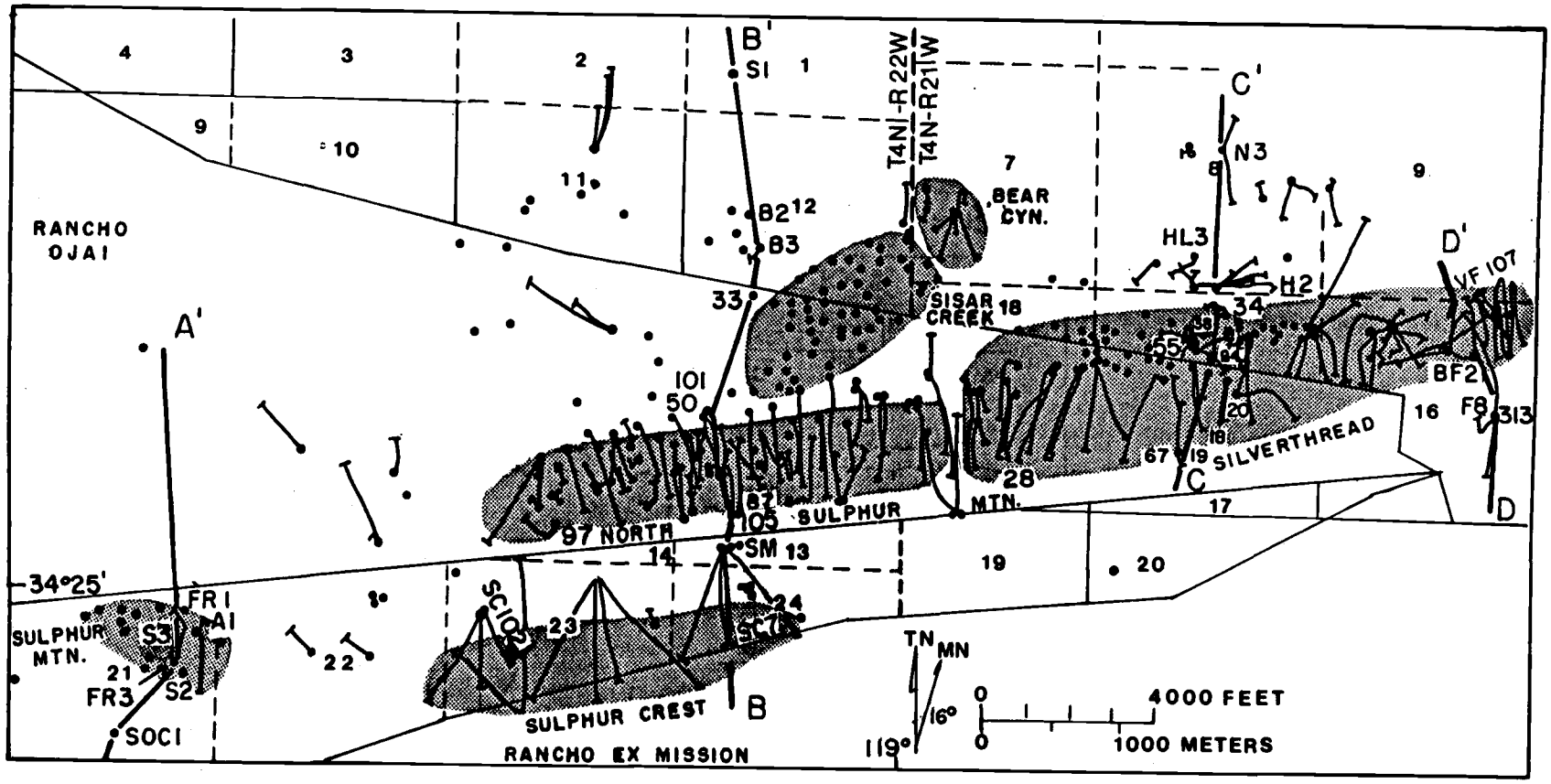
RANCHO OJAI
A'
B'
C'
D'
T4N-R22W
T4N-R21W
BEAR CYN.
SISAR CREEK
SILVERTHREAD
SULPHUR MTN.
97 NORTH
SULPHUR CREST
RANCHO EX MISSION
SULPHUR MTN.
34°25'
TN
MN
16°
119°
0
4000 FEET
0
1000 METERS

Figure 1-3

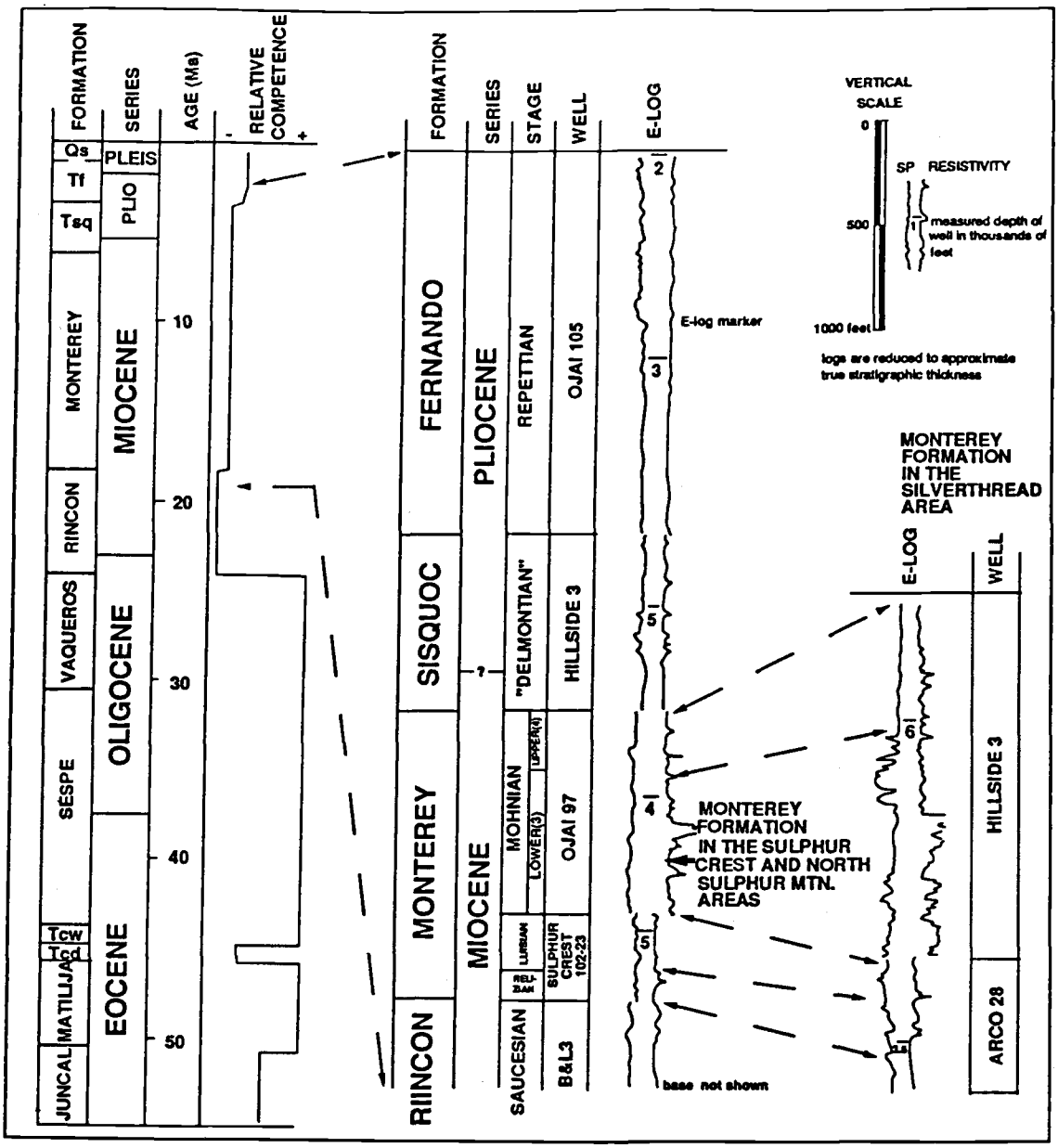

Figure 1-4: Generalized stratigraphic section showing age and relative competence of strata. Strata well defined in the subsurface are shown in the typical electric-log sections to the right, corrected to true stratigraphic thickness. Formation abbreviations same as Figure 1-2. Saucesian, Relizian, Luisian, Mohnian, and "Delmontian" are microfaunal stages of Kleinpell (1938), and Repettian is the lowermost microfaunal zone of Natland and Rothwell (1954).

STRATIGRAPHY

Figure 1-4 summarizes the stratigraphy in the Upper Ojai Valley. Those strata that are well defined in wells of the Ojai oil field are shown in the type electric-log section.

The stratigraphic descriptions are limited to the thickness and lithologic constraints on the strength of the formations. Descriptions of younger formations are more detailed where clast composition infers uplift of structures. Rocks exposed in the area are Eocene to Pleistocene in age. Eocene to Oligocene rocks are primarily well-indurated sandstone and form a thick, competent sequence. Uppermost Oligocene to lower Pliocene rocks are primarily shale and mudstone, and are relatively weak. These rocks are referred to as the Miocene incompetent section. The overlying Plio-Pleistocene strata are composed of sandstone, siltstone, mudstone, and conglomerate; they are trough turbidites at the base, grading upward into Pleistocene nonmarine sedimentary rocks.

Eocene and Oligocene competent section. Eocene and Oligocene strata, with the exception of the Juncal Formation and the Cozy Dell Shale, are primarily sandstone and are the most competent strata in the area.

The nomenclature used for the Eocene strata is that of Vedder (1972). The Eocene strata crop out in the hanging-wall block of the San Cayetano fault (Figures 1-2 and 1-5b-d).

Figure 1-5: Cross sections A-A' through D-D'. Locations of cross sections are shown on Figures 1-2 and 1-3; Figure 1-5a is located on Figure 1-1. No vertical exaggeration. The Miocene Monterey Formation, the source and reservoir rock, is shaded. The scale is equal to that in Figure 1-2. See Figure 1-2 for formation abbreviations. Well symbols are given in Table 1-1.

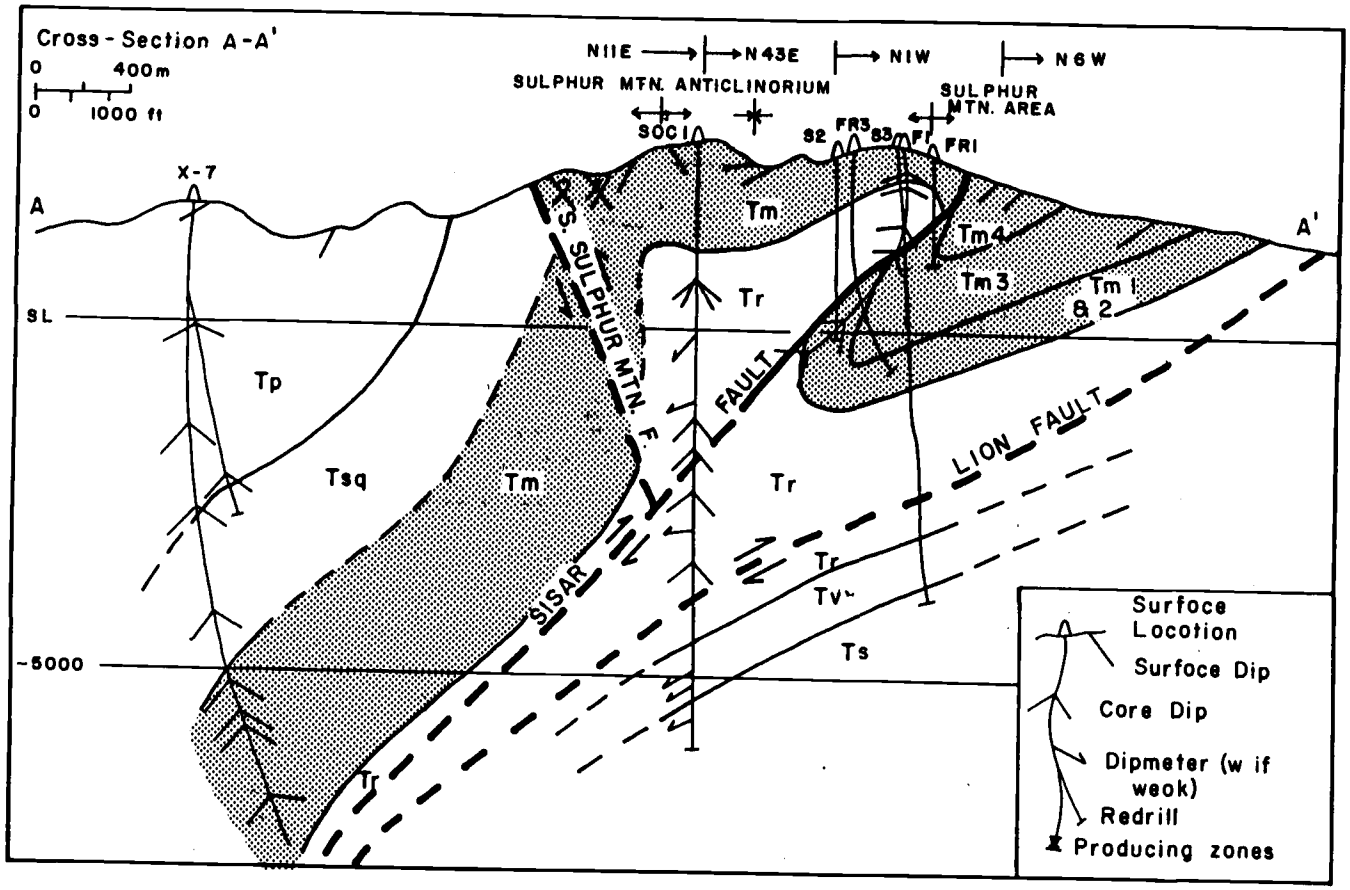
Cross-Section A-A'
0 400m
0 1000 ft
N11E
N43E
N1W
N6W
SULPHUR MTN. ANTICLINORIUM
SULPHUR MTN. AREA
SOC1
S2
FR3
S3
Fr'
FR1
X-7
A
A'
Tm
Tm4
Tm3
Tm1
S2
SL
Tr
Tp
Tsq
Tm
Tr
Tr
Tv
Ts
Tr
-5000
S. SULPHUR MTN. F.
FAULT
LION FAULT
SISAR
Surface Location
Surface Dip
Core Dip
Dipmeter (w if weak)
Redrill
Producing zones

Figure 1-5a

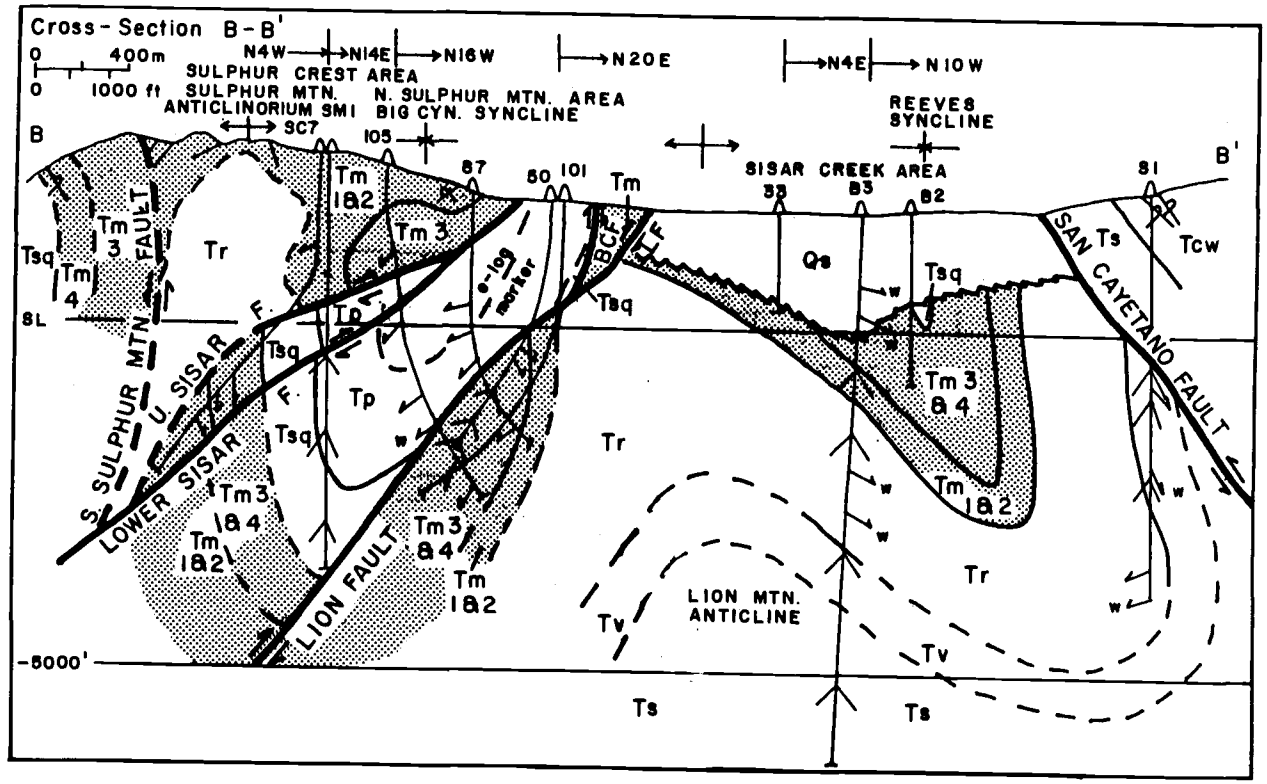
Cross-Section B-B'
0 400m
0 1000 ft
N4W
N14E
N16W
N20E
N4E
N10W
SULPHUR CREST AREA
SULPHUR MTN. ANTICLINORIUM
N. SULPHUR MTN. AREA
SMI
BIG CYN. SYNCLINE
REEVES SYNCLINE
SISAR CREEK AREA
B
B'
SC7
105
87
50
101
Tm
33
83
82
81
Tm 182
Tm 3
Tm 3 FAULT
Tsq
Tm 4
Tr
Qs
Ts
Tcw
SAN CAYETANO FAULT
SL
F.
Tp
Tm 3 84
Tm 182
U. SISAR
S. SULPHUR MTN.
LOWER SISAR
Tm3 184
Tm 182
LION FAULT
Tm3 84
Tm 182
LION MTN. ANTICLINE
Tv
-5000'
Ts
Ts

Figure 1-5b

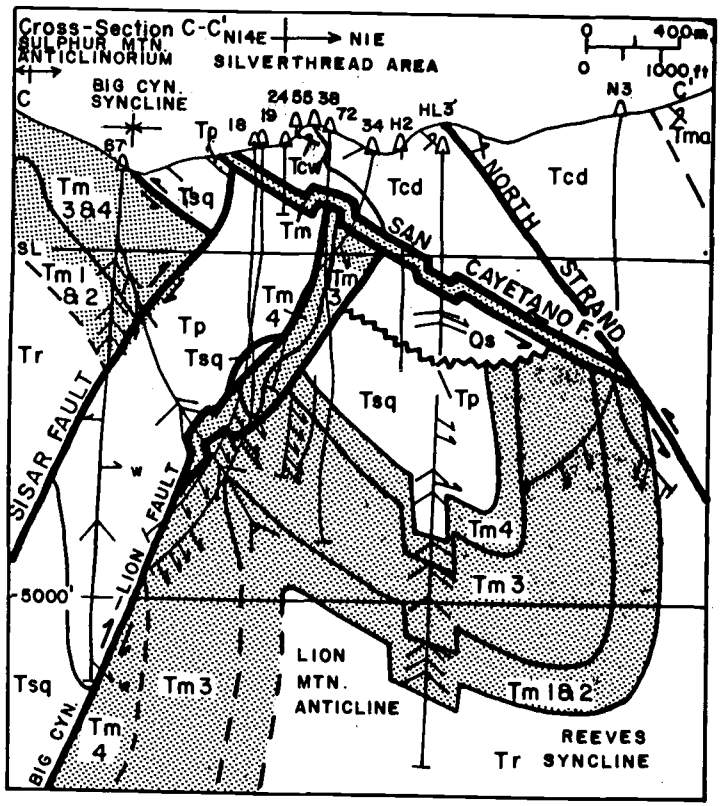

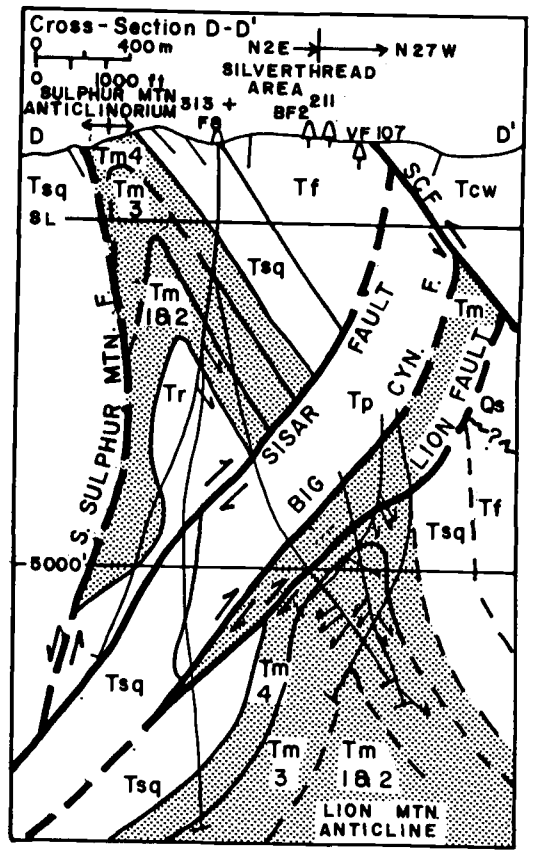

Figures 1-5c and 1-5d

The base of the Juncal Formation is not seen or penetrated by wells in the study area. Dibblee (1985, 1987b) mapped Juncal Formation overlying unnamed Cretaceous marine strata near the Santa Ynez fault to the northwest; there it is 1130 m thick (Dibblee; 1987c). Elsewhere, the Juncal rests on lower Eocene Sierra Blanca Limestone which itself rests on Upper Cretaceous turbidite sandstone and conglomerate (Vedder, 1972) and on Mesozoic granite (Dibblee, 1979). The Matilija Formation is about 425 m thick (Figure 1-2). The middle-late Eocene Cozy Dell Shale is approximately 730 m thick over much of the study area, but increases to 1040 m thick in the Silverthread area (Figure 1-3) because of the presence of interbeds of fine-grained sandstone. The Cozy Dell Shale is relatively less competent than the underlying Matilija or the overlying Coldwater and Sespe sandstones.

The upper Eocene Coldwater Sandstone is 760 m thick in the hanging-wall block of the San Cayetano fault (Figure 1-2) and at its type section in a tributary to Sespe Creek (Figure 1-1; Kerr and Schenk, 1928). The upper Eocene and Oligocene Sespe Formation (Kew, 1924) is cut by the San Cayetano fault, so that a complete section is not found at the surface in the study area. To the west, the Sespe Formation crops out in the core of the Lion Mountain anticline (Figure 1-2), where it is 1370 m thick, based on a well that reaches the Coldwater Sandstone (Fine, 1954). The Oligocene Vaqueros Formation is 275 m thick in outcrop south of Wilsie Canyon (Bush, 1956; Figure 1-2) and it is 245 m thick in the subsurface. The Vaqueros, Sespe, and

Coldwater formations form a sequence of competent strata about 2350 m thick (Figure 1-4).

Miocene incompetent section. The uppermost Oligocene-lower Miocene Rincon Formation crops out on the flanks of Reeves syncline (Figure 1-2). It is a ductile mudstone that is tectonically thickened in the hinges of folds (Figures 1-5, 1-6). Isopach contours (Edwards,1971) show that it should be approximately 460 m thick in undistorted sections in the study area.

The Miocene Monterey Formation is predominantly siliceous shale and is divided into four members based on the microfaunal stages of Kleinpell (1938): Tm1 is Relizian (lower middle Miocene), Tm2 is Luisian (upper middle Miocene), Tm3 is lower Mohnian (lower upper Miocene), and Tm4 is upper Mohnian (upper upper Miocene). Its thickness varies from 460 m to as much as 700 m (Figures 1-4, 1-5). Berger (1977) showed that the thickness of the Monterey Formation increases east of Sespe Creek (Figure 1-1) to about 1240 m accompanied by an increase in the amount of sandstone. The increased thickness in the Silverthread area is from the addition of intercalations of sandstone turbidites in the upper part of the section (Figures 1-4, 1-5c; Berger, 1977). The Monterey Formation is ductile and is tectonically thickened in fold hinges in the footwall blocks of the Sisar and San Cayetano faults (Figures 1-5a-d), and it forms disharmonic folds in the Sulphur Mountain anticlinorium (Figures 1-5a, 1-5b).

Figure 1-6: (a) Subcrop geologic map showing Lion Mountain anticline, Reeves syncline. This map is a subcrop map beneath younger, unfolded features including the San Cayetano fault, Saugus Formation, Lion fault, and alluvial-fan deposits as illustrated in cross section A-A'. Note the change in structural response to folding between the Vaqueros and Rincon Formations, viewing downplunge on the Lion Mountain anticline. (b) Subcrop geologic map showing the south flank of the Big Canyon syncline beneath the Sisar fault and at the surface as illustrated in cross section B-B'. To the left is the unnamed syncline that produces in the Sulphur Mountain area of the Ojai oil field (Figure 1-5a). Scale is the same as Figure 1-2. See Figure 1-2 for formation abbreviations.

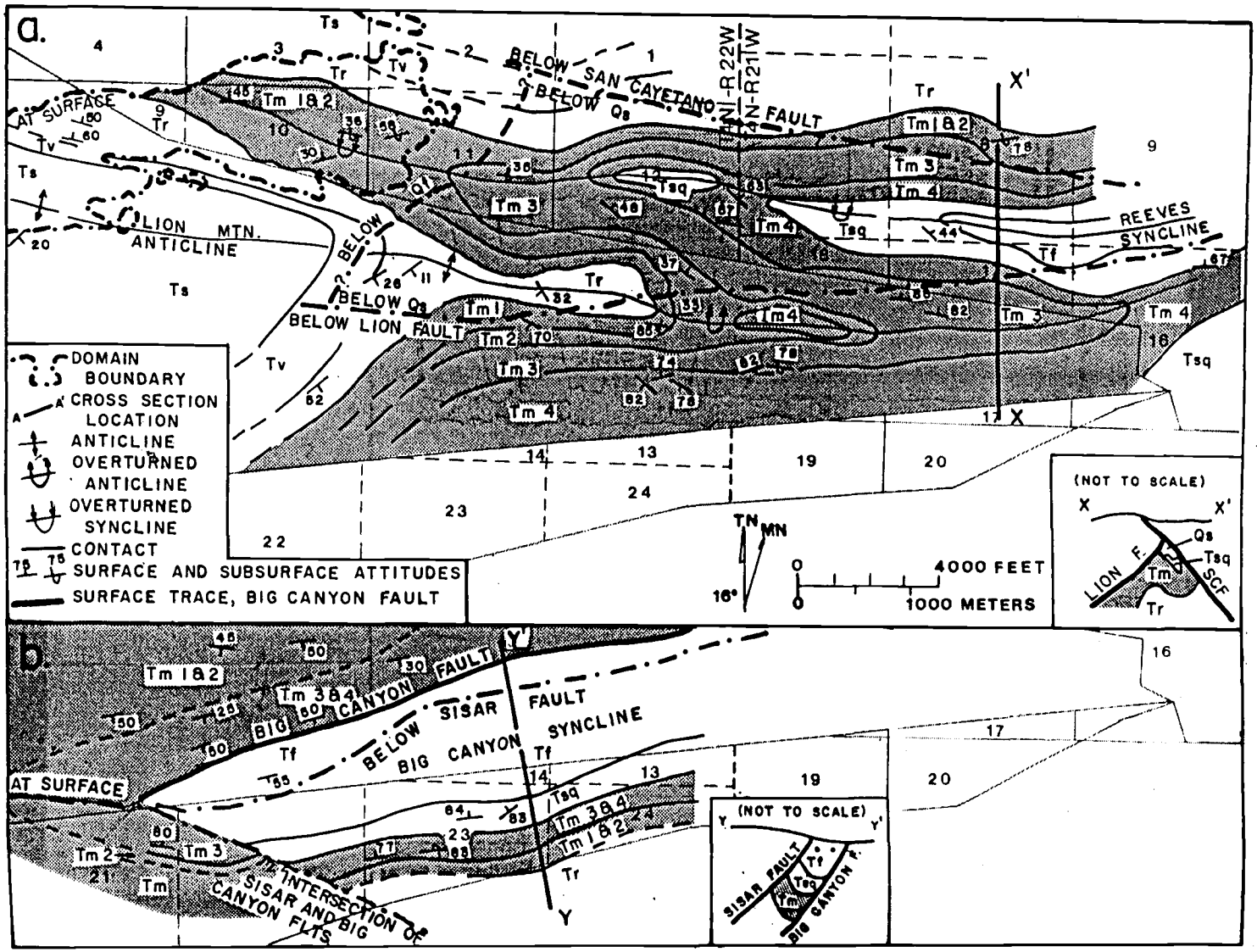
a.
b.
AT SURFACE
LION MTN. ANTICLINE
BELOW SAN CAYETANO FAULT
BELOW LION FAULT
REEVES SYNCLINE
BIG CANYON FAULT
BELOW SISAR FAULT
BIG CANYON SYNCLINE
INTERSECTION OF SISAR AND BIG CANYON FLATS
T2N-R22W
T2N-R21W
DOMAIN BOUNDARY
CROSS SECTION LOCATION
ANTICLINE
OVERTURNED ANTICLINE
OVERTURNED SYNCLINE
CONTACT
SURFACE AND SUBSURFACE ATTITUDES
SURFACE TRACE, BIG CANYON FAULT
4000 FEET
1000 METERS
(NOT TO SCALE)
SISAR FAULT
BIG CANYON F.
LION F.
SCF

Figure 1-6

The upper Miocene-Pliocene Sisquoc Formation is primarily shale and lies between strata with microfossils of the Mohnian stage of Kleinpell (1938) and strata with Repettian (lower Pliocene) microfossils as described by Natland and Rothwell (1954). In the subsurface of the Upper Ojai Valley, it has a thickness of 220-305 m (Figures 1-5c, 1-5d); south of Sulphur Mountain, it is 280-370 m thick (Figures 1-2, 1-5a). In the subsurface, it is tectonically thickened in the fold hinge of the Reeves syncline (Figures 1-5c, 1-6).

Plio-Pleistocene strata. The name Fernando Formation is used for middle Pliocene-middle Pleistocene deep-water sandstone, siltstone, mudstone, and conglomerate. These strata were described by Eldridge and Arnold (1907) and named the Fernando Group by Kew (1924), including the Repetto, Pico, Santa Barbara, and Saugus formations. Fine (1954), Bush (1956), Crowell et al. (1966), Schlueter (1976), Dibblee (1982, 1987a) include the Pliocene rocks in the Pico Formation. Jennings and Strand (1969) reduced the Fernando Group to formation status with the Repetto, Pico, and Santa Barbara members overlain by the Saugus Formation. This terminology was used by Rockwell (1988) and it is repeated here. The Santa Barbara member is equivalent to the Mudpit Shale of Nagle and Parker (1970). The Saugus is retained as a separate, overlying formation.

Strata in the Upper Ojai Valley are subdivided into Repettian and Pico members based on microfauna. Although the Repettian and Venturian are generally believed to be lower Pliocene and lower upper Pliocene, respectively,

they are characterized by microfauna that indicate water depth rather than age. Lagoe and Thompson (1988) use the coiling dominance of certain planktonic foraminifera as chronostratigraphic indicators, reasoning that changes between sinistral and dextral coiling are due to climatic shifts and, thus, are not time-transgressive. The Repettian-Venturian boundary is calculated to be 2.8 Ma at Wheeler Canyon (Figures 1-1, 1-7a), immediately south of the study area, based on data from Lagoe and Thompson (1988) and assuming constant deposition rates. The Repettian and Venturian deep-water faunas and sedimentary facies in the Fernando of the Upper Ojai Valley are similar to those in the Santa Clara syncline to the south, indicating that the Fernando was deposited as part of the main Ventura trough, and the Sulphur Mountain anticlinorium had not yet begun to form (Figure 1-8a).

In the subsurface of the Upper Ojai Valley, the Fernando is as much as 610 m thick (Figure 1-5b). It is tectonically thickened in the hinge of the Big Canyon syncline (Figure 1-5b). To the south, in the Santa Clara syncline, the Repettian section is 1120 m thick (Figure 1-7a). The greatly thinned section to the north implies differential subsidence during Repettian time, but there is no evidence of detritus from the Sulphur Mountain anticlinorium (Figure 1-8). Electric logs show a shaly Repettian section, except where sandstone and conglomerate occur in the upper section (above the E-log marker in Figures 1-4, 1-5b). These coarse-grained sandstones and conglomerates may represent proximal turbidite fan deposits derived from the north. In contrast, the

Figure 1-7: (a) Area-balanced cross section. Location is on Figure 1-1; the Upper Ojai Valley part is equivalent to Figure 1-5b. Cretaceous strata are marine turbidites at the surface; Eocene-Oligocene (shaded) is the base of the Juncal Formation to the top of the Vaqueros Formation; Miocene is the base of the Rincon Formation through the top of the Sisquoc Formation; Tf is Plio-Pleistocene Fernando Formation; Qs is upper Pleistocene Saugus Formation. SM, Sulphur Mountain; UOV, Upper Ojai Valley. (b and c) Schematic explanation of area-balancing. The area (A) equals the thickness of the strata (t) times the original bed-length (L).

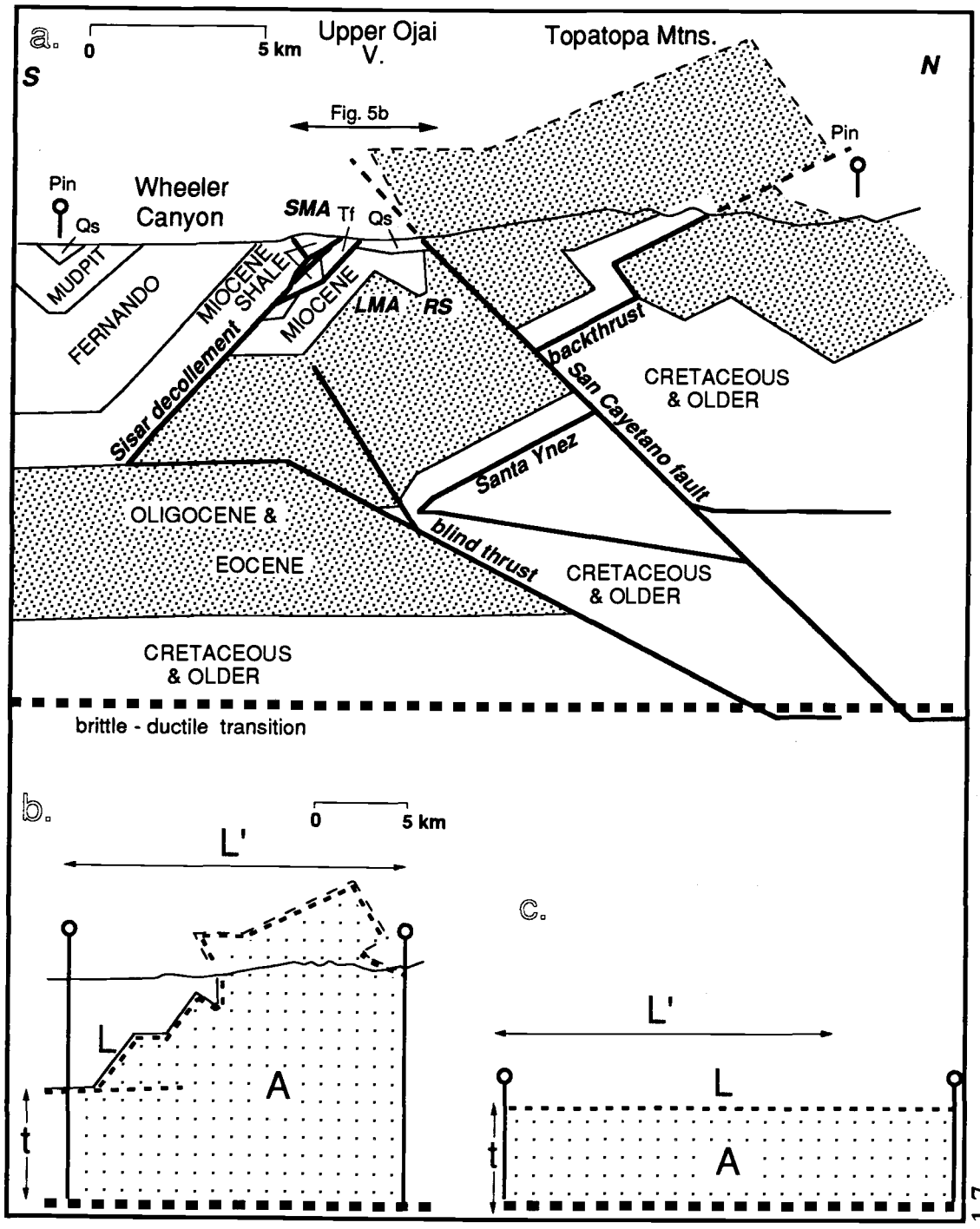
a.
0
5 km
S
N
Upper Ojai V.
Topatopa Mtns.
Fig. 5b
Pin
Qs
Wheeler Canyon
SMA
Tf
Qs
Pin
MUDPIT
FERNANDO
MIOCENE SHALE
MIOCENE
LMA
RS
backthrust
San Cayetano fault
CRETACEOUS & OLDER
Sisar decollement
Santa Ynez
OLIGOCENE & EOCENE
blind thrust
CRETACEOUS & OLDER
CRETACEOUS & OLDER
brittle - ductile transition
b.
0
5 km
L'
L
A
t
c.
L'
L
A
t

Figure 1-7

Figure 1-8: (a and b) Schematic illustration of unroofing of the uplifted area north of the San Cayetano fault, depositing clasts of progressively older formations in progressively younger deposits. Squares are clasts derived from Miocene formations; circles are derived from Eocene formations. (c) uplift of Sulphur Mountain anticlinorium deposits clasts derived from the Monterey formation in alluvial-fan deposits to the north. See Figure 1-3 for formation abbreviations.

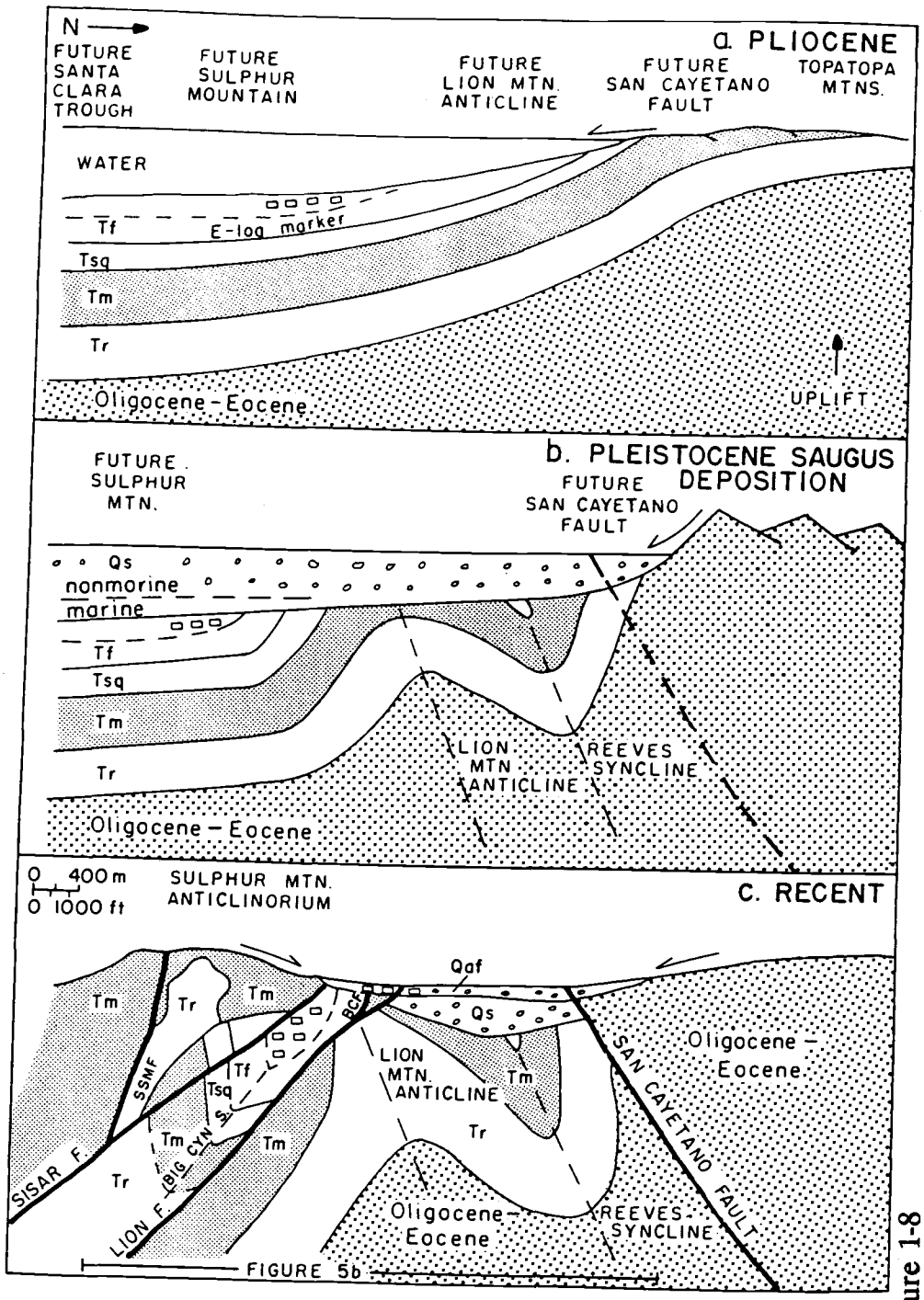
N
FUTURE SANTA CLARA TROUGH
FUTURE SULPHUR MOUNTAIN
FUTURE LION MTN. ANTICLINE
FUTURE SAN CAYETANO FAULT
TOPATOPA MTNS.
a. PLIOCENE
WATER
Tf
E-log marker
Tsq
Tm
Tr
Oligocene-Eocene
UPLIFT
FUTURE SULPHUR MTN.
b. PLEISTOCENE SAUGUS DEPOSITION
FUTURE SAN CAYETANO FAULT
Qs
nonmarine
marine
LION MTN ANTICLINE
REEVES SYNCLINE
0 400 m
0 1000 ft
SULPHUR MTN. ANTICLINORIUM
C. RECENT
Qaf
SSMF
RCF
SISAR F.
LION F.
BIG CYN
LION MTN. ANTICLINE
SAN CAYETANO FAULT
REEVES SYNCLINE
FIGURE 5b

Figure 1-8

Repettian section south of Sulphur Mountain consists of turbidite sandstone alternating with hemipelagic mudstone. Microfaunal ages in the sandstone section in the footwall block of the Sisar fault range from Repettian to Relizian. The dates older than Repettian are from redeposited microfossils from the Sisquoc and Monterey formations. This implies that nearby areas to the north, underlain at that time by Sisquoc and Monterey, were being uplifted and eroded, perhaps accompanying south-verging folding during the time of Repettian deposition (Figure 1-8a). One Repettian microfossil species found in sandstone in the Arco Ojai 105 well (Figure 1-3), Bulimina rostrata, is so fragile that it is unlikely to be reworked (G. H. Blake, personal communication, 1987); thus, the sands are probably no younger than Repettian. The Pico Member with Venturian microfauna is the youngest unit folded in the Big Canyon syncline in the footwall block of the Sisar fault.

The nonmarine Saugus Formation of the Upper Ojai Valley (Figures 1-2, 1-5b-d) contains clasts predominantly of Eocene sandstone (Figure 1-8). Natland and Kuenen (1951) show that clasts of Eocene sandstone predominate in Saugus conglomerate of middle Pleistocene age in the Santa Clara syncline south of Sulphur Mountain, indicating that the Saugus Formation in the Upper Ojai Valley is at least as young as it is farther south, and also that Sulphur Mountain had not yet begun to shed detritus into the basin (Figure 1-8b). In the Upper Ojai Valley, the Saugus lies with angular unconformity on rocks ranging from Oligocene to Repettian age (Figures 1-5b-d, 1-6). South of

Sulphur Mountain, the Saugus Formation lies conformably on the "Mudpit Shale" of early Pleistocene age (Figure 1-7a). The "Mudpit Shale" contains ash beds dated at 1.2 Ma (Izett et al., 1974) and 0.7 Ma (Sarna-Wojcicki et al., 1984). The "Mudpit Shale" is absent in the Upper Ojai Valley, suggesting that early Pleistocene strata were eroded away from the Upper Ojai Valley area. Near Ventura, the Saugus Formation has been dated by tephrochronology and amino-acid stereochemistry as between 0.63 and 0.2 Ma (Lajoie et al., 1982; Sarna-Wojcicki et al., 1984). In the study area, it attains a maximum thickness of 730 m. In the Santa Clara syncline, south of Sulphur Mountain, it is 1340 m thick (Figure 1-7a). In the subsurface of the Upper Ojai Valley, gently folded Saugus Formation occurs in the footwall block of the San Cayetano and Lion faults (Figures 1-5b, 1-5c).

STRUCTURE

The discussion of structures is divided into sections covering south-vergent and north-vergent structures. South-vergent structures include reverse faults that dip north, folds with more steeply dipping south limbs, and blind thrusts. North-vergent structures include south-dipping reverse faults and the Sulphur Mountain anticlinorium. North-vergent structures are interpreted to be the result of passive backthrusting above the foreland fault tip of a south-vergent blind thrust, as modeled by Namson (1987) and Namson and Davis (1987) south of Ojai Valley to the west (Figure 1-1).

South-vergent structures. The Lion Mountain anticline and Reeves syncline (Figures 1-5b, 1-5c, 1-5d) are south-verging folds related to early movement on the blind thrust in the footwall block of the San Cayetano fault (Figure 1-7a). The overturned strata in the hanging-wall block of the San Cayetano fault are part of the eastern extension of the Matilija overturn of Kerr and Schenk (1928). The Lion Mountain anticline and the Reeves syncline have north-dipping axial surfaces (Figures 1-5b, 1-5c).

The Lion Mountain anticline and Reeves syncline are interpreted to have formed as a south-verging fault-propagation fold (Figure 1-7a). Folded strata are deeply eroded and overlain unconformably by the late Pleistocene Saugus Formation (Figures 1-5b, 1-5c). To the south, in what is now the footwall block of the Sisar fault, clasts of Miocene strata are found in the uppermost Repettian Pico Member of the Fernando Formation. These clasts

are presumably from Miocene formations north of the San Cayetano fault that are now completely eroded away (Figure 1-8a). The Sulphur Mountain anticlinorium could not have been the source of the clasts because it did not form until later. The deep-water Pico Member of the Upper Ojai Valley was still connected to the Pico of the Santa Clara syncline. Northward thinning of the Pico Member between the Santa Clara and Upper Ojai Valleys may be related to coeval uplift of the region north of the San Cayetano fault (Figure 1-8a). Thus, folding of the south-vergent structures occurred between the end of Repettian deposition and the onset of Pleistocene Saugus deposition, and it probably preceded the folding of the north flank of the Reeves syncline. Strata as young as Repettian are tightly folded and deeply eroded. Folding ceased prior to the late Pleistocene deposition of the Saugus Formation, which is tilted only 10-20° and has its synclinal axis on the south flank of the Reeves syncline (Figures 1-5b, 1-5c).

The San Cayetano fault, first recognized as active by Putnam (1942), dips approximately 50° north (Figure 1-5b) to the west of Bear Canyon (Figure 1-3). In the Silverthread area (Figure 1-3), the main strand of the fault has a lobate surface trace (Figure 1-2). The fault zone contains a sliver of Monterey Formation that has been dragged up along the fault (Figure 1-5c), probably from the north limb of the Reeves syncline. This strand dips as little as 10°, but is generally 25-30° (Figures 1-5c, 1-9). This shallow-dipping main strand is

Figure 1-9: Structure-contour map of the San Cayetano and Sisar faults. The San Cayetano fault has main and north strands, and the Sisar fault has upper and lower strands. Contours on the upper Sisar fault and the north strand of the San Cayetano fault are shown in heavy lines. The Contour interval is 1000 feet (3.05 km). The scale is the same as that of Figure 1-2. Contours are shown only where controlled by well data.

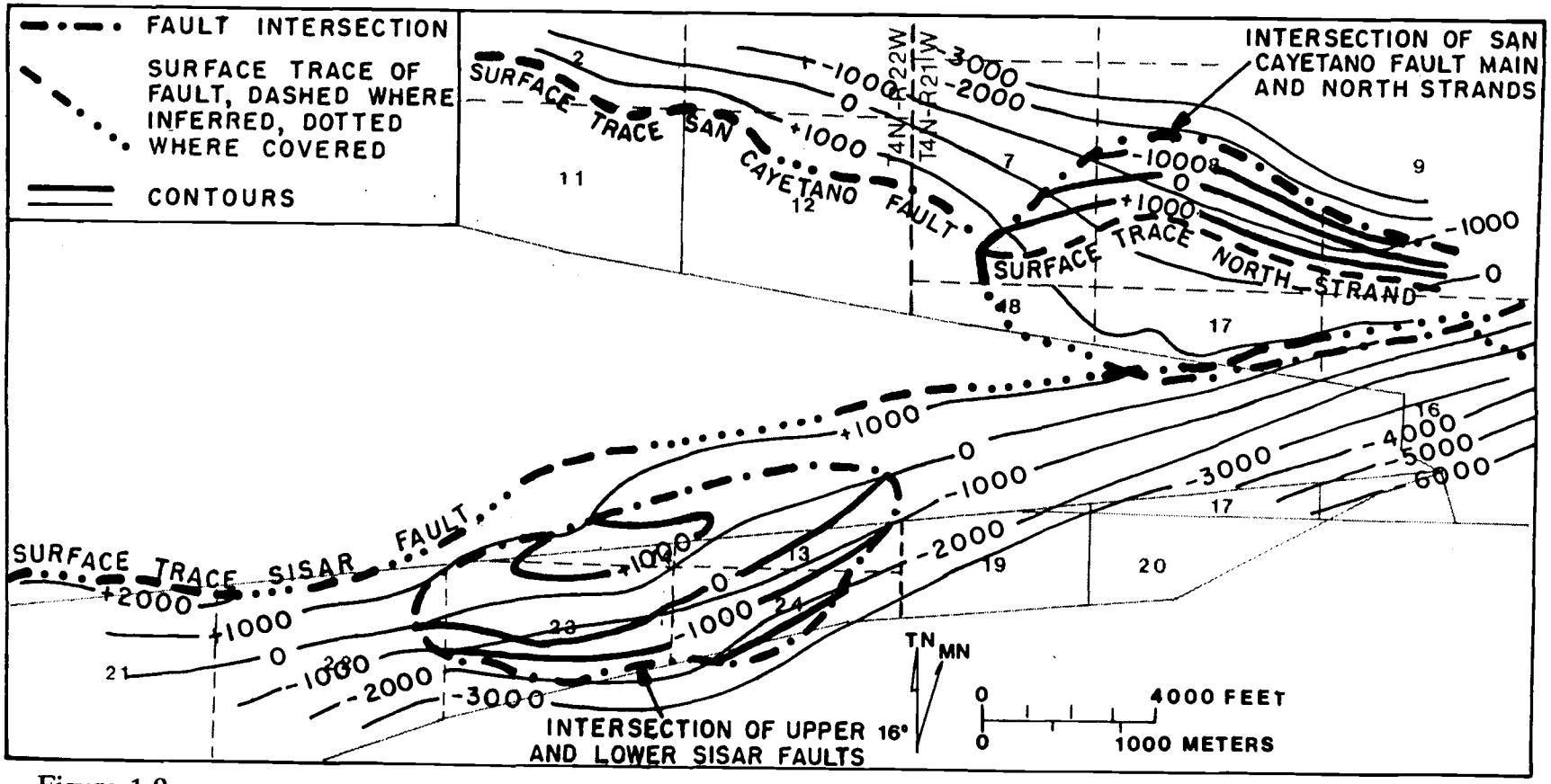
FAULT INTERSECTION
SURFACE TRACE OF FAULT, DASHED WHERE INFERRED, DOTTED WHERE COVERED
CONTOURS
INTERSECTION OF SAN CAYETANO FAULT MAIN AND NORTH STRANDS
SURFACE TRACE SAN CAYETANO FAULT
SURFACE TRACE NORTH STRAND
SURFACE TRACE SISAR FAULT
INTERSECTION OF UPPER AND LOWER SISAR FAULTS
T4N-R22W
T4N-R21W
TN
MN
0
4000 FEET
0
1000 METERS

Figure 1-9

interpreted to be an inactive strand of the San Cayetano fault that became abandoned in favor of the more steeply dipping north strand.

The north strand of the San Cayetano fault dips about 55° north (Figure 1-5c, 1-9) and is associated with tilted alluvial-fan gravels. The north strand brings Eocene rocks over upper Pleistocene alluvial deposits. Tilting of the surficial gravels is the only documented example of late Quaternary hanging-wall deformation on the San Cayetano fault (Rockwell, 1988). The north strand splays off from the main strand near Bear Canyon (Figure 1-2). Rockwell (1988) shows it merging with the main strand farther east near Santa Paula Creek, but the contacts there are not offset as they are in the west. Thus, the fault is interpreted to die out into bedding within the Cozy Dell Shale east of Santa Paula Creek (Figure 1-2), or to merge with the main strand still farther east. The apparent normal offset of the Coldwater-Cozy Dell contact at the west end of the north strand requires that the overturning of the strata preceded faulting by the north strand (Figure 1-2) and that bedding dip more gently than the fault at the fault cut-offs.

Yerkes and Lee (1979) show depths as great as 17 km to earthquake foci north of the San Cayetano fault, and northeast of the study area. Focal-plane solutions give an average dip of 65° north-northeast. Northeast of the study area, Simila et al. (1987; G. Simila, written communication, 1988) show a June, 1984 earthquake swarm that defines a 50° dip on a fault plane to 16 km depth. A focal mechanism for the 12 June 1984 main shock defines a 54° dip

at 12 km depth. Focal mechanisms on other major faults in the western Transverse Ranges have been shown to flatten at the mid-crustal level (Webb and Kanamori, 1985). If this is true for the San Cayetano fault as well, the upper block moved south-southwest over a decollement at the brittle-ductile transition at mid-crustal depth. Yeats (1981a) argued that a mid-crustal decollement is geologically reasonable assuming that the Transverse Ranges comprise a "tectonic flake." The surface flake is composed of brittle crystalline rocks riding over a ductile mid-crustal zone of decollement. Yeats (1983) proposed that the decollement occurred at the rheological boundary between upper high-strength and lower weaker rocks. In the Transverse Ranges, this decollement appears to ramp to the surface along north-dipping reverse faults including the Red Mountain, San Cayetano, and Santa Susana faults (Figure 1-1).

Along cross section C-C' (Figures 1-2, 1-3, 1-5c), stratigraphic separation is 6.0 km on the San Cayetano fault. Along cross section B-B'(Figures 1-2, 1-3, 1-5b, 1-7a, 1-11), there is no more than 2.6 km of stratigraphic separation. Separation diminishes to zero at the west end of Figure 2 in the Ojai Valley.

Folding associated with the San Cayetano fault may have begun as long ago as the Repettian because lowermost Repettian Fernando Formation is found in the core of Reeves syncline and north-derived clasts from Miocene strata are found in the uppermost Repettian Fernando Formation found in the core of the Big Canyon syncline. However, the clasts of Miocene strata may

Figure 1-10: Schematic cross sections illustrating the development of Sulphur Mountain anticlinorium. No vertical exaggeration. See Figure 1-2 for formation abbreviations. Dotted faults represent restored movement on faults. Tfp, Pico Member of the Fernando Formation; Tfr, Repetto Member. (a) Mid-late Pleistocene. Sulphur Mountain anticlinorium is rising as a fault-propagation fold with the fault tip of Big Canyon fault (BCF) in the hinge of the Big Canyon syncline (BCS). (b) Late Pleistocene. Movement on the Big Canyon, Upper Sisar (SF), and South Sulphur Mountain (SSMF) faults. (c) Represents present structure including that shown in Figure 1-5b following movement on the Lower Sisar (LSF) and Lion (LF) faults.

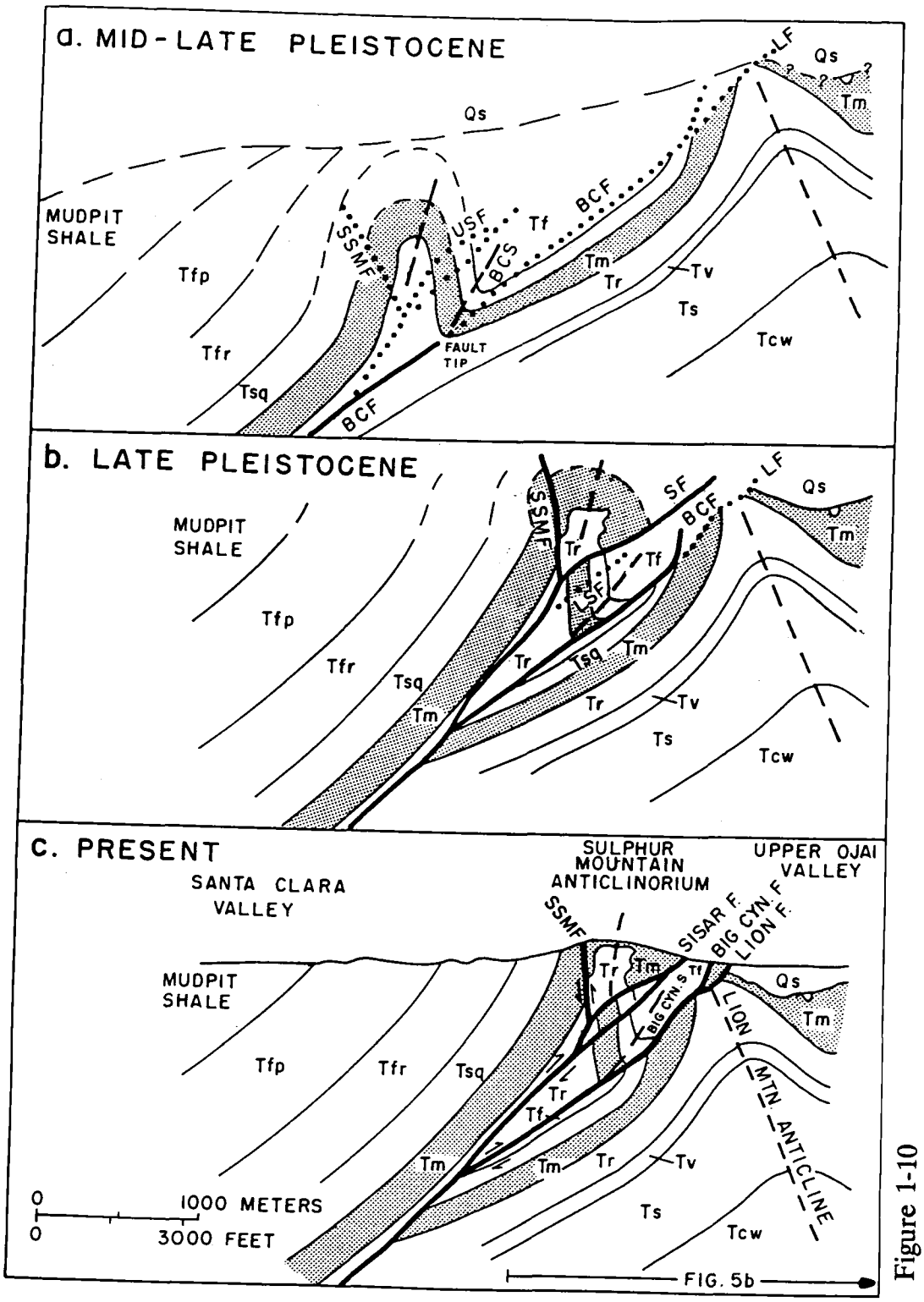
a. MID-LATE PLEISTOCENE
Qs
LF
Qs
Tm
MUDPIT SHALE
Tfp
Tfr
Tsq
SSMF
USF
BCS
Tf
BCF
Tm
Tr
Tv
Ts
Tcw
FAULT TIP
BCF
b. LATE PLEISTOCENE
MUDPIT SHALE
Tfp
Tfr
Tsq
Tm
SSMF
Tr
SF
BCF
Tf
LSF
LF
Qs
Tm
Tr
Tsq
Tm
Tr
Tv
Ts
Tcw
c. PRESENT
SANTA CLARA VALLEY
SULPHUR MOUNTAIN ANTICLINORIUM
UPPER OJAI VALLEY
SSMF
SISAR F.
BIG CYN. F.
LION F.
MUDPIT SHALE
Tfp
Tfr
Tsq
Tr
Tm
Tf
BIG CYN. S
Qs
Tm
LION MTN. ANTICLINE
Tr
Tf
Tm
Tm
Tr
Tv
Ts
Tcw
0
1000 METERS
0
3000 FEET
FIG. 5b

Figure 1-10

Figure 1-11: Structure contour map of the Lion and Big Canyon faults. The contour interval is 2000 feet (0.61 km). The scale is the same as that of Figure 1-2. Contours are shown only where controlled by well data.

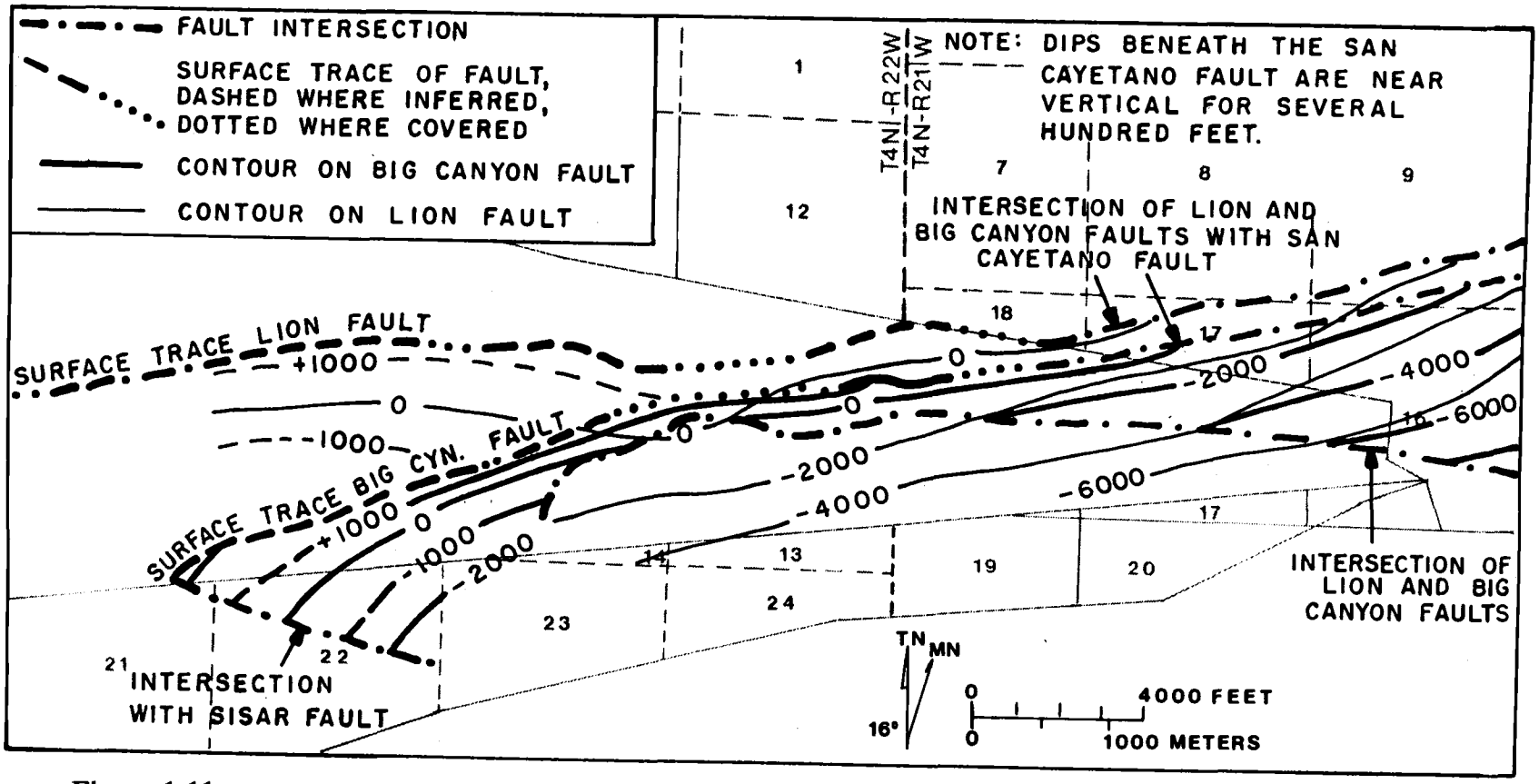
FAULT INTERSECTION
SURFACE TRACE OF FAULT, DASHED WHERE INFERRED, DOTTED WHERE COVERED
CONTOUR ON BIG CANYON FAULT
CONTOUR ON LION FAULT
NOTE: DIPS BENEATH THE SAN CAYETANO FAULT ARE NEAR VERTICAL FOR SEVERAL HUNDRED FEET.
T4N-R22W
T4N-R21W
INTERSECTION OF LION AND BIG CANYON FAULTS WITH SAN CAYETANO FAULT
SURFACE TRACE LION FAULT
SURFACE TRACE BIG CYN. FAULT
+1000
0
-1000
-2000
-4000
-6000
INTERSECTION WITH SISAR FAULT
INTERSECTION OF LION AND BIG CANYON FAULTS
TN
MN
16°
0
4000 FEET
0
1000 METERS

Figure 1-11

have been derived from structures farther north, leaving the age of the onset of deformation of the western San Cayetano fault uncertain. The eastern San Cayetano fault, in the Piru area, cuts rock as young as late Quaternary. The Pico Member of the Fernando Formation is much thinner on the upthrown side of the fault (L. Stitt, personal communication, 1987) but it is not clear whether the Repetto Member is also thinned. This implies that the eastern San Cayetano fault was probably active by the time that the Fernando Formation with Venturian microfossils was being deposited.

North-vergent structures. The Sulphur Mountain anticlinorium and Big Canyon syncline developed as a fault-propagation fold pair as early as 2.0-2.2 Ma according to Lagoe and Thompson (1988) and G. H. Blake (personal communication, 1987), because Venturian Pico Formation is the youngest unit folded in the Big Canyon syncline (Figure 1-5c, well 67). If the anticlinorium began forming prior to the onset of "Mudpit Shale" deposition, beginning ~1.2 Ma, the "Mudpit Shale" would thin towards and onlap onto the south flank of the fold. However, the "Mudpit Shale" shows no such thinning, so the Upper Ojai Valley probably was undergoing erosion at the time, and the Sulphur Mountain anticlinorium is younger than the Mudpit Shale (Figure 1-10).

The Sulphur Mountain anticlinorium and the Big Canyon syncline are cut by the Lion, Big Canyon, and Sisar reverse faults (Figures 1-2, 1-5, 1-9, 1-11; Lion fault set on Figure 1-1). All the faults dip to the south and, for the most part, postdate the folding. Map relations show that the Big Canyon fault

is truncated by the Sisar fault (Figure 1-2), which itself is truncated by the Lion fault west of the study area (Dibblee, 1987a). The overturned bedding on the north limb of the Sulphur Mountain anticlinorium, in the hanging-wall block of the Sisar fault, suggests that the anticlinorium be described as a fault-propagation fold. A fault-propagation fold represents deformation that takes place above, and in front of, a propagating fault tip. The tip of the propagating fault is in the core of the syncline beneath a rising anticline (Figure 1-10a; Suppe, 1985). Figure 1-10 shows schematically the development of the north-verging folds and faults. The Sulphur Mountain fault-propagation fold became locked (Figure 1-10a), and the Big Canyon fault tip propagated across the fold axis of the Big Canyon syncline as a backlimb thrust and cut across the north-dipping axial plane of the pre-existing Lion Mountain anticline (Figure 1-10b). The Sisar fault propagated across the anticlinal axis as a forelimb thrust (Figure 1-10b). Finally, the Lion fault moved along the Big Canyon fault surface at depth but ramped up to the surface along a new trace beneath the Big Canyon fault (Figures 1-5b-d, 1-11). These faults approach the San Cayetano fault obliquely (Figures 1-1, 1-2) and are folded by it near the surface (Figures 1-5c, 1-5d, 1-9, 1-10). They are interpreted to merge at depth to form a decollement, named the Sisar decollement by Yeats et al. (1988), in the ductile Rincon Formation (Figures 1-5a, 1-7a, 1-11). These faults do not cut the subjacent Vaqueros Formation, as documented by wells in the structurally higher west end of the study area (Figure 1-5a). The Lion fault set, the

Sulphur Mountain anticlinorium, and the Big Canyon syncline are interpreted to result from passive backthrusting from a blind thrust at depth (Figure 1-7a) based on seismic reflection data (Huftile, 1988b, 1989). This suggestion was made earlier for the Lion fault farther west in the Ojai Valley by Namson (1987) and Namson and Davis (1988).

Some folding continued during movement on the upper Sisar fault. The upper Sisar fault was folded and rotated out of the plane of maximum shear stress, and the planar lower Sisar fault cut through its footwall block forming the first horse in an antiformal stack (Figures 1-5b, 1-9). The lower Sisar fault has only about 120 m of stratigraphic separation, whereas the upper Sisar fault has a separation of 670 m (Figures 1-5b, 1-10). These faults truncate the South Sulphur Mountain fault, which appears to have formed as a pop-up structure with small reverse separation (Figures 1-5a, 1-5b, 1-5d). Schlueter (1976) shows the Sisar fault to be overturned near the surface as it obliquely approaches the San Cayetano fault. However, the Santa Fe Energy Arco 20 well (Figure 1-3) has upper Mohnian overlying Repettian benthic foraminifera near the surface; the well penetrated the hanging-wall block of the Sisar fault (Figure 1-5c) to the north of the mapped trace of Schlueter (1976), Dibblee (1982), and Rockwell (1983). The fault south of the well (Figure 1-5c) and parallel to Sisar Creek (Figure 1-2), that was shown by Schlueter (1976) and Rockwell (1983) to offset a terrace of Sisar Creek with the north side up, is not the surface trace of an overturned Sisar fault. The Sisar fault would have the

south side up. The fault is interpreted to be a backthrust along bedding in the Sisquoc Formation (Figure 1-5c), possibly due to the folding of the Sisar fault and its hanging-wall block by the overriding San Cayetano fault (Figures 1-5c, 1-5d).

The Big Canyon fault has normal separation with Pliocene Pico Member of the Fernando Formation in the hanging-wall block over Miocene Monterey Formation (Figure 1-2, 1-5b-d). However, movement on it is interpreted to be reverse; the normal separation is a consequence of the fact that, as a backlimb thrust, the fault cuts the north limb of the Big Canyon syncline and the axis of the pre-existing Lion Mountain anticline, bringing the core of the syncline over its flank (Figure 1-10). The Big Canyon fault generally dips south, but is near vertical where it is overridden by the San Cayetano fault (Figures 1-5c, 1-5d, 1-11). Wells shown on Figure 1-5c prove that the Big Canyon and Lion faults intersect at depth as was first suggested by Mitchell (1967, 1969). The Big Canyon fault zone defined in the subsurface by Fine (1954) is, in fact, bordered by the Lion and Big Canyon faults. The Big Canyon fault has about 3000 m of stratigraphic separation as shown on Figure 1-10b. This amount is required by bed-length balancing methods and seismic reflection data (Huftile, 1988b, 1989) which suggest the depth at which the Miocene strata in the footwall intersect the Lion fault set. Schlueter (1976) suggested that the Big Canyon fault was overlain by the Saugus Formation with clasts of dominantly Miocene rocks. More recent work by Dibblee (1987a) and Rockwell (1983) showed that this

overlying deposit is a late Pleistocene alluvial-fan rather than Saugus Formation, thus leaving the upper age limit on the fault less restricted.

The Lion fault is the youngest fault in the Lion fault set because it truncates all the other faults (Figure 1-2; Dibblee, 1987a). It is the only south-dipping fault that cuts the late Pleistocene Saugus Formation. The Lion fault has expression as a linear mountain front at the base of Sulphur Mountain. In map view, the Lion fault converges obliquely eastward toward the Big Canyon fault, and it is parallel to the Big Canyon fault where both faults are overridden by the San Cayetano fault (Figures 1-2, 1-5c, 1-5d, 1-11). Beneath the San Cayetano fault, the Lion fault is folded to a near-vertical dip (Figures 1-5c, 1-5d, 1-11). The Lion fault has 910 m of stratigraphic separation (Figure 1-5b); this is the amount necessary to restore the Mohnian Monterey Formation in the hanging-wall block of the Lion fault at the surface, down to where it is juxtaposed to equivalent strata on the south limb of the Lion Mountain anticline (Figure 1-5b).

The Richfield fault (Figure 1-2) is a connecting splay between the Big Canyon and Lion faults. The north limb of the syncline in the footwall block of the Sisar fault in Figure 1-5a can be traced eastward in the footwall block of the Big Canyon fault to where it is truncated by the Richfield fault (Figure 1-2). East of the Richfield fault, the fault zone between the Big Canyon and Lion faults is composed of Rincon and Monterey Formations (Huftile, 1988a). Farther east, another connecting splay between the Big Canyon and Lion faults

separates that block from a syncline with upper Mohnian Monterey Formation in its core (Figure 1-5c).

HORIZONTAL SHORTENING AND CONVERGENCE RATES

Yeats (1983) suggested that the large active reverse faults bordering the Ventura basin ramp upward from a horizontal decollement at the brittle-ductile transition. If so, the horizontal component of movement at the brittle-ductile transition should be equal to the sum of the fault-plane separation nearer the surface on the San Cayetano fault, the shortening taken up by folding related to movement on the San Cayetano fault, and the folding and faulting associated with blind thrusts beneath Upper Ojai Valley and Sulphur Mountain (Figure 1-7a). Huftile (1987) constructed a retrodeformable cross section including Figure 1-5b, presented here as an area-balanced cross section (Figure 1-7a). It is assumed that the pin lines were originally vertical and that the formation thicknesses in the Santa Clara syncline are fairly well known from surface and subsurface data. Seismic-reflection data (Huftile, 1988b, 1989), the wells in Figure 1-5a, and map relations (Figure 1-2; Dibblee, 1987a) all support a shallower decollement surface in the lower Miocene Rincon Formation. Namson (1987) and Namson and Davis (1988) also interpreted a decollement at the same horizon. The top of the Eocene-Oligocene competent section is a fairly well constrained horizon; the location of the fault tip, the flat beds beneath the Sisar decollement, and the dips on the Sisar decollement and the ramp are constrained by seismic reflection data (Huftile, 1988b, 1989). The brittle-ductile transition is based on the base of the zone of earthquakes. Bed-length times the thickness of the sedimentary rocks between the brittle-ductile

transition and the top of the Eocene-Oligocene strata should equal the area defined by the local pin lines, the brittle-ductile transition, and the top of the Eocene-Oligocene competent sequence (Figure 1-7b). Conversely, if the area and the bed-length are known, the thickness and thus, the depth to the brittle-ductile transition can be calculated (Figures 1-7b, 1-7c). The bed length of the top of the Oligocene is 38 km based on a brittle-ductile transition of 17 km, the approximate base of earthquakes. If the depth to the brittle-ductile transition is allowed to range between 15 and 19 km and the area for each level is measured, the bed length changes from 43 to 35 km (Table 1-2), indicating that the bed length is not very sensitive to the depth of the brittle-ductile transition.

The local pin lines at the top of the Oligocene are now 22.5 km apart, allowing for a total horizontal shortening of 15.5 km. If shortening began to occur immediately after the end of the Repettian, 2.8 m.y. ago (calculated from Lagoe and Thompson, 1988), then the average shortening rate is 5.5 mm/y. If shortening began later, the shortening rate would be higher.

Figures 1-5b and 1-7a indicate stratigraphic separation is 2.6 km on the San Cayetano fault. This separation increases eastward along the fault; at Figure 1-5c, it is 6.0 km combining both strands. Rockwell (1988) showed by ^{14}C dating and correlation of alluvial-fan materials that the displacement rate since the late Pleistocene is 1.05 ± 0.2 mm/y at Sisar Creek and 1.35 ± 0.4 mm/y at Bear Canyon (Figure 1-2). Assuming a constant displacement rate like that

at Bear Canyon, it would take only 1.9 Ma to accomplish the displacement shown on Figure 1-7a.

Table 1-2

Comparison between depth to the brittle-ductile transition and original bed length.

Depth to brittle-ductile transition (km)	Thickness (t) from top Vaqueros to brittle-ductile transition (km)	Area (A) (km^2)	Original bed-length (L=A/t) (km)
15	7	299	43
16	8	321	40
17	9	342	38
18	10	364	36
19	11	385	35

OIL ACCUMULATION

Oil is both sourced and produced from the Miocene Monterey Formation. Production is from Mohnian sandstone where present, and from fractured shale where sandstone is absent. Most of the production is from the lower Mohnian section (Figures 1-4, 1-5c).

In the Silverthread area, oil is produced from Mohnian sandstone and fractured shale of the Monterey Formation in the Lion Mountain anticline, which has been overthrust by both the Lion and San Cayetano faults (Figures 1-5c, 1-5d). The trapping mechanism for the south limb is the Lion fault. It is an inefficient trap because the fault is overlain by fractured Monterey Formation wedged between the Lion and Big Canyon faults (Figures 1-5c, 1-5d). Some of this oil has migrated to the surface where it occurs as oil seeps between the Lion and Big Canyon faults (Figure 1-2).

In the Bear Canyon and Sisar Creek areas, oil is produced from Mohnian sandstone and fractured shale in the north limb of the Lion Mountain anticline, below the unconformity at the base of the Saugus Formation (Figure 1-5b). In the Sisar Creek area, sands above the unconformity are also productive (Mitchell, 1968). The trapping mechanism, again inefficient, is provided by fine-grained strata within the Saugus Formation.

In the North Sulphur Mountain area, oil is produced from lower Mohnian fractured shale on the south limb of the Lion Mountain anticline where it is cut by the Big Canyon-Lion fault (Figure 1-5b). Here, the trapping

mechanism is the Lion fault, as in the Silverthread area, but it is an efficient trap because the fault is overlain by thick mudstone of the Repettian Pico Member of the Fernando Formation (Figure 1-5b).

In the Sulphur Crest area, oil is produced from lower Mohnian fractured shale that has been overthrust by the upper and lower Sisar fault. The trapping mechanism is efficient and is provided by the upper Sisar fault that juxtaposes the mudstones of the Rincon Formation over the producing zone (Figure 1-5b).

In the Sulphur Mountain area, oil was produced from Relizian sandy shales and lower Mohnian fractured shale of the Monterey Formation in the south limb of the syncline overthrust by the Sisar fault (Figure 1-5a). The Rincon Formation in part overlies the producing zone and provides a seal.

It is enigmatic why the Monterey Formation has not produced oil in the north limb of the Reeves syncline. Several wells have penetrated the formation there, but no new oil field areas have been discovered (Figures 1-5b, 1-5c). This suggests that oil migrated into the Lion Mountain anticline as the north limb of the anticline formed as a fault-propagation fold in Figure 1-7a, while much of the folding of the north limb of the Reeves syncline results from later movement on the San Cayetano fault. Consequently, while the fold limb shared by the Lion Mountain anticline and the Reeves syncline is productive, the north limb of the Reeves syncline is not because it would have then been down dip. Oil produced from fractured shales in the Sulphur Crest area could not migrate until the formation became fractured. Thus, it is speculated that

oil has remained essentially where it matured, and was trapped by the Sisar fault as the Sulphur Mountain anticlinorium was formed.

CONCLUSIONS

Deformation in the Upper Ojai Valley began with the folding of sedimentary strata as young as late Pliocene (Venturian Stage). The Lion Mountain anticline is associated with a fault-propagation fold beneath the Upper Ojai Valley. Mohnian and Delmontian reworked fossils in Repettian deep-water sandstone in the footwall block of the Sisar fault are probably the result of uplift north of the San Cayetano fault.

The Sulphur Mountain anticlinorium developed as a fault-propagation fold beginning in the middle Pleistocene. The folding was a result of back-thrusting from the fault tip of a blind thrust (Figure 1-7a). The fold became locked, and the Big Canyon fault propagated as a backlimb thrust (Figure 1-10a). Though the Big Canyon fault has normal separation near the surface, it is a reverse fault that brought the core of the Big Canyon syncline over its flank. The Sisar fault then propagated as a forelimb thrust. Some folding of the Sulphur Mountain anticlinorium continued during movement on the upper Sisar fault. Eventually, the Sisar fault was rotated out of the plane of maximum stress, and a more planar lower Sisar fault cut through the footwall block of the upper fault, producing an antiformal stack. The South Sulphur Mountain fault is a reverse fault with small offset, forming a pop-up structure at Sulphur Mountain. The Lion fault was the last south-dipping fault to move, cutting the late Pleistocene Saugus Formation. The Big Canyon, Sisar, and

Lion faults (Lion fault set) merge at depth to form the Sisar decollement in the ductile Rincon Formation.

A total horizontal shortening of 15.5 km has occurred in the Upper Ojai Valley-Sulphur Mountain area, calculated by area-balancing the cross section in Figure 1-5b (Figure 1-7a). If shortening has occurred since the end of Repettian time, 2.8 m.y. ago, then the average rate is 5.5 mm/y.

DISCUSSION

To the east of the Upper Ojai Valley, the San Cayetano fault accounts for all the south-vergent horizontal shortening (see Figure 1-11 of Yeats, 1983; 1981b). To the west, in the Ojai Valley, south-vergent horizontal shortening is taken up on a blind thrust with the Lion fault forming a passive backthrust (Namson, 1987; Namson and Davis, 1988; Huftile, 1988a; Yeats and Huftile, 1989). The area of the Upper Ojai Valley is a transition between the two forms, with shortening occurring on both the surface reverse fault and the blind thrust. The Lion fault set forms the passive backthrust. The level of the basal decollement, the brittle-ductile transition, is estimated to be about 17 km by area-balancing methods (Figure 1-7) and the recorrelation of seismic reflection data (Huftile, 1989). West of Ojai Valley, the eastern Red Mountain fault is a tear fault. The central and western Red Mountain fault is another south-verging surface reverse fault with focal mechanism solutions to 12 km depth (Yeats et al., 1987), which accounts for all the south-vergent shortening (Huftile, 1988a).

Chapter 2:

Cenozoic Structure of the Piru 7½-minute Quadrangle, California

by

Gary J. Huftile and Robert S. Yeats
Department of Geosciences
Oregon State University
Corvallis, OR 97331-5506

ABSTRACT

The Piru 7½-minute quadrangle in the central Ventura basin contains a thick accumulation of Plio-Pleistocene sedimentary rocks bordered by opposing reverse faults, on the north by the north-dipping San Cayetano fault and on the south by the south-dipping Oak Ridge fault. Deformation in the Piru quadrangle can be separated into three phases: (1) pre-Vaqueros (late Oligocene-early Miocene) tilting in the hanging-wall block of the Oak Ridge fault that is coincident with normal faulting farther south at Big Mountain, (2) pre-Pleistocene reverse faulting of the Torrey fault, and (3) Quaternary deformation. Strands of the San Cayetano and Oak Ridge faults offset late Quaternary surfaces. East of Sespe Creek, the San Cayetano fault has a lobate surface trace, and the dip of the fault shallows to as much as 27°N. Farther east, the fault bifurcates into two strands; the northern, Main strand trends northeast, cuts an alluvial fan 2½ km ENE of Piru, and dies out; the southern, Piru strand trends east and dies out near the eastern boundary of the quadrangle. The Oak Ridge fault has variable, low dips in its upper 2.5 km to

the west and is more steeply dipping to the east where it bifurcates into three strands and dies out south of the eastern terminus of the San Cayetano fault. Near the eastern termini of the San Cayetano and Oak Ridge faults, displacement is taken up on east-trending folds and south-dipping reverse faults of the East Ventura fold belt.

INTRODUCTION

The Piru quadrangle is located in the central Ventura basin, part of the western Transverse Ranges of southern California. The Ventura basin contains the world's thickest sequence of Pleistocene age strata (Yeats, 1977), found in the subsurface in the Santa Clara Valley in the southwestern corner of the quadrangle (Figure 2-1, Plate I). This sequence occurs in the Santa Clara syncline which is bounded on the north by the San Cayetano reverse fault and on the south by the Oak Ridge reverse fault (Figure 2-1). The surface traces of these two reverse faults are only about 1 km apart in the southwestern part of the quadrangle, but at depth, the area between the faults is more than 10 km wide.

On the south side of the Santa Clara Valley, the hanging-wall block of the Oak Ridge fault contains strata as old as Oligocene at the surface. Farther east, the Oak Ridge fault divides into three strands (Figure 2-1, Plate I), and only the northern strand at the edge of the Santa Clara Valley appears to be active. In the subsurface of the hanging-wall block of the Oak Ridge fault, wells penetrate strata as old as Paleocene (Seedorf, 1983). On the north side of the Santa Clara Valley, the Modelo lobe (Figure 2-1) of the San Cayetano fault consists of a fold belt of Miocene strata with fold axes parallel to the southward-convex surface trace of the fault. One well reaches Oligocene strata, and Oligocene and Eocene strata are exposed west and north of the quadrangle.

Figure 2-1: Index map showing the major structural features of the Ventura basin and surrounding areas, and the location of the Piru quadrangle. BC-Balcom Canyon, BM-Big Mountain, DVF-Del Valle fault, EVFB-East Ventura fold belt, LSC-Little Sespe Creek, MC-Modelo Canyon, PC-Piru Creek, S-Saticoy, SC-Sespe Creek, SP-Santa Paula, WC-Wiley Canyon.

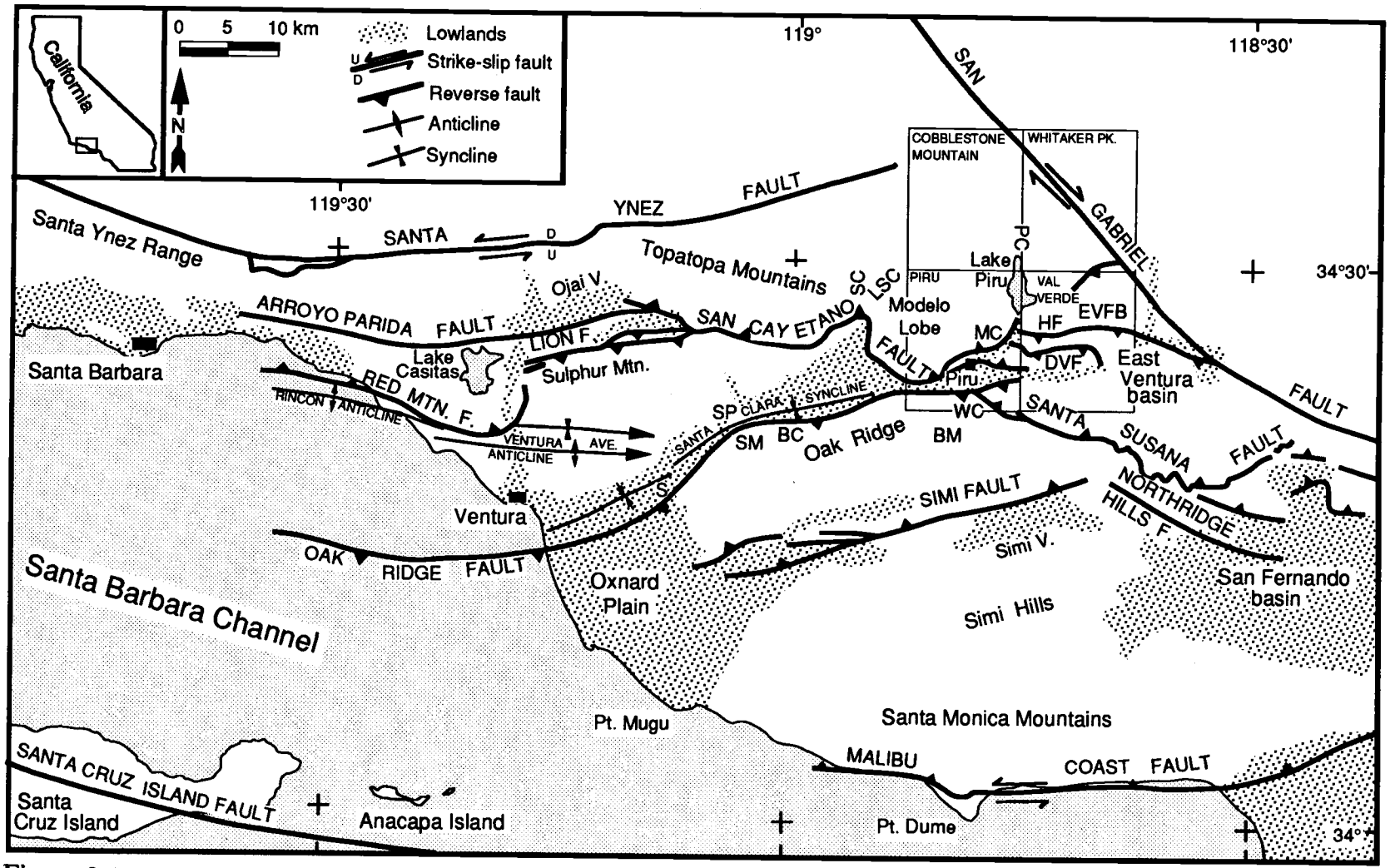
California
0 5 10 km
N
Lowlands
Strike-slip fault
Reverse fault
Anticline
Syncline
119°30'
119°
118°30'
34°30'
34°
Santa Ynez Range
SANTA YNEZ FAULT
Topatopa Mountains
Ojai V.
ARROYO PARIDA FAULT
LION F.
Sulphur Mtn.
Lake Casitas
Santa Barbara
RED MTN. F.
RINCON ANTICLINE
VENTURA AVE. ANTICLINE
SAN CAY ETANO FAULT
SC
LSC
Modelo Lobe
COBBLESTONE MOUNTAIN
WHITAKER PK.
PC
PIRU
Lake Piru
VAL VERDE
HF
EVFB
MC
DVF
East Ventura basin
Piru
WC
BM
SP CLARA SYNCLINE
SANTA
SM
BC
Oak Ridge
SAN GABRIEL FAULT
SANTA SUSANA FAULT
NORTHRIDGE HILLS F.
SIMI FAULT
Simi V.
Simi Hills
San Fernando basin
Ventura
OAK RIDGE FAULT
Oxnard Plain
Santa Barbara Channel
Pt. Mugu
Santa Monica Mountains
MALIBU COAST FAULT
Pt. Dume
SANTA CRUZ ISLAND FAULT
Santa Cruz Island
Anacapa Island

Figure 2-1

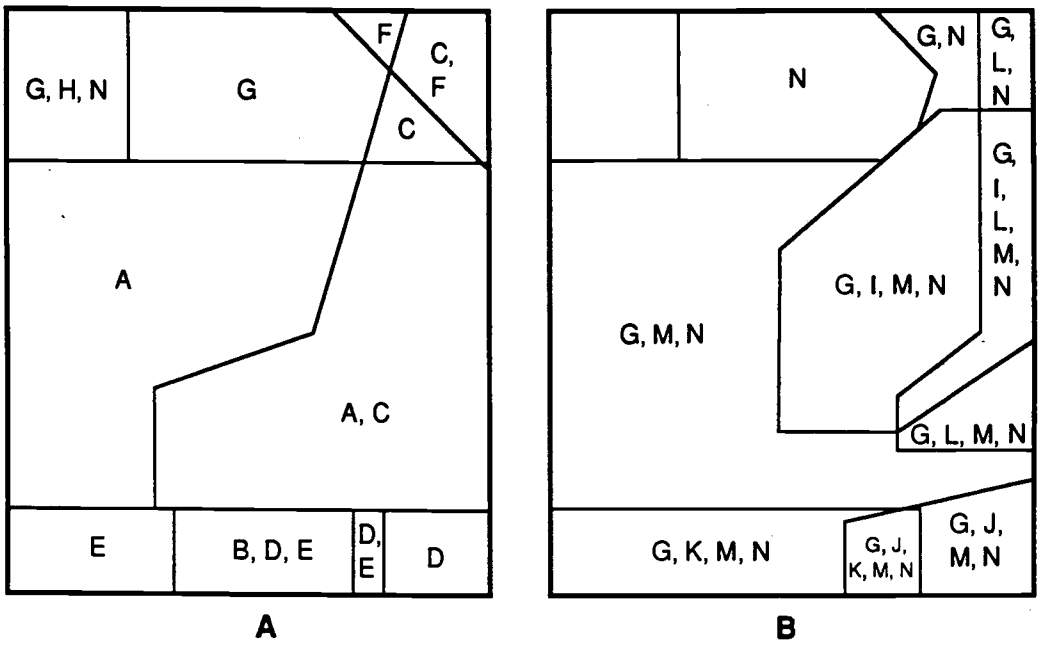

Figure 2-2: Sources used in map compilation. **(A)** Sources used extensively in compilation: A-Çemen (1977); B-Huftile (1988a, b); C-Huftile (1988, unpublished map); D-Ricketts and Whaley (1975); E-Rieser (1976); F-Crowell (1953, unpublished map); G-Argo Petroleum (1982); H-Bailey (1951, unpublished map); Morton (1972, entire quadrangle). **(B)** Sources consulted but not used extensively in compilation: I-Cordova (1956); J-Bain (1954); K-Jestes (1957); L-Robinson (1956); M-California Division of Mines and Geology (1972); Welsh (1972, unpublished map, entire quadrangle).

In the eastern part of the quadrangle, the San Cayetano fault bifurcates into the Main strand along the lower part of Piru Creek andthe Piru strand at the northern edge of the Santa Clara Valley (Figure 2-1, Plates I, V). Both strands cut late Quaternary deposits. Both the San Cayetano and Oak Ridge faults lose separation eastward as they bifurcate. The Main strand of the San Cayetano fault dies out in Piru Creek, and the other strands of both faults die out near the eastern boundary of the quadrangle. The folds of the Modelo lobe continue eastward across Piru Creek and form part of the East Ventura fold belt (Figure 2-1). The western ends of the south-dipping Holser and Del Valle faults can be traced to Piru Creek, but cannot be found west of the creek. These faults increase separation eastward.

The geologic map (Plate I) was compiled (Figure 2-2) from Çemen (1977), Ricketts and Whaley (1975), Rieser (1976), Morton (1972), Argo Petroleum (1982), Dibblee (1991), and from unpublished maps by T. L. Bailey (1951) and J. C. Crowell (1953). Other maps consulted but not extensively used in the compilation include California Division of Mines and Geology (1972), an unpublished map by G. J. Welsh (1972), and University of California at Los Angeles masters theses by Bain (1954), Cordova (1956), Robinson (1956), and Jestes (1957). Dibblee (1991) published a geologic map of the Piru quadrangle, but did not consider the subsurface. Because of our interpretation of the subsurface, we disagree with several areas of Dibblee's surface map, particularly the trends of the Oak Ridge fault and the Buckhorn anticline.

The present study began with surface and subsurface mapping by Ricketts and Whaley (1975) of the Oak Ridge fault set east of Wiley Canyon (Plate I), Rieser (1976) of the Oak Ridge fault west of Wiley Canyon, and Çemen (1977) of the Modelo lobe of the San Cayetano fault.
Further work was done by Stitt and Yeats (1983) north of the Santa Clara Valley and by Huftile in the Piru Creek area and south of the Oak Ridge fault in the Wiley Canyon and Torrey Canyon area. Open-file maps, including subsurface cross sections, of the Val Verde and Whitaker Peak quadrangles east of the Piru quadrangle were published by Yeats et al. (1985); the present report follows the same format.

Data were collected from wells drilled by the petroleum industry (Plate III). Well data, provided by the California Division of Oil and Gas and by various petroleum companies, include electric logs, core descriptions, mud logs, dipmeter logs, directional surveys, and paleontological reports. Paleontologic data were used without reexamining the fossils ourselves or reevaluating the biostratigraphic correlations. Critical areas had to be remapped entirely (Huftile 1988a, b; and previously unpublished mapping along Piru Creek and Piru Lake; Figure 2-2), while others required only minor revisions. We concentrated on Quaternary structural relations. Cross sections were compiled from Çemen (1977), Ricketts and Whaley (1975), Rieser (1976), Huftile (1988 a, b), and L. T. Stitt (unpublished cross sections) drawn with electric logs at

larger scales, reduced to 1:24,000 (map scale) and redrafted without electric logs on Plate IV.

This paper is part of a larger effort to calculate crustal convergence rates across the Ventura basin through the balancing and retrodeforming of cross sections. Balancing cross sections requires detailed knowledge of the geology and the timing of structures. Thus, we have found it necessary to do detailed studies of areas in preparation for drawing a balanced cross section. This is one of those studies, as is Huftile (1991) and Yeats et al. (in prep.).

STRATIGRAPHY

Basement rocks are not observed in the Piru quadrangle. To the northeast, in the Whitaker Peak quadrangle (Figure 2-1), basement is composed of Precambrian gneiss and Mesozoic granodiorite (Yeats et al., 1985). There, basement is overlain by unnamed Eocene strata (Squires, 1981) that are not observed in the subsurface of Piru quadrangle. South of the Oak Ridge fault, the Eocene Llajas Formation and underlying Paleocene or Cretaceous strata are penetrated by wells just south of the quadrangle boundary (Ricketts and Whaley, 1975; Seedorf, 1983; Yeats, 1988b). The late Eocene to early Miocene nonmarine Sespe Formation and the lower Miocene shallow marine Vaqueros Formation form the top of a sandstone-rich, competent sequence. The early Miocene Rincon Formation is composed of deep-water mudstone and siltstone that are less competent than the underlying strata. The Rincon Formation is not found south of the Oak Ridge fault. The middle Miocene to lower Pliocene Modelo and Towsley Formations constitute part of a submarine fan system deposited in deep water, becoming shallower water upsection (Winterer and Durham, 1962). The Pliocene Fernando Formation was deposited as turbidites transported down the axis of the Santa Clara syncline. Water depths continued to shallow upsection through deposition of the Pleistocene Saugus Formation, which is nonmarine in its upper part.

Llajas Formation (Tll). The Eocene Llajas Formation in the subsurface is interbedded gray, fine- to medium-grained, silty sandstone and dark gray silty sandstone. The Texaco Shiells 165 well (Plate III, Plate IV, A-A') penetrated 721 m of Llajas (Rieser, 1976) and the Union Torrey 92 well penetrated 548 m. Mallory (1959) and Schmidt (1970) placed the formation in the Penutian and Ulatisian (middle Eocene) Stages. Canter (1974) listed benthic Foraminifera of the Ulatisian Stage from Big Mountain to the south (Figure 2-1). At its type locality in the Simi Hills, Squires (1981) noted foraminifera of the late Eocene Narizian Stage near the top of the formation.

Sespe Formation (Tsp). The Sespe Formation is composed of nonmarine sandstone, siltstone and conglomerate. Generally, red sandstone and conglomerate characteristic of the type section at Sespe Creek (Figure 2-1) west of the quadrangle are absent on Oak Ridge, and the maroon and green silty claystone and greenish gray sandstone characteristic of the Oak Ridge section is not found at the type locality. Correlation of vertebrate fossils to benthic foraminiferal stages yielded ages of late Eocene (Uintan Stage) to early Miocene (Arikareean Stage; Stock, 1932; Wilson, 1949; Savage et al., 1954; Durham et al., 1954; Mason and Swisher, 1988). Berggren and Van Couvering (1973) suggested that the Sespe Formation is Refugian and Zemorrian. More recently, Lander (1983) used vertebrate fauna to infer a range of middle Eocene to late Oligocene for the Sespe.

The Sespe Formation crops out in the cores of anticlines in the hanging-wall block of the Oak Ridge fault in the southwestern part of the quadrangle. The Sespe Formation is composed of variegated fine- to very-coarse-grained silty sandstone that is in places massive, interbedded with maroon to dark green sandy claystone, red to white to green siltstone and claystone, and red to gray, thin-bedded, sandy siltstone (Ricketts and Whaley, 1975).

Thicknesses south of the Oak Ridge fault are 1860 m in the southwest corner of the quadrangle (Rieser, 1976), 1830 m in the Oxy Davis-USL 83X-1 well just south of cross section B-B' (Plates III and IV), and greater than 2100 m in the Texas Hunter 1 well just south of cross section D-D'.

North of the San Cayetano fault, the Sespe Formation is not exposed in the Piru quadrangle. To the west, at the type section along the lower Sespe Creek (Figure 2-1), Eschner (1957) reported 853 m of exposed section. Wells in the Sespe field produce from the Sespe Formation. Downplunge, the Union Moran 1 well (Plates III and IV, A-A') is the easternmost well in the Piru quadrangle to reach the Sespe Formation, north of the San Cayetano fault; it penetrated 15 m of maroon, massive, hard, fine- to medium-grained sandstone interbedded with maroon to red sandy shale and greenish-gray, thin-bedded, sandy siltstone.

To the northeast, in the Whitaker Peak quadrangle, Bohannon (1976) reported 700 m of the Sespe Formation at Canton Canyon. Yeats et al. (1985)

divided the formation into two members, a basal conglomerate and breccia member overlain by a red-brown sandstone and red mudstone member.

North of the Piru quadrangle, in the Cobblestone Mountain quadrangle, J. C. Crowell (1953, unpublished mapping) shows approximately 150 m of the sandstone member.

Vaqueros Formation (Tv). The Vaqueros Formation is composed of transgressive marine sandstone and siltstone deposited in shallow water (Edwards, 1971; Jestes, 1957). Its age was considered by Edwards (1971) to be Zemorrian. Canter (1974) found evidence for the formation at Big Mountain, to the south (Figure 2-1), to be, in part, Saucesian; Blake (1983) determined that only the lowermost part of the formation is latest Zemorrian to early Saucesian and that the overlying strata are early Saucesian neritic equivalents to the overlying, bathyal Rincon Formation.

The Vaqueros is exposed south of the Oak Ridge fault and west of Torrey Canyon (Plate I). It was shown by Jestes (1957) to be 472 m thick at Wiley Canyon, and by Ricketts and Whaley (1975) to be 305-396 m thick in Torrey Canyon. The formation thins to the east because of pre-middle Miocene erosion. It is composed of gray to brown, fine-grained, massive to thin-bedded sandstone interbedded with tan to light gray sandy siltstone (Ricketts and Whaley, 1975). It is distinguished from the underlying Sespe Formation by the presence of megafossils. Hall et al. (1967) and Canter (1974)

show that the contact with the underlying Sespe Formation is unconformable at Big Mountain (Figure 2-1) as does Huftile (1988a, b) at Wiley Canyon.

North of the San Cayetano fault, the Vaqueros Formation is exposed just west of the northwest corner of the Piru quadrangle (Dibblee, 1990; Eschner, 1957; Edwards, 1971; Çemen, 1977, 1989; Argo Petroleum, 1982) and to the northeast of the quadrangle (J. C. Crowell, 1953, unpublished mapping; Yeats et al., 1985). Edwards measured 165 m of Vaqueros along Little Sespe Creek (Figure 2-1). North and northeast of the Piru quadrangle, Crowell (1953, unpublished mapping) mapped a 110 m thick section and Edwards (1971) measured an 80 m section along Piru Creek, The Union Moran 1 well (Plate III) penetrated 83 m of greenish gray, massive, medium- to fine-grained sandstone.

Rincon Formation (Tr). The Rincon Formation is not found south of the Oak Ridge fault and Miocene strata are not penetrated in the footwall block of the Oak Ridge fault. The Rincon Formation is exposed in the northwest corner of the Piru quadrangle along Tar Creek (Plate I). The Union Moran 1 well penetrated 732 m (Plate I, A-A', Plate III) of massive, gray to black, hard, dense, brittle siltstone and mudstone. Eschner (1957) measured 275 m of bluish-black mudstone and shale to the west, along Little Sespe Creek (Figure 2-1). To the north of the Piru quadrangle, along Piru Creek, Edwards (1971) found 280 m of section that was predominantly mudstone. Eschner (1957) determined its age to be late Zemorrian to Saucesian (early Miocene).

Modelo Formation (Tm). The type section, first described by Eldridge and Arnold (1907), is in Modelo Canyon, west of Piru Creek. Kew (1924) identified five members, the upper shale, upper sandstone, middle shale, lower sandstone, and lower shale although he included the Rincon Formation and part of the Vaqueros Formation in his lower shale member and the Towsley Formation in his upper member. The Modelo Formation ranges in age from Relizian through Mohnian (middle and upper Miocene). The formation was deposited by turbidity currents at bathyal water depth (Natland and Kuenen, 1951; Berger, 1977).

The Modelo Formation is exposed between the north and south strands of the Oak Ridge fault (Plate I). There the Modelo ranges in age from Luisian to Mohnian (Ricketts and Whaley, 1975), and it unconformably overlies the Vaqueros Formation. Ricketts and Whaley (1975) divided the formation south of the Oak Ridge fault into three members: (1) the basal member is Luisian and is composed of gray to grayish tan to brown, predominantly fine- to very fine-grained, soft, friable sandstone interbedded with gray to tan to brown, fossiliferous, sandy siltstone and shale (Tmss) overlain by light brown to gray to black, fossiliferous, silty shale interbedded with grayish tan to brown, fossiliferous, sandy siltstone (Tmsh); (2) the middle member (Tmd) is lower Mohnian in age and is composed of white to light brown, siliceous shale, dark brown diatomaceous shale, and tan to gray, impure chert; and (3) the upper member (Tms) is upper Mohnian in age and is composed of interbedded light

brown siliceous siltstone, dark brown diatomaceous siltstone, and light reddish brown chert. Cross sections A-A', B-B', and C-C' (Plate IV) show a sliver of Modelo Formation wedged into the fault zone of the Oak Ridge fault.

North of the San Cayetano fault, Kew (1924) defined five members of the Modelo Formation, all of which are exposed in the Modelo lobe area (Figure 2-1). The lower shale member (Tm1) is penetrated by the Getty Temescal 14, McCulloch Hopper Canyon 1, McCulloch Hopper Canyon 1A, and Pacific Western Crocker Fee 1-D wells (Plate III, Plate IV, E-E', F-F', A-A, and D-D'). It is Relizian to Luisian in age (Çemen, 1977) and is composed of dark gray to brown to black, massive, hard, fractured shale interbedded with light gray, medium- to coarse-grained sandstone. The Union Moran 1 well penetrated 794 m of the lower shale member. In the northwest corner of the quadrangle, the contact between the Rincon Formation and the overlying lower shale member of the Modelo Formation is convex to the east; the overlying contact between the lower shale and lower sandstone members of the Modelo is highly deformed (Plate I), implying that the décollement beneath the Modelo lobe is in the lower shale member of the Modelo Formation.

The overlying lower sandstone member (Tm2) is penetrated by several wells (Plate IV, A-A', D-D', E-E, and F-F') and it is Luisian in age (Çemen, 1977). It is composed of white-gray to dark brown, fine- to medium-grained sandstone interbedded with dark brown, massive siltstone and claystone. Its

thickness ranges from 550 m to 1005 m; it is about 700 m thick in the McCulloch IDS 1-16 and Getty Temescal 14 wells.

The middle shale member (Tm3) is lower Mohnian in age (Eschner, 1957; Çemen, 1977). In the subsurface, it ranges from 152 m to 640 m thick (Plate IV). The middle shale is composed of dark brown, hard, cherty, porcelaneous and calcareous shale.

The upper sandstone member (Tm4) ranges in thickness between 275 m at the surface north of Piru and 825 m at the surface near the Temescal anticline (Cordova, 1956); in the subsurface, McCulloch IDS 1-16 penetrated a complete section, 640 m thick. It is composed of white to gray. thick- to thin-bedded, fine- to coarse-grained arkosic sandstone interbedded with subordinate amounts of siliceous and silty clay shale (Çemen, 1977). Truex (1977) correlated this member with the lower Mohnian.

The upper shale member (Tm5) was determined by Kleinpell (1938) to be upper Mohnian to lower Delmontian at outcrops in Modelo Canyon. At the surface, the upper shale member is 200 m thick in the Santa Felicia syncline to 488 m thick east of Piru Creek. Dibblee (1991) maps this member as the Sisquoc Formation, which is Delmontian to the west. However, Mohnian benthic forams are found throughout this member and in the overlying Towsley Formation in the Arco Black Ranch 7-15 and Arco Hamilton Brothers Black Ranch 12-84 wells to the east in the Val Verde quadrangle (Yeats et al., 1985).

We believe that sufficient reason exists to continue calling this section the upper shale member of the Modelo Formation.

Towsley Formation (Tt). Coarse-grained sandstone deposited in deep water by turbidity currents and overlying the Modelo was named by Winterer and Durham (1951) the Towsley Formation. Winterer and Durham (1962) reported a late Miocene to early Pliocene fauna. The lower part of the Towsley contains Mohnian Foraminifera and the upper part is Delmontian; Rotalia miocenica, one of the key foraminifera used in establishing the Delmontian Stage at Oak Ridge, was found in the Oceanic Marr-Sloan 1 well (Ricketts and Whaley, 1975), in the southwest corner of the Val Verde quadrangle (Figure 2-1).

South of the Santa Clara River, the Towsley Formation is exposed between the middle and north strands of the Oak Ridge fault. There, Ricketts and Whaley (1975) divided the formation into two members based on lithology: The lower member (Tts) is composed of tan, coarse-grained, poorly sorted, massive sandstone interbedded with chocolate brown, foraminiferal siltstone; the upper member (Ttu) is composed of tan, sandy siltstone interbedded with chocolate brown siltstone and red to white, iron-stained, coarse-grained, pebbly, indurated sandstone lenses (Ricketts and Whaley, 1975). Thickness ranges from 1097 m to 1433 m (Plate IV, E-E', F-F').

Two wells penetrate the upper part of the Towsley in the footwall block of the Oak Ridge fault (Plate IV, E-E'). The Shell Sloan 1 well penetrated 282

m of gray to black, hard, massive siltstone interbedded with light brown, fine- to medium-grained sandstone and light gray to gray-brown conglomerate overlain by a conglomerate bed, 78 m thick.

North of the San Cayetano fault, the Towsley was divided into four members by Çemen (1977). The basal conglomerate member is called the Hasley conglomerate (Tthc) by the oil industry. It is composed of reddish-brown, fine-to coarse-grained, pebble- to boulder-conglomerate with clasts of igneous rock. The lower siltstone member (Tts) is composed of light brown to dark greenish brown, thin-bedded siltstone. The upper conglomerate member (Ttc) is composed of white to light gray to reddish brown, thin- to thick-bedded conglomerate interbedded with fine-grained, pebbly sandstone and siltstone. The upper siltstone member (Tts) is composed of siltstone interbedded with white sandstone. Thickness of the Towsley Formation ranges from 378 m just north of the Holser fault to 747 m south of the Holser fault.

Fernando Formation. Fernando Formation is used for middle Pliocene to lower Pleistocene deep-water clastic sedimentary rocks deposited from the east by turbidity currents (Hsü, 1977; Hsü et al., 1980). The strata were described by Eldridge and Arnold (1907) and named by Kew (1924) the Fernando Group which included the Repetto, Pico, Santa Barbara, and Saugus Formations. Bain (1954), Cordova (1956), Robinson (1956), Eschner (1957), Jestes (1957), Crowell et al. (1966), Yeats et al. (1985) include the Pliocene rocks in the Pico Formation. Jennings and Strand (1969) reduced the

Fernando Group to formation status with the Repetto, Pico, and Santa Barbara Members overlain by the Saugus Formation; this terminology was used by Ricketts and Whaley (1975), Rieser (1976), Rockwell (1988), Yeats (1988a, b), and Huftile (1991), and is repeated here. The Santa Barbara Member is equivalent to the Mudpit Shale of Nagle and Parker (1971); although it is not observed in the Piru quadrangle.

The Repetto member (Tfr) corresponds to the Repettian Stage of Natland and Rothwell (1954). It is exposed in the eastern part of the Piru quadrangle on both sides of the Santa Clara syncline, in the hanging-wall blocks of the Piru strand of the San Cayetano fault and of the Camulos fault-north strand of the Oak Ridge fault. It is composed of green to tan siltstone interbedded with tan, lenticular sandstone and conglomerate (Ricketts and Whaley, 1975; Çemen, 1977). It is about 734 m thick, determined from surface outcrops and well data, about 2.5 km east of Piru quadrangle (Çemen, 1977); along cross sections E-E' and F-F' (Plate IV), the thickness is about 730 m.

The Pico Member (QTf) contains microfossils referred to the Venturian and lower Wheelerian Stages of Natland and Rothwell (1954). Blackie and Yeats (1976) showed that the Olduvai normal event, near the Plio-Pleistocene boundary at 1.6-1.8 Ma, is within the Pico member at Saticoy oil field, about 10 miles west of the Piru quadrangle, however, the member's boundary is time-transgressive. Thus, the Pico member is Plio-Pleistocene. Winterer and Durham (1962) reported a trend from deep-water faunas near the base of the

Pico to shallow-water faunas near the top. Pico strata crop out in the footwall block of the Oak Ridge fault and between the Main and Piru strands of the San Cayetano fault (Plate I). The Pico is composed of interbedded tan to buff to brown, phosphatic, fine- to medium-grained sandstone, silty sandstone, and olive-green to tan to brown, thin-bedded, friable, glauconitic, sandy siltstone and siltstone. Lenses of brown to tan, medium- to coarse-grained sandstone and brown to white cobble-conglomerate are common. The conglomerate beds contain clasts of crystalline rocks derived from the San Gabriel Mountains to the east (Jestes, 1957; Hsü, 1977; Hsü et al., 1980). The Texaco Lawton 1 well (Plate III, Plate IV, A-A') penetrates 1630 m of Pico without reaching the Repetto Member. Farther east, cross sections E-E' and F-F' (Plate IV) constrain the Pico Member to be 1890 m thick.

Saugus Formation (Qs). The Saugus Formation probably overlies the Pico member of the Fernando Formation conformably in the western part of the Piru quadrangle (Plate IV, A-A' through D-D'). Just east of the Piru quadrangle, in the Val Verde quadrangle, Yeats et al. (1985) show that the contact at the base of the Saugus is an angular unconformity; and east of there, the Saugus pinches out. The Saugus Formation is informally divided into two members, a basal marine member (Qsm) and a nonmarine member (Qsnm) equivalent to the Sunshine Ranch member of Winterer and Durham (1962). Based on a magnetostratigraphic section in the East Ventura basin, east of the Piru quadrangle, Levi et al. (1986) estimate the base of the Saugus Formation

to be younger than 2.5 Ma and the top of the Saugus to be ~0.4 Ma. To the west, near Ventura, the Saugus Formation has been dated by tephrachronology and amino-acid stereochemistry as between 0.63 and 0.4-0.2 Ma (Lajoie et al., 1982; Sarna-Wojcicki et al., 1984; K. R. Lajoie, written communication to R. S. Yeats, 1988). The base of the Saugus Formation in cross sections A-A' and B-B' (Plate IV) corresponds to foraminiferal horizon 5, shown by Yeats (1981) to be ~1 Ma.

The lower marine member is composed of greenish gray-white to gray, fine- to medium-grained, locally conglomeratic and silty sandstone, greenish gray, soft siltstone and sandy siltstone, and gray and white, coarse-grained conglomerate (Çemen, 1977). In the subsurface of the Santa Clara Valley, the marine member varies in thickness between 427 m in the east and 960 m in the west.

The overlying nonmarine member is composed of light to dark gray, medium- to very fine-grained, firm, massive sandstone and silty sandstone, brown to light gray, friable, fine- to coarse-grained pebble- and cobble-conglomerate. In the subsurface, it ranges from 2926 m thick in the west at A-A' (Plate IV), to 1950 m thick at D-D'; farther east the section is faulted and incomplete.

Alluvial fan material (Qaf). Poorly consolidated to unconsolidated sand and gravel with soil developed at the surface. The fan at the mouth of Modelo Canyon contains abundant platy chips of Modelo Formation.

Terrace material (Qt). Reddish brown, poorly bedded, poorly consolidated gravel, sand, and silt. Terrace surfaces are preserved above present drainage, and terrace deposits rest with angular unconformity on underlying formations.

Landslide material (Qls). Landslides are common throughout the quadrangle with fine-grained Modelo Formation especially susceptible to sliding.

Modern alluvium (Qal). Unconsolidated gravel, sand, and silt with poorly developed soils.

STRUCTURE

The late Quaternary structure of the Piru quadrangle includes the east ends of the Oak Ridge and San Cayetano faults and the west end of the East Ventura fold belt with its south-dipping faults that extend down into bedding. Discussion of structures is divided into five groups: (1) the San Cayetano fault strands and folding of the Modelo lobe, (2) the Oak Ridge fault strands and related folds in its hanging-wall block, (3) the east Ventura fold belt, (4) the Santa Clara syncline, and (5) older faults.

San Cayetano fault and Modelo lobe. The Piru quadrangle covers the eastern half of the Modelo lobe and the eastern end of the San Cayetano fault (Figure 2-1). Near Hopper Canyon (Plate I), the fault bifurcates into two strands. In the lobate part of the fault, the dip on the fault is 22-34°N at the western edge of the Piru quadrangle; the Main strand dips 40°N just east of the intersection between the Main and Piru strands and as much as 66°NW at its eastern end; the Piru strand has a low dip at its western end and steepens to 54°N at its eastern terminus (Plate V). Çemen (1977, 1989) estimated 5.2-7.3 km of stratigraphic separation at Hopper Canyon, and 4.6-5.3 km at Edwards Canyon (Plate I).

Both strands of the San Cayetano fault have evidence of late Quaternary displacement. On the north, the Main strand of Çemen (1977) trends roughly east-northeast and turns more northerly on the west side of Piru Canyon where it dies out. Across Piru Canyon, older strata exposed on the west are

juxtaposed against younger strata on the east, suggesting a component of left-lateral movement on the eastern end of the fault strand. North of the Holser syncline, there is no apparent offset of formation contacts, suggesting the fault strand dies out near the Holser syncline. The fan at the mouth of Modelo Canyon (Plate I) seems to be cut by the Main strand. Aerial photographs show that drainages are more incised west of the fault than they are east of the fault, suggesting uplift west of the Main strand. Offset of the drainages increases to the south where dip-slip offset should be greater. Some drainages seem to be offset left-laterally, implying oblique offset for this part of the fault as would be expected for a reverse fault that turns in the direction of stress as shown by Mount and Suppe (1987) and dies out.

The southern, Piru strand of Çemen (1977) extends to the east through Piru and north of Camulos (Plate I). The surface trace can be followed by a warp in alluvium that extends through the town of Piru. The easternmost well that penetrates the strand is the Gulf Rubel 1 well (Plate III).

The Modelo lobe extends between Sespe Creek (Figure 2-1) and Piru Creek (Plate I) and is almost entirely overlain by the Modelo Formation at the surface. Miocene and older rocks are tightly folded providing closure for oil production within the Modelo Formation. Folds are 0.8-16 km in axial length and are roughly parallel to the San Cayetano fault (Çemen, 1977). An exception , is the Buckhorn anticline which trends northwest at the western edge of the Piru quadrangle. It was mapped by Dibblee (1991) and Cemen

(1977, 1989) to turn and trend west-southwest in the central part of the quad. But Morton (1972) showed much of that area to be covered with landslide debris, and subsurface cross sections A-A' and B-B' (Plate IV) show that the crest of the anticline is south of the location shown by Dibblee (1991) and Çemen (1977, 1989). The structural style changes between the two cross sections, with bedding-plane faulting in the west but only ramping in the east. This change in structural style can be explained only by the Buckhorn anticline trending obliquely to and dying out into the San Cayetano fault (Plate I).

Some of the folds extend across Piru Canyon, including the Holser syncline, Temescal anticline, and the Santa Felicia syncline, and thus they are transitional structures between the Modelo lobe and the East Ventura fold belt. Named folds within the Modelo lobe include the Pole Canyon anticline, Buckhorn syncline, Buckhorn anticline, Hopper Basin syncline, Modelo anticline, Blanchard syncline, and South Temescal anticline (Plate I). All of the larger, named anticlines have steeper or overturned south limbs, and the named synclines have steeper north limbs, implying southward vergence for the fold belt. South vergence is not always apparent for smaller, unnamed folds (Plate IV, A-A'). Most folds plunge to the east, as exhibited by the general exposure of younger strata to the east (Plate I).

The Hopper Ranch fault (Plate I: Çemen, 1977, 1989) does not connect with the western San Cayetano fault north of Fillmore as mapped by Jennings and Strand (1969); rather it is likely a flexural-slip fault between the competent

lower sandstone and incompetent lower shale members of the Modelo Formation (Çemen, 1977; Yeats, 1983). Its age is uncertain, but is assumed to be coincident with folding. Several folds, above and below the fault, are truncated by the fault.

The Arundell fault (Plate I; Çemen, 1977, 1989), like the Hopper Canyon fault, separates competent sandstones and incompetent shales of the Modelo Formation and is possibly a flexural-slip fault.

Oak Ridge fault and related structures. The Oak Ridge fault is a post-Saugus steeply south-dipping fault that forms the southern boundary of the central Ventura basin. Yeats (1988a, b) divided the fault into five segments: (1) the western coastal and offshore segment that does not offset the Pleistocene Saugus Formation; (2) the Saticoy to Santa Paula segment that trends roughly N40°E and has oblique slip because of its trend; (3) the Santa Paula to Balcom Canyon segment that has a steeply south-dipping fault and dip-slip displacement; (4) the Balcom Canyon to Wiley Canyon (Plate I) segment which has a lobate surface trace, has shallow dips in the upper 2 km of the fault surface, and has dip-slip displacement, and (5) the eastern segment that separates into three splays and dies out (Figure 2-1). The Piru quadrangle covers parts of segments 4 and 5 (Figure 2-1, Plate I). Throughout the Pliocene and early Pleistocene, the Oak Ridge fault had no topographic expression, but both sides of the fault subsided and received sediments, with

the north side subsiding more (Yeats, 1965; 1988b). Yeats (1988a) calculated a slip rate of 5.9-12.5 mm/y since the end of Saugus deposition at 0.4-0.2 Ma.

The western half of the Piru quadrangle contains part of segment 4. In this segment, the fault surface dips 64-77°S at depth but is much shallower in its upper 2.5 km (Plate IV, A-A'). Strike and dip on the fault surface is highly irregular. Dibblee (1991) maps this segment along the mountian front, south of the trace of the fault on Plate III. However, subsurface mapping (Rieser, 1976) shows that the fault trace is north of the mountain front and has been eroded by the Santa Clara River. Within the Piru quadrangle, the fault zone is composed of fractured Modelo Formation (Huftile, 1988a, b). This segment juxtaposes Oligocene-Miocene Vaqueros Formation and older strata against Pliocene-Pleistocene Fernando and Saugus Formations. The fault dips 70-75°S near Wiley Canyon (Plate I, Plate IV, B-B'), shallowing to 59°S near the surface, between Wiley and Eureka canyons with control as deep as 2.65 km (Plate I; Huftile, 1988a, b). This segment of the fault postdates the folding of the Wiley Canyon anticline in the hanging-wall block because the fold axis is truncated by the fault (Huftile, 1988a, b).

The Wiley Canyon anticline is one of several en echelon folds in the hanging-wall block of the Oak Ridge fault. It plunges gently to the west and steeply to the east. An east-trending cross section demonstrated that the Sespe Formation was broadly anticlinal when the Vaqueros Formation was deposited (Huftile, 1988a, b). This folding would have been coincident with tilting and

normal faulting of the Sespe Formation at the Big Mountain oil field (Hall et al., 1967; Canter, 1974). This pre-Vaqueros anticline was not necessarily parallel to the younger Wiley Canyon anticline.

To the east, in segment 5, the fault surface steepens to 83-85°, and the South and Middle strands diverge from the North strand (Plate I). West of Torrey Canyon, the South strand dips 78-90°S and juxtaposes Oligocene-Miocene Sespe and Vaqueros formations against middle and upper Miocene Modelo Formation. It has a separation of ~1220 m. The South strand trends southeast, extending south and southeast of the Piru quadrangle where it is rotated so that it dips north with normal separation, and is truncated by the Santa Susana fault (Ricketts and Whaley, 1975). The Middle strand trends southeast of the Oak Ridge fault. It dips 80°S near the North strand (Plate IV, D-D'), merges with the South strand, and is rotated to a north dip (Plate IV, E-E'; Ricketts and Whaley, 1975).

The North strand is generally a range-front fault that dips steeply to the south. The surface trace is commonly covered by landslide debris and alluvium (Plate I). The North strand is considered to be the younger strand because it cuts folded Fernando and Saugus formations (Yeats, 1988b). In the eastern part of the Piru quadrangle, the North strand forms a north-facing scarp. A frontal strand is called the Camulos fault by Yeats (1988b); this strand may offset alluvium, and it cuts previously folded Fernando and Saugus Formations.

East Ventura fold belt. At the eastern termini of the Oak Ridge and San Cayetano faults, displacement is transferred to the East Ventura fold belt and the north-dipping Santa Susana fault (Figure 2-1). The eastern edge of the Piru quadrangle covers the westernmost part of the East Ventura fold belt. The fold belt is composed of east-trending, north-vergent folds and south-dipping reverse faults that may extend down into bedding-plane faults.

The Holser fault is the largest of the south-dipping reverse faults in the fold belt (Stitt and Yeats, 1983). In the Piru Canyon area, the Holser fault can be traced to Piru Canyon, but not across it (Figure 1, Plate I). West of Piru Creek, a south-side-up disturbed zone follows the old road, just north of the Modelo Canyon fan. However, it makes little sense structurally because the Holser fault would be in the hanging-wall block of the Piru strand east of Piru Creek and in the hanging-wall block of the Main strand west of Piru Creek. In the Piru Creek area, the fault parallels bedding (Çemen, 1977; Weber, 1982; Stitt and Yeats, 1983; Yeats et al., 1985). Movement on the fault is entirely post-Saugus (Stitt and Yeats, 1983; Yeats et al., 1985). Reverse separation is 460-1850 m with the maximum separation at Ramona oil field in Val Verde quadrangle (Yeats et al., 1985).

The Del Valle fault is the only other south-dipping reverse fault in the East Ventura fold belt that extends westward into the Piru quadrangle. It is the southernmost reverse fault in the fold belt. Stratigraphic separation ranges from 400 m to 670 m (Yeats et al., 1985). Çemen (1977, 1989) mapped the Del

Valle fault on the east side of Piru Canyon along the contact between the Towsley Formation and the Repetto Member of the Fernando Formation. We have mapped the Towsley-Repetto contact north of Çemen's (1977, 1989) and the western Del Valle fault where he mapped the easternmost Main strand of the San Cayetano fault. This agrees with the mapping of Yeats et al. (1985) which shows, by offset contacts 1 km to the east of the Piru quadrangle, that that part of the fault must be south-side-up. The west end of the Del Valle fault is not associated with folding in either the hanging-wall or footwall blocks, implying that the fault is dying out to the west (Yeats et al., 1985).

Folds trend easterly, generally plunge to the east, and fold late Cenozoic strata. Northward vergence is evidenced by steeper north limbs of anticlines, steeper south limbs of synclines, and the convex northward surface traces of some folds such as the Santa Felicia syncline (Plate I; Yeats et al., 1985). The Holser syncline, exposed at the surface west of Piru Canyon, is overridden to the east of Piru Canyon by the Holser fault (Plate IV, F-F'; Yeats et al., 1985).

Santa Clara syncline. The Santa Clara River generally follows the axis of the Santa Clara syncline from southwest of Piru to the west. The eastern terminus of the Santa Clara syncline is southwest of Piru where an anticline-syncline pair, trending N70°W and named the Piru anticline and Piru syncline by Çemen (1977, 1989), occurs. These folds strongly deform the Pleistocene Saugus Formation (Plates IV, VI). Comparison of Plate VI with Plate XXI of Çemen (1977), shows that the axial planes of these folds dips south. Their

trend is roughly perpendicular to maximum horizontal stress in the East Ventura basin determined by borehole breakouts by Mount and Suppe (1987) and may reflect the direction of transport. Çemen (1977) showed the trend of the Piru syncline changed trend to westerly at its northern end, but this change in trend was not supported by new data; dipmeter measurements from the McCulloch Hopper Canyon 1A well imply that the syncline trends WNW throughout the Piru quadrangle. The folds plunge to the northwest, possibly from loading by movement on the San Cayetano fault.

CONCLUSIONS

Pre-Pliocene deformation in the Piru quadrangle is observed only in the hanging-wall block of the Oak Ridge fault. The north-dipping Torrey fault does not cut strata younger than late Mohnian (Ricketts and Whaley, 1975). The Sespe Formation in the Wiley Canyon anticline (Plate I) seems to have been broadly anticlinal at the time of Oligocene-Miocene Vaqueros Formation deposition (Huftile, 1988a, b). This fold was not necessarily parallel to the present Wiley Canyon anticline, and was refolded prior to movement on the Oak Ridge fault.

The Ventura basin is a Plio-Pleistocene accumulation of sedimentary rocks between opposing reverse faults, the San Cayetano and the Oak Ridge faults. Both faults cut strongly deformed Pleistocene Saugus Formation and are believed to have Holocene offset. West-northwest-trending folds not parallel to the faults, the Piru anticline and the Piru syncline, occur in the footwall block, between the faults. So the depositional trough between the San Cayetano and Oak Ridge faults forms a zig-zag pattern synclinorium.

Fold axes of folds in the Modelo lobe, in the hanging-wall block of the San Cayetano fault, generally parallel the surface trace of the fault. The close spacing of folds may indicate a shallow décollement surface separating highly deformed Miocene strata from more competent strata; folded contacts in the northwest corner of the Piru quadrangle indicate that the décollement is in the Miocene Modelo Formation Lower Shale member. These folds generally verge

southward and plunge to the east; the eastward plunge is evidenced by generally younger strata to the east.

As the San Cayetano and Oak Ridge faults die out to the east, displacement is taken up by folds and south-dipping reverse faults of the East Ventura fold belt and by the north-dipping Santa Susana fault.

SEISMIC HAZARD

Post-Saugus faults include the San Cayetano, Oak Ridge, Holser and Del Valle faults. Relatively few tectonic landforms associated with the Holser and Del Valle faults have been preserved (Yeats et al., 1985). Thus, if these faults do produce earthquakes, their recurrence interval is very long; if these faults become bedding-plane faults at depth, they are unlikely to penetrate rocks of such high strength that they would generate large-magnitude earthquakes.

The faults with the greatest hazard in the area for seismic rupture are the San Cayetano and Oak Ridge faults. Both the Main and Piru strands of the San Cayetano fault appear to cut Holocene surfaces. The Main strand turns north at its east end and offsets the top of an alluvial fan at the mouth of Modelo Canyon. The Piru strand offsets alluvium to the west of, and in Piru. The two strands merge at depth and extend down at a moderate dip to seismogenic depth. There has been no historical seismicity on the onshore Oak Ridge fault. South of the Santa Clara Valley, the North strand of the Oak Ridge fault and the Camulos fault form a north-facing scarp and cut alluvium. East of Torrey Road (Plate I), alluvial deposits have a linear boundary with the Santa Clara River channel deposits. This could be related to faulting or merely be a terrace riser of the Santa Clara River. The landslides that cover much of the North strand are possibly coseismic. Seismicity on the San Cayetano fault

has been recorded by Lee et al. (1979) and by Simila et al. (1987); G. W. Simila, written communication, 1989).

ACKNOWLEDGEMENTS

This work was supported by U. S. Geological Survey Contracts 14-08-0001-G1194, -G1372, and -G1798 from the Earthquake Hazard Reduction Program. We wish to thank Leonard T. Stitt, John Truex, and Edward A. Hall for their assistance in the field and discussions that have improved the paper. The geologic map was also reviewed by Thomas W. Dibblee. Alton Albin was an able field assistant. The figures were drafted by Huftile and the plates were drafted by Paula Pitts and Linda Haygarth.

Chapter 3:

Convergence Rates Across a Displacement Transfer Zone in the Western Transverse Ranges near Ventura, California

Gary J. Huftile and Robert S. Yeats
Department of Geosciences
Oregon State University
Corvallis, OR 97331-5506

ABSTRACT

Three cross sections are balanced and retrodeformed to 250±50 ka and 975±75 ka to yield crustal shortening and shortening rates for the western Transverse Ranges of California. The cross sections compare the shortening that occurs along a transfer zone in which displacement is transferred eastward from a surface reverse fault (Red Mountain fault) to a blind thrust and to a combination of both a surface reverse fault (San Cayetano fault) and the blind thrust. Crustal shortening rates have increased through time. For the three cross sections, crustal shortening rates were 4±4 mm/y, 5±2 mm/y, and 6±5 mm/y for the interval between 250 ka and 975 ka. Since 250±50 ka, crustal shortening rates increased to 23±12 mm/y, 29±7 mm/y, and 27±11 mm/y. Crustal convergence rates determined by GPS surveys, taken over a length of 2.7 years, indicate a shortening rate of 7±2 mm/y across the basin. The discrepancy between a rate of strain over a time period of little seismic activity, and a faster rate determined by the offset of bedrock horizons indicates that

much of the crustal movement is being stored as elastic strain and could result in the release of energy in intermediate-sized earthquakes.

INTRODUCTION

Shortening in the western Transverse Ranges is taken up on both north- and south-verging structures, including outcropping reverse faults, blind thrusts, and folds. The western Transverse Ranges are cut by a series of active, north-dipping reverse faults, the Santa Susana, San Cayetano, and Red Mountain faults (Figure 3-1). This paper addresses crustal shortening and shortening rates across the transfer zone between the western two north-dipping faults, the Red Mountain and the San Cayetano faults and is an update of Huftile [1987, 1988b, 1991]. To the east, in the Modelo lobe segment of the San Cayetano fault (Figure 3-1), south-verging displacement is taken up entirely on the San Cayetano fault and associated folding [Yeats, 1983a]. To the west, displacement is entirely taken up on the Red Mountain fault and associated folding. In between, in the Ojai Valley area, there is no north-dipping reverse fault at the surface. Displacement is taken up on a blind thrust, first modeled by Namson [1987] and Namson and Davis [1988]. The surface expression of the blind thrust is the south-dipping homocline south of Sulphur Mountain and also the Lion fault set (Figure 3-1) which dips south and extends downward into bedding within the homocline, forming a passive backthrust above the blind thrust. The presence of both the south-dipping homocline and a surface reverse fault between Ojai Valley and the Modelo lobe suggests that the displacement is partitioned between the two structural types.

Figure 3-1: Index map showing the surface traces of western Transverse Ranges faults and major folds, and cross-section locations of Figures 2-4. The domain boundary separates a region to the east where late Pleistocene surface reverse fault displacement occurs on the Oak Ridge fault and a region to the west where displacement is transferred along a décollement in Miocene mudstones to the Ventura Avenue anticline and Rincon anticline. Abbreviations are: ACS-Ayers Creek syncline, CB-Carpinteria basin, CLS-Cañada Larga syncline, E11-Edwards 11 oil well, HC-Hall Canyon, MC-Matilija Canyon, MF-Montalvo fault, RMA-Red Mountain anticline, SC-Sexton Canyon, SCr-Sespe Creek, SPC-Santa Paula Creek, T653-Shell T653 oil well, UOV-Upper Ojai Valley, and VAA-Ventura Avenue anticline.

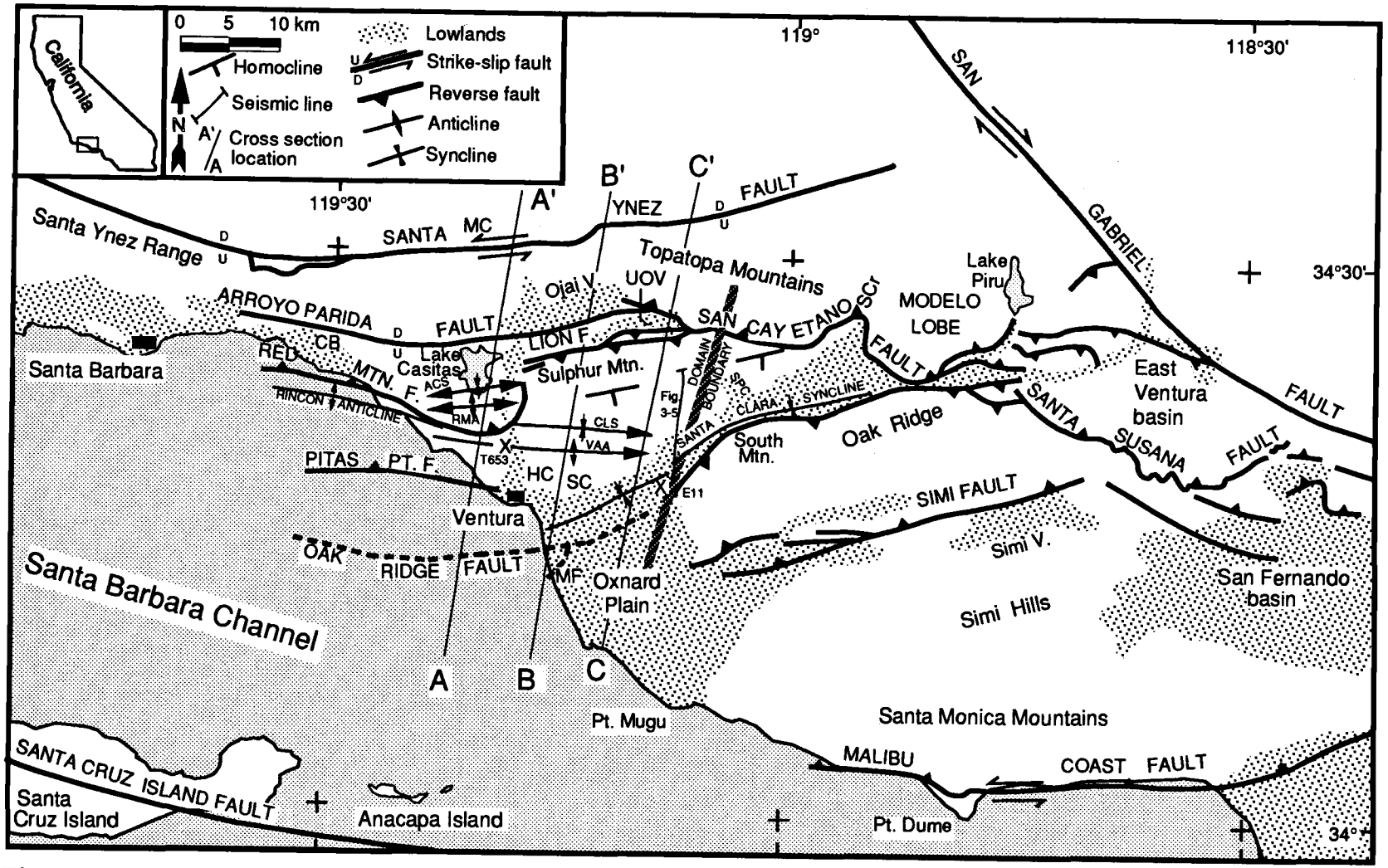
California
0 5 10 km
Homocline
Seismic line
Cross section location
Lowlands
Strike-slip fault
Reverse fault
Anticline
Syncline
119°
118°30'
119°30'
34°30'
34°
SAN GABRIEL FAULT
Santa Ynez Range
SANTA YNEZ FAULT
SANTA MC
Topatopa Mountains
Ojai V.
UOV
Lake Piru
ARROYO PARIDA FAULT
LION F.
SAN CAY ETANO SCr
MODELO LOBE
Santa Barbara
RED MTN. F.
CB
Lake Casitas
Sulphur Mtn.
DOMAIN BOUNDARY
RINCON ANTICLINE
ACS
RMA
CLS
VAA
Fig 3-5
SANTA CLARA SYNCLINE
East Ventura basin
SANTA SUSANA FAULT
Oak Ridge
South Mtn.
PITAS PT. F.
T653
HC
SC
E11
SIMI FAULT
Ventura
OAK RIDGE FAULT
Simi V.
San Fernando basin
Santa Barbara Channel
MF
Oxnard Plain
Simi Hills
A
B
C
A'
B'
C'
Pt. Mugu
Santa Monica Mountains
MALIBU COAST FAULT
SANTA CRUZ ISLAND FAULT
Santa Cruz Island
Anacapa Island
Pt. Dume

Figure 3-1

Models of the structural geology are presented in three balanced cross sections. Cross section A-A' crosses the Red Mountain fault (Figure 3-2), B-B' crosses the blind thrust at Ojai Valley (Figure 3-3),and C-C' crosses the western San Cayetano fault and the blind thrust at Upper Ojai Valley (Figure 3-4). All three sections cross the Oak Ridge fault. The cross sections are retrodeformed back to the top of the Pleistocene Saugus Formation, estimated to be 250±50 ka [Lajoie et al., 1982; Yerkes et al., 1987; Lajoie et al., 1991), in order to determine the amount of structural shortening and rate of deformation since Saugus deposition ended. This allows the determination of convergence rates for only the youngest structures formed after the end of Saugus deposition. The cross sections are then retrodeformed to horizon 5 of Yeats [1981], estimated to be 975±75 ka, to document the increase in convergence rates over the last 250±50 ka. Emphasis is placed on putting upper and lower bounds on the deformation, rather than defending a favorite interpretation. See the Appendix for further constraints on the method.

Figure 3-2: Cross section A-A': The Pleistocene Saugus Formation is lightly shaded, and the Oligocene Sespe Formation, near the top of the competent sandstones, is darkly shaded. **(a)** present-day structure. Cross bars are earthquake locations near the Red Mountain fault with horizontal and vertical error bars. A heavier, shaded, and dipping line through the cross bars is the north-dipping fault-plane solution of the earthquake. Identified oil wells are: 1-Bankline Dunshee 1, 2-McCulloch Brothers-Baldwin 1, and 3-the Continental Casitas 1 and 2. Wells show dipmeter data with a line to one side of the well bore; core dips are shown with dipping lines to each side of the well bore. **(b)** retrodeformed to the top of the Pleistocene Saugus Formation, 250±50 ka. Faults entirely restored are shown with dashed lines. The Ventura Avenue anticline and Mid-Channel fault are entirely retrodeformed (see text for discussion). Displacement shown on the Red Mountain fault is the maximum amount. **(c)** retrodeformed to the benthic foraminifera horizon 5 of Yeats [1976, 1981b], dated as 975±75 ka. Displacement on the Red Mountain fault is the maximum possible. Water depth is from Yeats [1981b]. Abbreviations are: Qs-Pleistocene Saugus Formation, Qca-Pleistocene Casitas Formation, Qmp-Pleistocene "Mudpit Shale", Qsb-Pleistocene Santa Barbara Formation, QTf-Plio-Pleistocene Fernando Formation, Tfr-Pliocene Fernando Formation bearing benthic foraminifera of the Repettian Stage, Tsq-Pliocene Sisquoc Formation, Tm-Miocene Monterey Formation, Tr-upper Oligocene to lower Miocene Rincon Formation, Tcv-Miocene Conejo Volcanics, Tv-Oligocene

Vaqueros Formation, Tsp-Oligocene to upper Eocene Sespe Formation, Tcw-upper Eocene Coldwater Formation, Tcd-upper Eocene Cozy Dell Formation, Tma-upper Eocene Matilija Formation, Tj- Eocene Juncal Formation, Tll-middle and upper Eocene Llajas Formation, Tpl-undifferentiated Paleocene strata, K-Cretaceous, PJF-Padre Juan fault, TCF-Tule Creek fault, APF-Arroyo Parida fault, SYF-Santa Ynez strike-slip fault, and MCF-Mid-Channel fault.

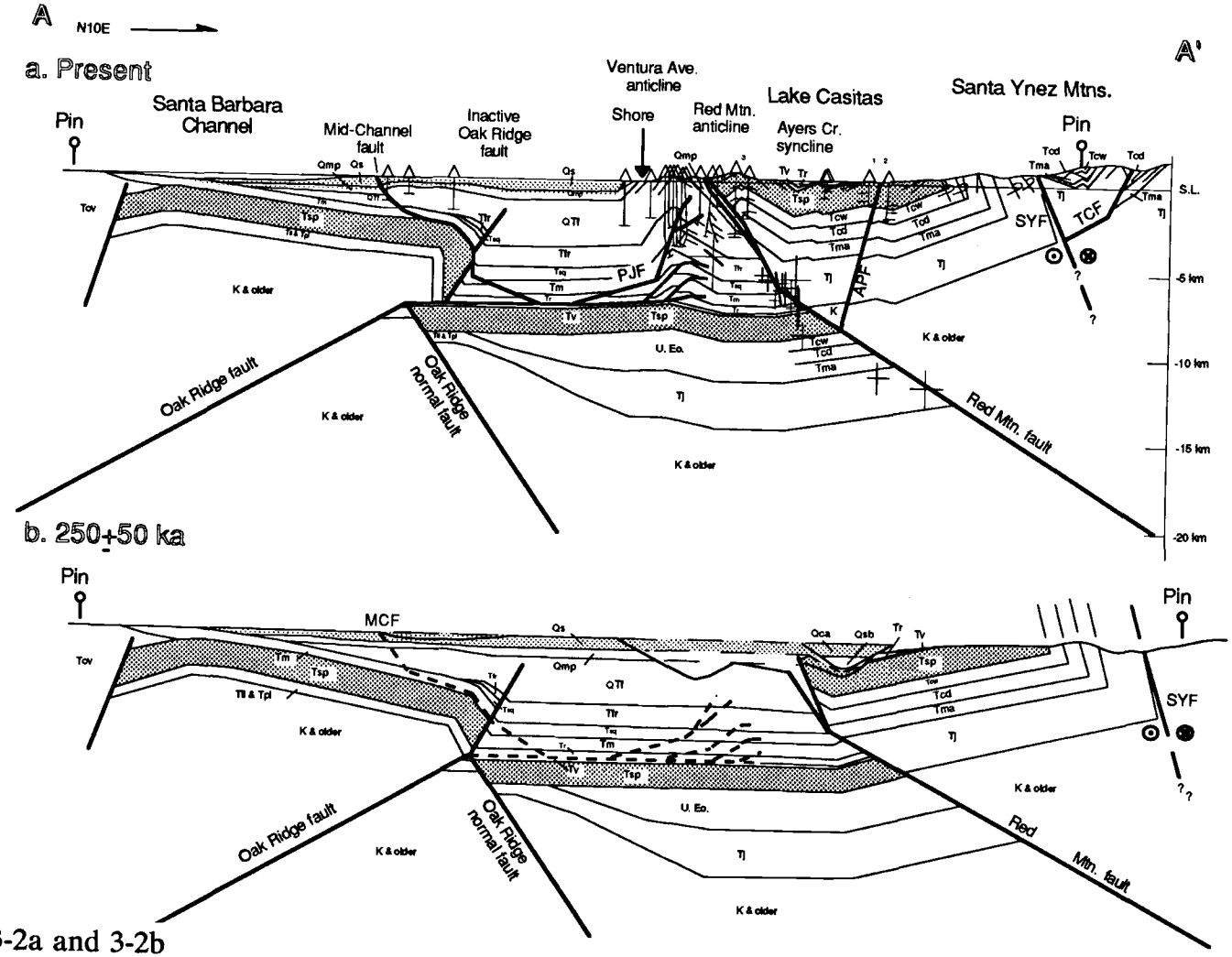

Figures 3-2a and 3-2b

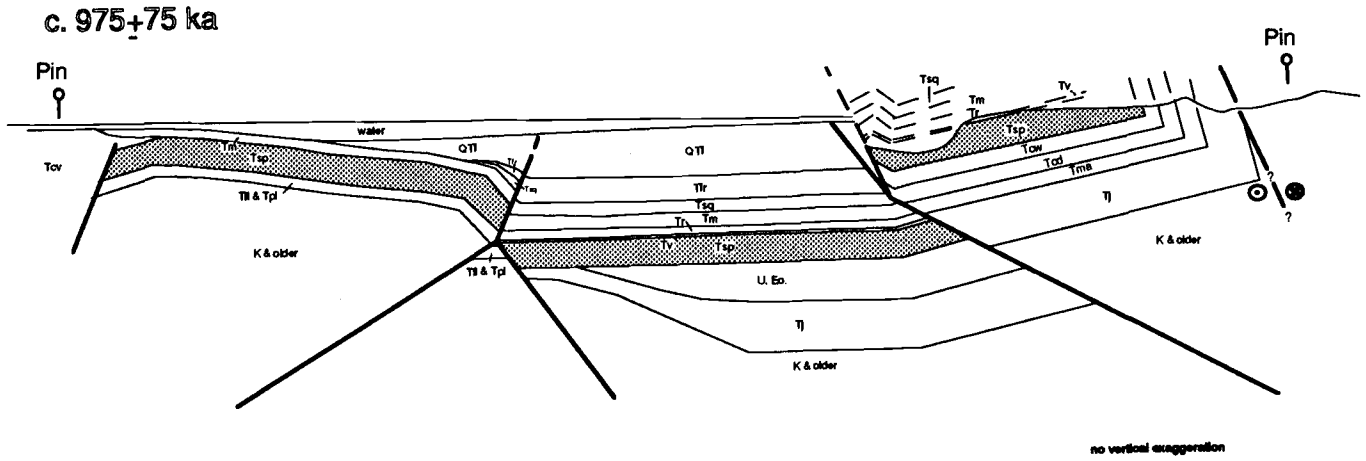
c. 975±75 ka
Pin
Pin
water
Tcv
Tm
Tsp
QTl
Tv
Tm
Tll & Tpl
K & older
Tlr
Tsq
Tm
Tr
Tv
Tsp
U. Eo.
Tll & Tpl
Tl
K & older
Tsq
Tm
Tr
Tv
Tsp
Tow
Tod
Tma
Tl
K & older
?
?
no vertical exaggeration

Figure 3-2c

Figure 3-3: Cross section B-B': **(a)** present-day. Abbreviations and shading are the same as in Figure 3-2; Mgr-Mesozoic granite, TT-Taylor thrust, BT-Barnard thrust. The movement on the Taylor thrust is out of the plane of the cross section [Hsü, 1977; Yeats, 1983a] **(b)** retrodeformed to 250±50 ka. The Ventura Avenue anticline is entirely retrodeformed. Displacement on the upper flat of the south-vergent blind thrust is shown by the distance between the present hinge and retrodeformed hinge. Movement on the Taylor thrust is constrained to between 1.3-0.65 Ma by Yeats [1983a], and offset along it must remain in the retrodeformed section. **(c)** retrodeformed to 975±75 ka. Offset on the Taylor thrust is partially restored.

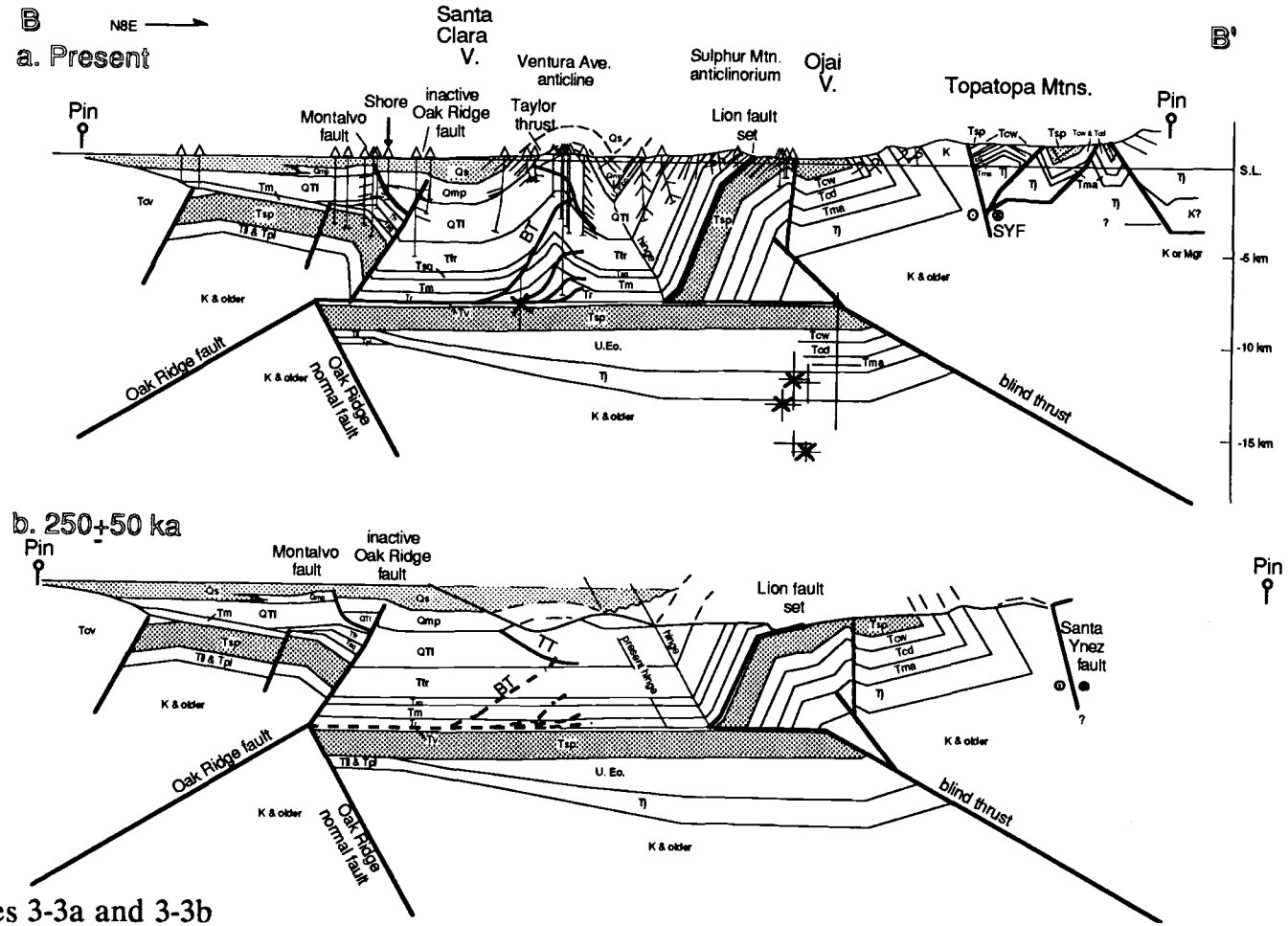

Figures 3-3a and 3-3b

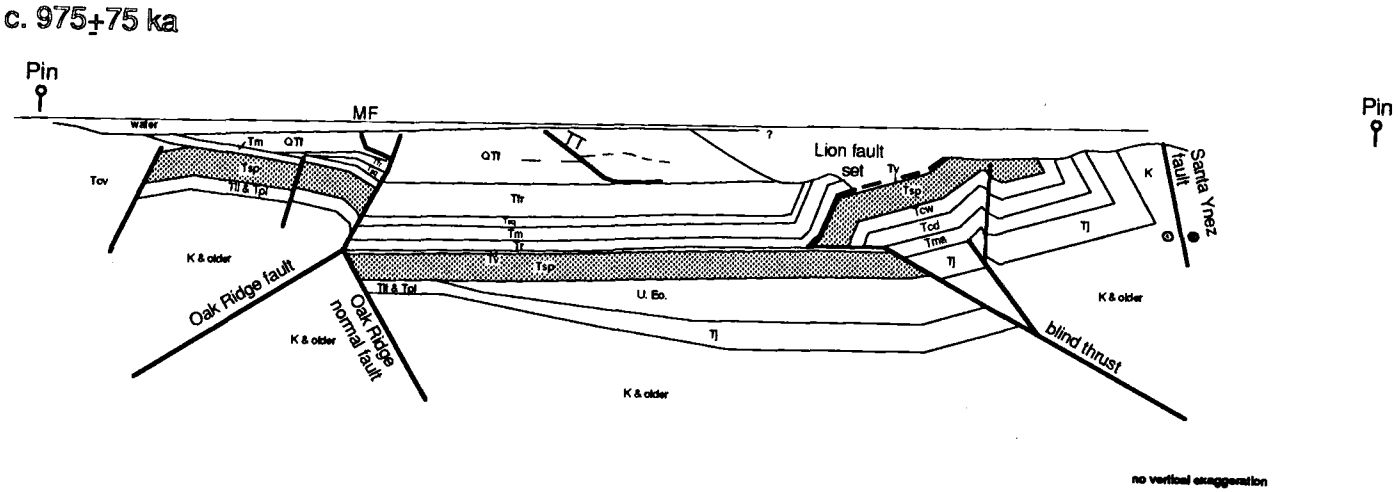
c. 975±75 ka
Pin
MF
water
Tm
QTf
Tsp
Tfl & Tpl
Tov
K & older
Oak Ridge fault
Oak Ridge normal fault
K & older
Tfl & Tpl
QTf
TT
Tfr
Tsp
Tm
Tr
Ty
Tsp
U. Eo.
Tj
K & older
Lion fault set
Ty
Tsp
Tcw
Tcd
Tmm
Tj
Tj
K & older
blind thrust
K
Santa Ynez fault
Pin
no vertical exaggeration

Figure 3-3c

Figure 3-4: Cross section C-C': **(a)** present-day. Abbreviations and shading are the same as in Figure 3-2; LMA-Lion Mountain anticline, and RS-Reeves syncline. **(b)** retrodeformed to 250±50 ka. The Ventura Avenue anticline has been retrodeformed, 0.7 km from the folding, and 1.8 km of north-vergent shortening is taken up at the Sulphur Mountain anticlinorium. The elevation of the top of the Saugus Formation (Qs) at Upper Ojai Valley has been lowered by restoring the movement on the south-vergent blind thrust. The amount of displacement on the upper flat of the south-vergent blind thrust is shown by the distance between the synclinal hinges. There is significant folding of the Sulphur Mountain anticlinorium left unrestored. **(c)** retrodeformed to 975±75 ka. A maximum of 0.3 km of Venturian Fernando Formation (QTf) is found in the Big Canyon syncline. None is found farther north. Displacement on the blind thrust is retrodeformed enough to allow deposition of that amount of QTf.

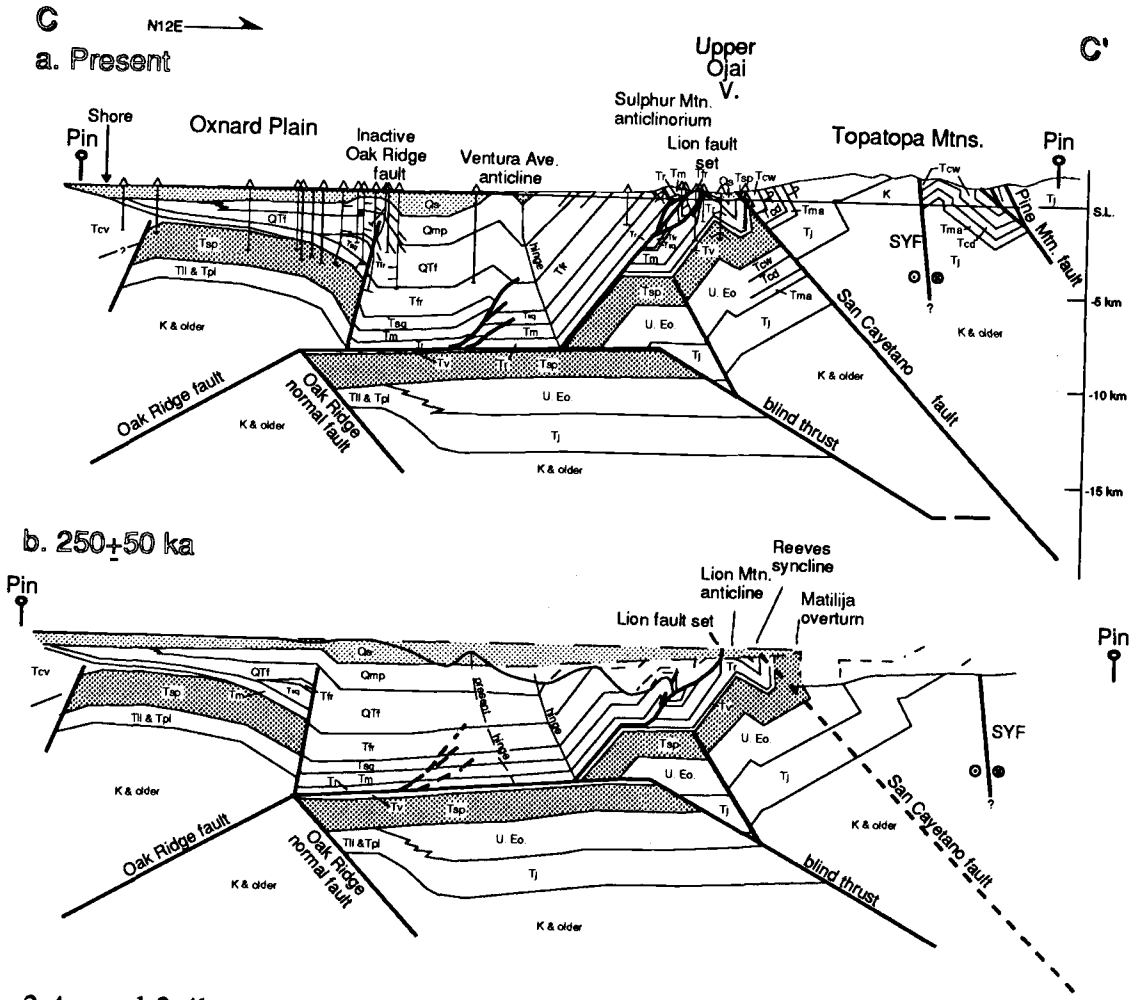

Figures 3-4a and 3-4b

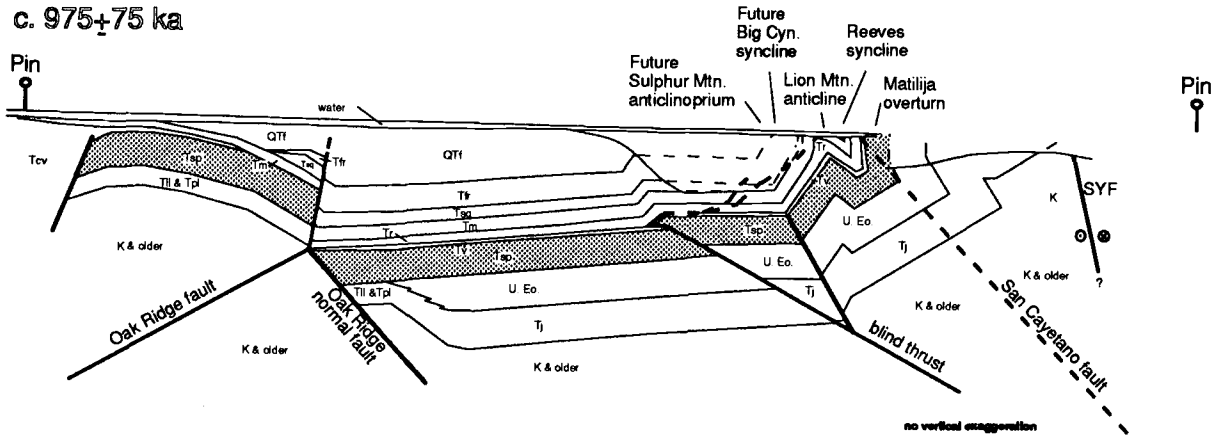
c. 975±75 ka
Pin
Future
Big Cyn.
syncline
Reeves
syncline
Future
Sulphur Mtn.
anticlinoprium
Lion Mtn.
anticline
Matilija
overturn
Pin
water
QTf
Tcv
Tsp
Tmv
Tsa
Tfr
Tll & Tpl
K & older
Oak Ridge fault
Oak Ridge
normal fault
Tll &Tpl
U Eo
Tj
K & older
K & older
blind thrust
U Eo.
U Eo
Tj
K & older
K
SYF
?
K & older
San Cayetano fault
no vertical exaggeration

Figure 3-4c

STRATIGRAPHY

Cretaceous through Paleogene strata are primarily sandstone and form a thick competent sequence. These strata include unnamed Cretaceous strata, and the Eocene Juncal, Matilija, Cozy Dell, and Coldwater formations.

The nonmarine Eocene and Oligocene Sespe Formation is dominated by competent sandstone. The overlying Vaqueros Formation is composed of shallow marine sandstone and is the uppermost formation of the competent sequence. The Sespe Formation is shaded on all cross sections because of its thickness and its position near the top of the competent sequence.

The overlying Miocene mudstone of the Rincon Formation is the least competent formation in the central Ventura basin. It forms the core of the Sulphur Mountain anticlinorium which has overturned limbs on both of its flanks, inferring ductile deformation within the formation. The Rincon Formation is also the most likely décollement horizon because of the strength contrast between it and the underlying sandstone-bearing formations. The Monterey and Sisquoc formations overlie the Rincon Formation and are relatively weak formations which are décollement horizons to the east [Huftile and Yeats, in prep.] and west [Grigsby, 1986]. The overlying Pliocene Fernando and Pleistocene Saugus formations contain more coarse clastic strata and are more competent. The Pleistocene Saugus Formation has also been shaded on the cross sections.

Age of top of Saugus. The top of the Saugus Formation was defined just east of Ventura as the uppermost strongly deformed sedimentary rock [Lajoie et al., 1982]. The age of the top of the Saugus Formation was estimated to be 250±50 ka on the basis of amino-acid racemization of marine shells at the top of the formation [Lajoie et al., 1982; Yerkes et al., 1987; Lajoie et al., 1991] . In the east Ventura basin, the top of the Saugus was estimated to be about 400 ka by paleomagnetic stratigraphy [Levi et al., 1986].

Age of horizon 5. Horizon 5 was defined by Yeats [1976] and labeled the 1 Ma datum by Yeats [1981b]. The age of horizon 5 is determined using the Edwards 11 oil well in West Saticoy oil field (Figure 3-1). In the Edwards 11 well, horizon 5 is within 10 measured feet of the base of the Jaramillo normal magnetic event [Blackie and Yeats, 1976; Yeats and Taylor, 1989]. The date of this event is determined by K-Ar dating of basalt, phonolite, and obsidian from various places in the world [Mankinen and Dalrymple, 1979] to be 975±75 ka.

At Hall and Sexton Canyons (Figure 3-1), horizon 5 occurs between the Bishop ash and the Bailey ash [Sarna-Wojcicki et al., 1987; Sarna-Wojcicki et al., 1991; Yeats, 1988], which are dated as 738±3 ka [Izett et al., 1988] and 1.2±0.2 [Izett et al., 1974] respectively. A date for horizon 5 can be estimated using its position between two ash beds and assuming constant deposition rates. Constant deposition rate is not a valid assumption because a plot of stratigraphic position in Sexton Canyon versus age of the Lava Creek B [0.62

Ma; Christiansen and Blank., 1972; Sarna-Wojcicki et al., 1984, 1987, 1991] Bishop, and Bailey ash beds does not lie on a straight line [Sarna-Wojcicki et al., 1987, their Figure 3-5]. The range of values estimated by assuming constant deposition rates includes the range of the base of the Jaramillo. Thus, the estimated age for horizon 5 used in this report is 975±75 ka.

CROSS SECTIONS

Cross sections must be drawn in the direction of tectonic transport so that displacements do not occur out of the plane of the cross section. The cross sections are straight and are drawn within 15° of the maximum horizontal stress. Maximum horizontal stress has been determined with focal plane solutions of earthquakes, piercing point offset of a turbidite sandstone edge across the Oak Ridge fault, and borehole breakouts of near-vertical oil wells [Zoback et al., 1987; Yeats et al., 1988]. The direction of maximum horizontal stress is ~N24°E [Yeats et al., 1988]. The cross sections are also located by the structures they cross and by the availability of oil well data. Arbitrarily limiting the lines of the cross sections to within 15° of the direction of maximum horizontal stress limits the error in shortening estimates to ±3% (cos 15° =0.97).

The cross sections are pinned to the south in the Oxnard Plain and its offshore extension because it has been stable since the Miocene. To the north, the cross sections are pinned just north of the Santa Ynez fault. The Santa Ynez fault has been proposed as the left-lateral fault that was the northern boundary of clockwise rotation in the Transverse Ranges [Luyendyk and Hornafius, 1987]. Several authors have inferred left-lateral offset along the fault because of offset stratigraphic facies and a laumontite isograd; a list of references, offset horizons, and sense and amount of offset is given in Table 3-1. In addition, Gordon [1978] noted left-stepping en echelon folds at the east

Table 3-1.

Estimates of lateral separation of the Santa Ynez fault

Author(s)	Age and formation offset	Amount and sense of offset
Dibblee [1950] & *O'Brien* [1973]	Oligocene and Early Miocene Sespe and Vaqueros fms.	244 m left-lateral
Edwards [1971]	Early Miocene, Vaqueros Fm.	60 km left-lateral
Link [1971]	Eocene, Matilija Fm.	1.6-3 km left-lat.
McCracken [1969]	Oligocene, Sespe Fm.	35 km left-lateral
McCulloh [1981]	laumontite isograd	37 km left-lateral
Page et al. [1951]	Eocene, Sierra Blanca Ls.	11-14 km left-lat.
Roubanis [1963]		3 km left-lateral
Schmitka [1973]	Eocene, Matilija Fm.	48 km right-lat.
Schroeter [1972]	Eocene, Sierra Blanca Ls.	15 km left-lateral

end of the fault, inferring a left-lateral sense of offset on the fault. At Matilija Creek, there are horizontal slickensides in a steeply-dipping fault zone.

Other authors [Namson, 1987; Namson and Davis, 1988] have noted that the south side of the fault is up along its entire length and that the fault appears to die out into folds at both ends. This would deny significant strike-slip displacement on the fault. They model the fault as an Oligocene backthrust because of an unconformity north of the fault. However, tectonism during the Oligocene was extensional [Muehlberger, 1958; Bohannon, 1975]. The stratigraphic offsets, the steepness of the fault, and the horizontal slickensides are sufficient reason not to balance across the fault.

Rotation of a crustal block implies that rocks have moved in and out of the plane of a cross section. Only the rocks at the axis of rotation would remain in the section. Older strata would have rotated more than strata deposited at the time of, or since rotation. Retrodeforming structures in a cross section is only valid when flattened to the time of the younger, unrotated strata. Shortening, measured on a balanced cross section along a horizon that has undergone rotation, is more than the actual shortening. A correction must be applied by multiplying the amount of measured shortening by the cosine of the rotation. Rotation of the western Transverse Ranges began in early Miocene time [Liddicoat, 1990; Hornafius et al., 1986] and rotated 50-60° clockwise during middle Miocene [10-16 Ma; Hornafius et al., 1986]. Liddicoat [1992] found that Pliocene Fernando Formation, ~500 m stratigraphically

beneath horizon 5 and exposed in Santa Paula Creek (Figure 3-1), is rotated 20.0±7.2° clockwise. Levi et al. [1986] found that nonmarine Saugus Formation (~0.4-2 Ma there) in east Ventura basin is rotated is rotated as much as 30° clockwise. Rotation of strata younger than horizon 5 has not yet been tested in the central Ventura basin, so there remains the possibility that the 250±50 ka and 975±75 ka horizons have been rotated as much as 20° clockwise. If this proved to be true, then the numbers stated in this paper could be as much as 6% greater than actual shortening (cos 20° =.94).

The Oak Ridge fault, at South Mountain, has 2.5 km of displacement in the last 250±50 ka [Yeats, 1988; Yeats and Huftile, 1991]. West of South Mountain, topographic relief due to uplift of the hanging wall of the Oak Ridge fault decreases to zero and there is no post-Saugus displacement on the fault in the Oxnard Plain and its offshore extension. The change is too to be attributed to a decrease in crustal convergence westward along the western Transverse Ranges. Yeats et al. [1988] proposed that the vertical displacement at South Mountain does not die out westward, but is transferred along a décollement in the Miocene Rincon Formation to the Ventura Avenue/Rincon anticline. Folding of the Ventura Avenue anticline is entirely WNW of a domain boundary (Figure 3-1) parallel to the tectonic transport direction marking the western limit of the post-Saugus surface displacement on the Oak Ridge fault. The location of the fold in the foreland is controlled by the location of the

hanging-wall block of the Red Mountain fault, composed of competent sandstones.

Namson [1987] and Namson and Davis [1988] proposed that the Ventura Avenue anticline is a south-vergent structure, rising from a décollement in the Rincon Formation at about 8 km depth. This is denied by the presence of the same anticline in the footwall block, south of the Red Mountain fault because earthquakes have occurred on the fault to depth much greater than their décollement depth. Faults within the fold dip north and south. Yet, those that dip north, such as the Taylor thrust (Figure 3-4), the Grubb fault, and the T-99 fault are older and have a trend that is not parallel to the fold axis of the Ventura Avenue anticline [Yeats, 1983a]. Movement on the Taylor thrust was constrained by Yeats [1983a] between 650-1,300 ka. Younger, south-dipping faults such as the Padre Juan (Figure 3-2) and the Barnard (Figure 3-4) faults are generally parallel to the fold axis and lose separation northward, as expected for a north-vergent fault-propagation fold.

The stratigraphic level of the décollement is determined from well penetrations at Sulphur Mountain and by a deep test at the Ventura Avenue anticline. Huftile [1988a, 1991] mapped the north-verging, south-dipping Lion fault set with post-Saugus displacement. These faults, the Big Canyon, Sisar, and Lion faults appear to merge at depth to form the Sisar décollement in the Rincon Formation. They do not appear to cut rocks older than the Rincon Formation [Huftile, 1991, his Figure 3-5a]. A deep-test oil well (Taylor 653,

located on Figure 3-1) was drilled in the core of the Ventura Avenue anticline to a depth of 6553 m. The well confirmed that the Ventura Avenue anticline was rootless and that the décollement must underlie the Monterey Formation [Yeats, 1983a; Yeats et al., 1988]. Thus we conclude that the décollement is most likely within the mudstone of the Rincon Formation, immediately above the competent sandstone sequence discussed above. Seismic reflection profiles (Figure 3-5) support this interpretation.

Hadley and Kanamori [1977] suggested that the surface trace of the San Andreas fault in the big bend area does not correspond with the plate boundary between the Pacific and North American plates, based on the identification of anomalous, high-velocity mantle that spans the fault. This interpretation implies that the plate boundary between the San Andreas fault and the eastern edge of the mantle anomaly must be a horizontal thrust. Hadley and Kanamori [1978] subsequently found some earthquakes at mid-crustal depths beneath the central Transverse Ranges with horizontal nodal planes. Webb and Kanamori [1985] found additional occurrences of near-horizontal nodal planes at mid-crustal depths beneath the Transverse Ranges and the San Emigdio Mountains. They argued that a regional, mid-crustal décollement lies beneath the Transverse Ranges. Yeats [1981a] suggested that the central Transverse Ranges are a "tectonic flake," using the terminology of Oxburgh [1972]. Yeats suggested that the Vincent thrust is an exposed mid-crustal thrust. Later, Yeats [1983a] noted that the mid-crustal décollement

coincides with the base of earthquakes and concluded that the décollement marked the rheological change between high-strength, brittle rocks and underlying ductile rocks. Shortening occurring at the horizontal brittle-ductile transition is equal to the dip-slip displacement of an associated surface reverse fault plus the shortening taken up in folding.

Cross section A-A'. The Red Mountain fault dips about 48°N at the surface and 60° to the base of well control at about 3 km depth [Yeats et al., 1987]. Below that, the distribution of earthquakes suggests the presence of a lateral ramp separating eastern and western segments of the fault at the western termini of the Red Mountain anticline and the Ayers Creek syncline where the plunge of the folds abruptly increases to 40°W. Based on seismicity during the period of 1970-1975 (Figure 3-6), the western segment extends down to seismogenic depths of about 12 km at a 66° dip, while the eastern segment shallows in dip at about 6 km depth. It is interpreted that the change in dip occurs at the intersection of the fault and the fold hinge of the Ayers Creek syncline. Using the methods of Woodward et al. [1989], a change in dip to 33° is interpreted. The structure of the hanging-wall block is constrained by the thickness of the Oligocene Sespe Formation, ~1.6 km at the surface and in the Bankline Dunshee 1, McCulloch Brothers-Baldwin 1, and Continental Casitas wells (wells 1, 2, and 3 on Figure 3-4a) that reach the underlying Eocene Coldwater Formation both south and north of the Arroyo Parida fault.

The timing of movement on the Red Mountain fault is poorly constrained. The Red Mountain fault is active. Yet, the Red Mountain anticline formed a seaknoll and affected turbidite deposition of the late Pliocene-early Pleistocene Pico Member of the Fernando Formation [Figure 3-7; Yeats et al., 1987] so that at least some of the folding would have to remain after retrodeforming back to the top of the Saugus Formation (Figure 3-4). Mapping by Dibblee [1988] and Yeats [unpublished mapping] shows that sandstones to the east of Red Mountain are thin and pinch out westward toward Red Mountain. South of Red Mountain, thick sandstones also lens out northward toward Red Mountain, inferring that Red Mountain was a sea knoll during deposition of the Fernando Formation (Figure 3-7).

The hanging-wall block of the Red Mountain fault contains no strata younger than Miocene, making the timing difficult to constrain. The amount of post-Saugus movement on the Red Mountain fault was determined at by projecting the approximately age-equivalent Pleistocene Casitas Formation of the Carpinteria basin (Figure 3-1) into the section from the west. Figure 3-8 shows three ways to project the Pleistocene strata into the cross section. Each allows for movement on the Rincon Creek fault, which was post-Saugus [Jackson and Yeats, 1982]. One projection is parallel to the synclinal axis of the Carpinteria basin and follows the axes of the Rincon Mountain and Ayers Creek synclines. This projects the base of the Pleistocene basin into the section just above topography. A second projection follows the 6°W plunge of

Figure 3-5: Profile 2, recorrelated and unmigrated Vibroseis seismic reflection line. Uninterpreted **(a)** and interpreted line sketch **(b)** recorrelated to 12 seconds, two-way time. The line is oblique to true dip and is horizontally exaggerated. Thus, the apparent dips shown are less than the true dips. Oil wells are the Union Ex-Mission X14 and X17. To the south, the Santa Clara syncline has horizontal reflectors down to about 6.6 seconds. To the north, there are dipping reflectors of the homocline overlying flat reflectors, inferring a blind thrust geometry. The ramp of the blind thrust is off the section to the north (see Figure 3-4a).

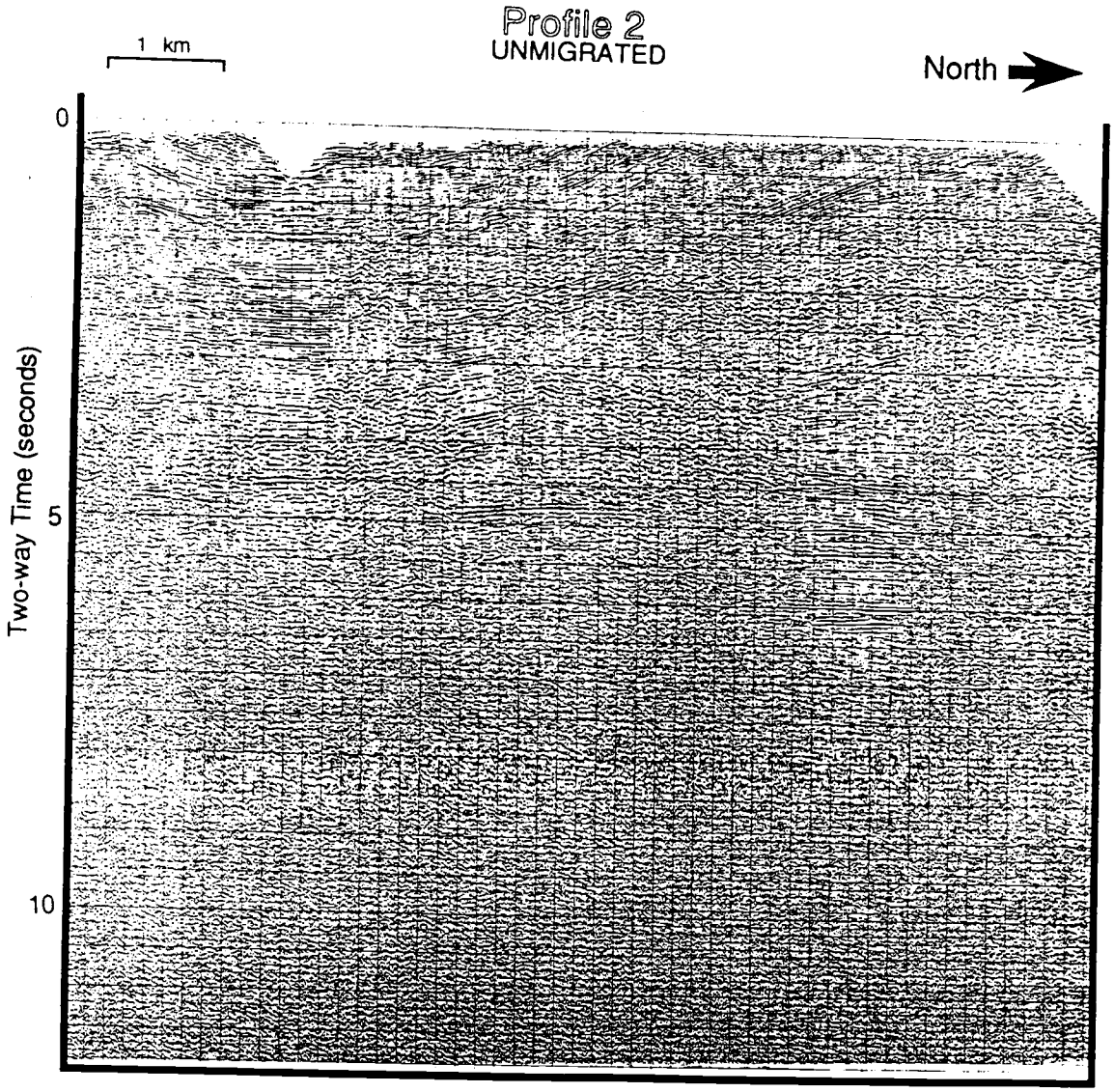

Figure 3-5a

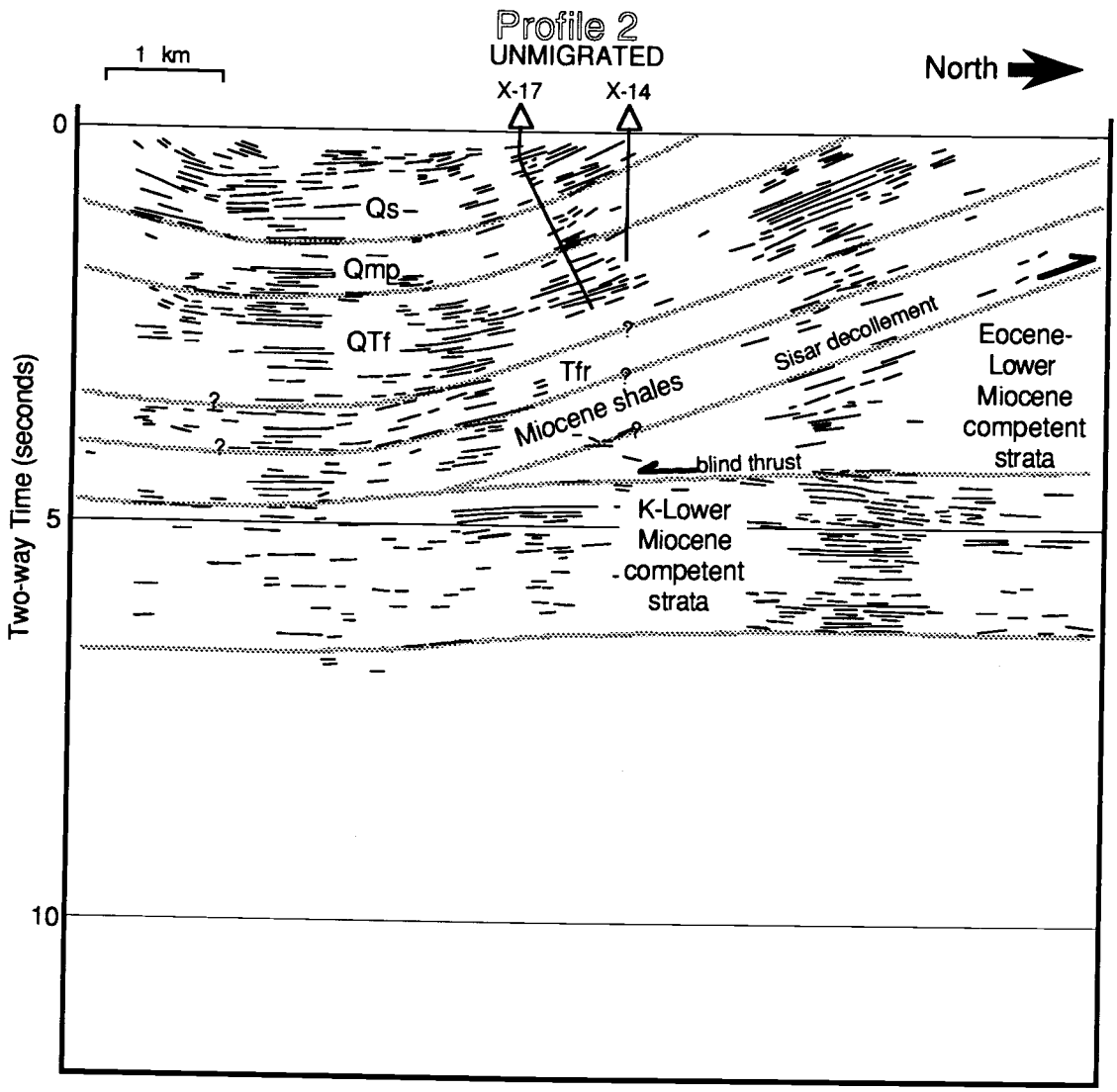
Profile 2
UNMIGRATED
1 km
North
X-17
X-14
0
5
10
Two-way Time (seconds)
Qs
Qmp
QTf
Tfr
Miocene shales
Sisar decollement
Eocene-
Lower
Miocene
competent
strata
blind thrust
K-Lower
Miocene
competent
strata

Figure 3-5b

Figure 3-6: Map showing seismicity related to the Red Mountain fault from 1980-1985. Shaded lines show the surface locations of the axial traces of the Ayers Creek syncline (ACS) and the Red Mountain anticline (RMA). The location of the change in plunge to 40°W is shown. Cross bars show the horizontal error in the locations of earthquakes. Depths in km subsea and vertical error are posted on each cross bar. Focal mechanism solutions [cf. Yeats et al., 1987] are shown with an arrow opposite the direction of slip and the inferred dip of the plane of movement. The surface locations of the Red Mountain anticline and the Ayers Creek syncline are shown with a shaded pattern. Dots are the surface location of oil wells with control on the Red Mountain fault [Yeats et al., 1987]. Lines from the dots are the well courses of directionally drilled wells. X marks the location of the intersection with the fault. The contour interval is 1 km. The upper 3 km is constrained by the wells and is the same as in Yeats et al. [1987]. There are two clusters of earthquakes. The western cluster has earthquakes at depths of 9.75-11.51 km which allow for a consistent dip on the fault of about 66°S. The eastern cluster has depths between 5.31-8.77 km. Below 5 km depth, an increase in contour spacing is required to honor all of the data. This infers a shallowing of the eastern end of the Red Mountain fault and the presence of a lateral ramp between the two clusters of earthquakes. The lateral ramp is observed at the surface where the western end of the Red Mountain anticline abruptly increases plunge to 40°W.

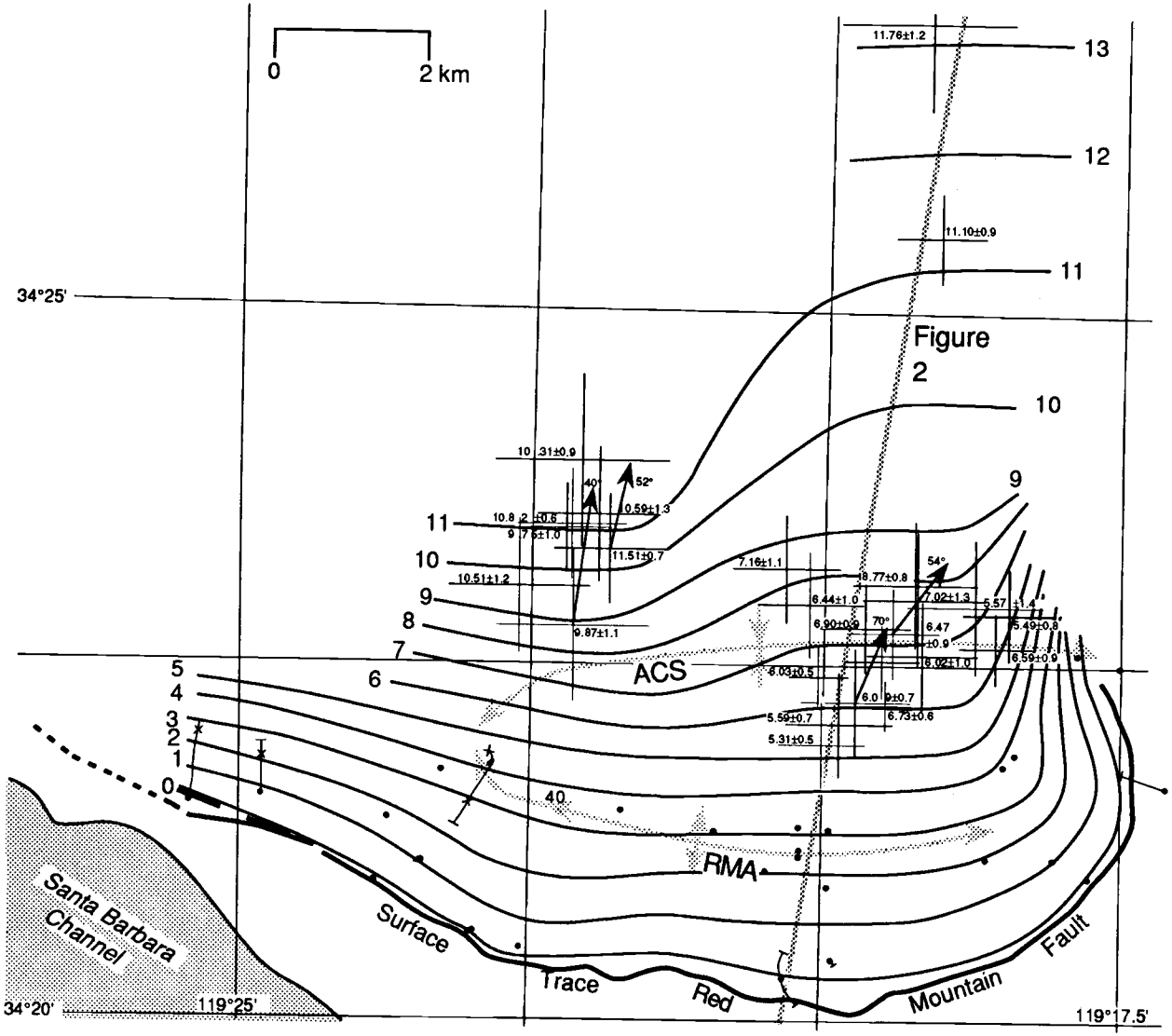
0
2 km
34°25'
34°20'
119°25'
119°17.5'
Figure 2
ACS
RMA
Surface Trace Red Mountain Fault
Santa Barbara Channel
11.76±1.2
11.10±0.9
10.31±0.9
11.51±0.7
10.51±1.2
9.87±1.1
7.16±1.1
8.77±0.8
6.44±1.0
6.90±0.9
6.47
±0.9
6.02±1.0
6.03±0.5
6.09±0.7
6.73±0.6
5.59±0.7
5.31±0.5
6.59±0.9
40°
52°
54°
70°
13
12
11
10
9
8
7
6
5
4
3
2
1
0
40

Figure 3-6

Figure 3-7: Map showing the distribution of sandstones (shaded) in the Fernando Formation at the surface using mapping by Dibblee [1988] and Yeats [unpublished mapping]. Abbreviations are the same as in Figure 3-2. The sandstones were deposited from the east and north by turbidity currents. North of the Cañada Larga syncline, the sandstones are thin and pinch out to the west before they reach the Red Mountain uplift. South of the syncline, sandstones in the same sequence are massive, very thick, and extend well to the west of Red Mountain. This infers that Red Mountain was uplifted as the Fernando Formation was deposited.

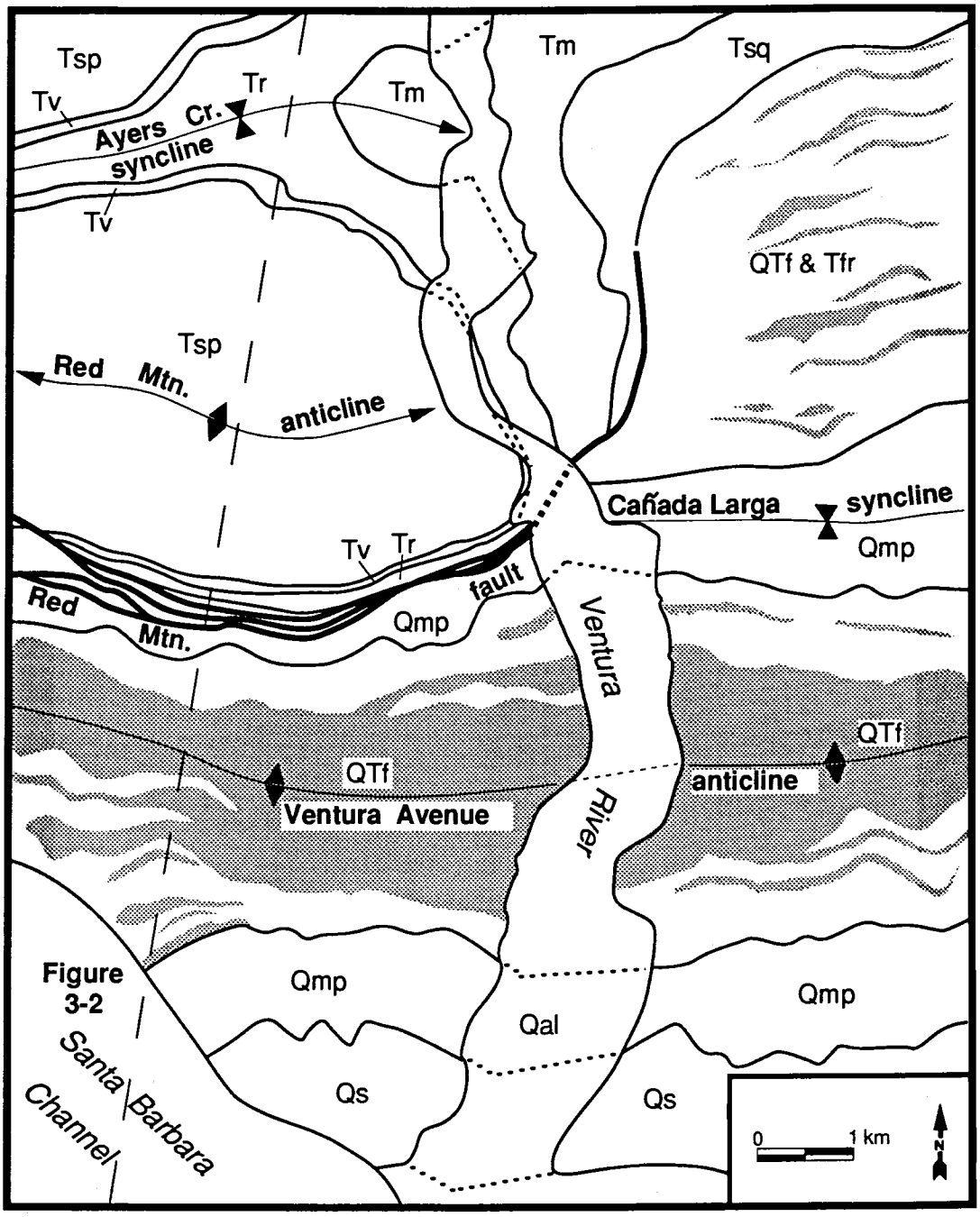
Tsp
Tv
Tr
Tm
Ayers Cr.
syncline
Tv
Tm
Tsq
QTf & Tfr
Tsp
Red Mtn.
anticline
Cañada Larga
syncline
Qmp
Tv Tr
fault
Red Mtn.
Qmp
Ventura
River
QTf
anticline
QTf
Ventura Avenue
Figure 3-2
Qmp
Qal
Qmp
Santa Barbara Channel
Qs
Qs
0
1 km
N

Figure 3-7

Aquifer B of Slade [1975] in the Carpinteria basin, the uppermost aquifer that is sufficiently penetrated by wells to accurately allow the determination of a plunge. This also projects the base of the Pleistocene basin just above topography. Both projections result in 3.5 km of dip-slip displacement, and thus, horizontal shortening that has occurred since Saugus deposition ended. This is considered to be the maximum offset for the Red Mountain fault in the last 250±50 ka. The minimum offset on the Red Mountain fault is determined by projecting the Carpinteria basin into the section with 0° plunge, assuming that Pleistocene strata were never deposited on Red Mountain. Minimum dip-slip displacement on the Red Mountain fault since 250±50 ka is 0.2 km. Because the displacement on the Red Mountain fault since 975±75 ka is determined independently of these projections, the total offset is unaffected. So the first two projections maximize the offset since 250±50 ka and the third projection maximizes the offset between 250 ka and 975 ka.

The south-vergent Mid-Channel fault is south of the Oak Ridge fault. Cross section A-A' crosses the Mid-Channel fault at its easternmost end. To the west of Figure 3-2, the CUSS 8-355 core hole has horizon 5 repeated the well. It is interpreted as a backthrust rising up from the décollement because the Ventura Avenue anticline, in the footwall of the Red Mountain fault, has locked up. This interpretation is somewhat speculative, but there is little shortening associated with the Mid-Channel fault along this cross section. We do not interpret that Mid-Channel fault is rooted to the north because of the

Figure 3-8: Map and cross section showing different eastward projections of Pleistocene strata in the Carpinteria basin, the only occurrence of Pleistocene strata in the hanging-wall block of the Red Mountain fault, into the line of section in Figure 2. Abbreviations: Qca-Casitas Formation, Qsb-Santa Barbara Formation, RCF-Rincon Creek fault. **(a)** map showing the location of outcropping Pleistocene strata and the surface location of reverse faults and folds. The shaded line is the line of projection shown in Figure 8b. Surface dips from Dibblee [1987a, 1987b, 1988] are used to determine the plunges of folds shown in larger numbers along the axial traces. **(b)** Three methods of projection are used to constrain the movement on the Red Mountain fault since 250±50 ka. The Rincon Creek fault truncates the top of the Casitas Formation and is therefore allowed to offset the projections. One projection is along the plunges of the synclines between the synclinal Carpinteria basin and the Ayers Creek syncline at the cross section. This is accomplished along a plunge of 0° east to the east end of Rincon Mountain syncline which plunges 22°E. Between the Rincon Mountain and Ayers Creek synclines, a plunge of 40°W is used because it is the maximum plunge observed in the area. At the west end of Ayers Creek syncline, there is a plunge of 22°W. A plunge of 0° is used from there to the section. This projection allows for deformation in the hanging-wall block of the fold, assuming that the Ayers Creek syncline was at the same elevation as the Carpinteria basin during deposition of the Pleistocene. This is considered to be the maximum amount of displacement

since 250±50 ka. Another projection used the plunge of the uppermost aquifer in the Carpinteria basin that is sufficiently penetrated by wells to allow the determination of a plunge. Aquifer B of Slade (1975) was found to have a plunge of 6° W. Projecting the top and base of the Pleistocene into the section places the Pleistocene just above topography, at the same elevation as in the previous projection. A third projection assumes that no Pleistocene was deposited at Red Mountain and is projected east at 0° plunge. This projection allows for the minimum displacement on the Red Mountain fault since 250±50 ka.

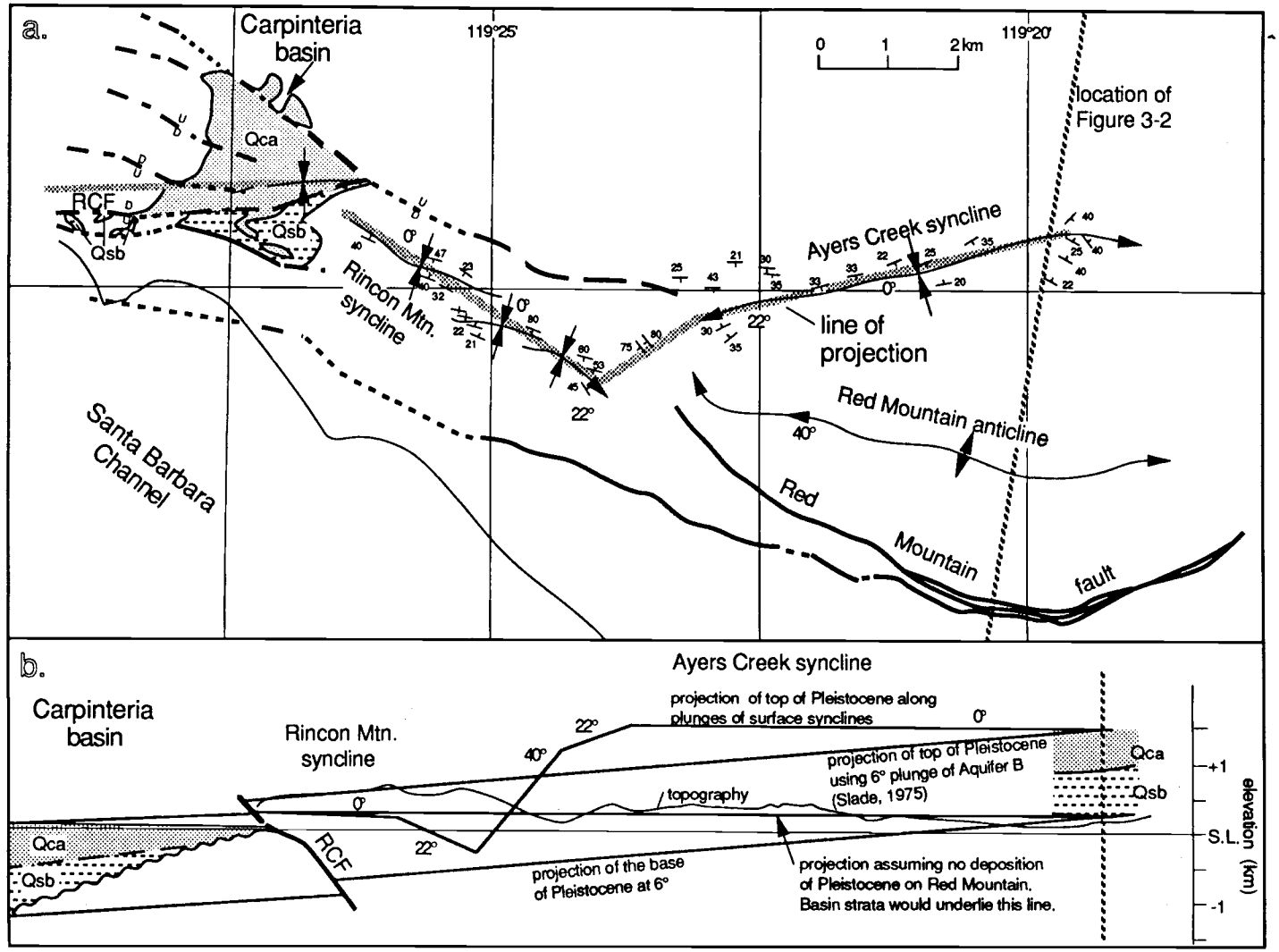
a.
Carpinteria basin
119°25'
119°20'
0 1 2 km
location of Figure 3-2
Qca
Qsb
RCF
Ayers Creek syncline
Rincon Mtn. syncline
line of projection
Red Mountain anticline
Santa Barbara Channel
Red Mountain fault
b.
Ayers Creek syncline
Carpinteria basin
Rincon Mtn. syncline
projection of top of Pleistocene along plunges of surface synclines
projection of top of Pleistocene using 6° plunge of Aquifer B (Slade, 1975)
topography
projection of the base of Pleistocene at 6°
projection assuming no deposition of Pleistocene on Red Mountain. Basin strata would underlie this line.
S.L.
+1
-1
elevation (km)

Figure 3-8

seismicity to 12 km depth on the Red Mountain fault to the north [Figure 3-6; Yeats et al., 1987]. Figure 3-4a implies that all the displacement on the fault is post-Saugus. This is based on the observation that Saugus is thinner on the structure and the top of the formation has been eroded. Suppe et al. [1992], using narrowing upward kink bands expressed on seismic reflection data, infers that much of the displacement could be older. Thus, the displacement on the Mid-Channel fault is 0-0.3 km since 250±50 ka.

South, and in the footwall block, of the Red Mountain fault is the Ventura Avenue anticline. The structure of the Ventura Avenue anticline in this section is from Grigsby [1986] and Yeats et al. [1988] extended down to the décollement in the Rincon Formation. The bend in the Padre Juan fault is modeled based on the synclinal hinge angle just south of the fault. Using the method of Woodward et al. [1989], a change in the dip of the fault to 18°S is calculated. There is 2.5 km of shortening at the Ventura Avenue anticline.

The Oak Ridge fault is modeled as a normal fault through the end of deposition of the Monterey Formation. The Oak Ridge anticline was a positive feature accompanied by normal faulting during the Miocene, and it is assumed that the Oak Ridge fault farther north was active and had normal displacement [Yeats, 1987; 1989]. On the three cross sections in this study, the Monterey Formation is the youngest conformable formation that is tilted northwest in the Oxnard Plain (Figures 3-2, 3-3, 3-4). A wedge of Pliocene sedimentary rocks as old as the Sisquoc Formation overlies the Monterey Formation with angular

unconformity [Yeats, 1983b]. The wedge accompanies contractile tectonics using the reasoning of Namson [1987, his figure 4]. The first deposition on the forelimb of the fold should form a wedge.

Retrodeformation of the Ventura Avenue anticline moves the inactive, upper part of the Oak Ridge fault south 2.5 km. Flattening of the north-dipping limb in the hanging-wall block adds 0.7-0.8 km of shortening.

Total horizontal shortening along cross section A-A' since 250±50 ka is 3.4-7.1 km, which occurred at a rate of 23±12 mm/y.

In the Carpinteria basin to the west, the Casitas Formation (Saugus equivalent) and the Santa Barbara Formation (Mudpit Shale equivalent) lie unconformably on folded Miocene and older rocks [Jackson and Yeats, 1982]. Pliocene strata are not found in the hanging-wall block of the Red Mountain fault. Mapping by Grigsby [1986] and Dibblee [1988] shows the Mudpit Shale truncated by the Red Mountain fault and Figure 3-2a [see Grigsby, 1986, his Plate VIII] shows that the base of the Mudpit Shale is truncated in the footwall block of the fault. So the minimum dip-slip displacement on the Red Mountain fault since 975±75 ka is considered to be that amount that would expose the Mudpit Shale in the footwall block of the fault. This is 3.6 km, only slightly more than the maximum displacement at 250±50 ka. Because the Sisquoc Formation is the youngest formation in the conformable sequence in the hanging-wall block of the Red Mountain fault, the maximum dip-slip

displacement is interpreted to be 5.5 km, the amount that would allow a full section of the Sisquoc Formation to overlie the Red Mountain anticline.

Unfolding of rocks in the hanging-wall block of the Oak Ridge fault adds ~0.1 km of shortening. Total shortening since 975±75 ka is 7.2-9.2 km. The shortening rate between 250±50 ka and 975±75 ka is 5±5 mm/y (Tables 3-2, 3-3).

Cross section B-B'. East of the east end of the Red Mountain fault, the Ojai Valley area has no north-dipping surface reverse fault. South-vergent movement is taken up on a blind thrust and associated fold, first modeled as a fault-bend fold by Namson [1987] and Namson and Davis [1988]. The surface expression of the blind thrust is a south-dipping homocline (Figure 3-1); this is underlain by flat-lying strata beneath the blind thrust, an interpretation confirmed by multichannel seismic reflection data [Figure 3-5; Huftile, 1988b]. A passive backthrust, the Sisar décollement of Yeats et al. [1988], is interpreted to extend up into bedding in the Miocene Rincon Formation from the blind thrust fault tip. The surface expression of the Sisar décollement is the Lion fault set, which includes the Lion fault, the Oak View faults to the west near Ventura River, and the Sisar and Big Canyon faults in Upper Ojai Valley.

Shortening on the Ventura Avenue anticline is 2.0 km. The 2.5 km of vertical uplift on the Oak Ridge fault at South Mountain is transferred to the Ventura Avenue anticline [Yeats et al., 1988]. This results in 2.5 km of

Table 3-2

Ranges of Horizontal Shortening (km)

Section A-A'					
	Flattening of hanging-wall Oak Ridge fault	**Mid-Channel fault**	**Ventura Avenue anticline**	**Red Mountain fault**	**Total**
250±50 ka	0.7-0.8	0-0.3	2.5	0.2-3.5	3.4-7.1
975±75 ka	0.8-0.9	0.3	2.5	3.6-5.5	7.2-9.2

Section B-B'						
	Flattening of hanging-wall Oak Ridge fault	**Ventura Avenue anticline**	**Taylor thrust**	**Upper flat of blind thrust**	**Flattening across hinge at top of ramp**	**Total**
250±50 ka	0.3	2.0-2.5	0.1	3.0-3.1	1.4	6.7-7.3
975±75 ka	0.3	2.0-2.5	0.1	5.2-5.3	2.6	10.2-10.8

Section C-C'						
	Flattening of hanging-wall Oak Ridge fault	**Ventura Avenue anticline & Sulphur Mtn. anticlinorium**	**Upper flat of blind thrust**	**Flattening across hinge at top of ramp**	**San Cayetano fault**	**Total**
250±50 ka	0.4	0.7-2.5	1.3	0.5	1.8-2.9	4.7-7.6
975±75 ka	0.5	0.7-2.5	4.2-4.4	1.0	1.8-2.9	8.2-11.3

Table 3-3

Summary of Horizontal Shortening and Shortening Rates

Cross Section	250 ± 50 ka		975±75 ka	250±50 to 975±75 ka
	Total shortening	Shortening rate	Total shortening	Shortening rate
A-A'	3.4-7.1 km	23±12 mm/y	7.2-9.1 km	4±4 mm/y
B-B'	6.7-7.3 km	29±7 mm/y	10.2-10.8 km	5±2 mm/y
C-C'	4.7-7.6 km	27±11 mm/y	8.2-11.3 km	6±5 mm/y

horizontal shortening at the Ventura Avenue anticline in Figure 3-2. East of the Red Mountain fault and northwest of the displacement on the Oak Ridge fault at South Mountain, folding of the Ventura Avenue anticline is less as it plunges east and dies out. It is possible that the displacement not taken up in the fold is taken up on the Sisar décollement, in addition to the displacement due to the blind thrust. It is not possible to determine how much that displacement would be, though it is reasonable to assume that the total displacement of the Oak Ridge contribution to the displacement on the Sisar décollement plus the folding of the Ventura Avenue anticline does not exceed the 2.5 km on cross section A-A' (Figure 3-2). Thus, the displacement is considered to be between 2.0 and 2.5 km.

The dip of the homocline is well constrained at the surface and in oil wells. The dip of 66° is too steep for a fault-bend fold and must be the result of a duplex [Woodward et al., 1989], a fault-propagation fold that became horizontal when it propagated up to a weak formation [Mitra, 1990], or it could have folded previously tilted strata. The latter interpretation is preferred because geologic mapping by Dibblee [1987a, 1987b] suggests a gently south-dipping limb beneath Ojai Valley. A fault-propagation fold would have a longer north-dipping limb beneath Ojai Valley and a duplex would also have a more extensive backlimb than is observed.

Dips within the Saugus Formation at the east end of the Ventura Avenue anticline average 18° less than the dips in underlying strata [Weber et

al., 1973]. The Saugus Formation is folded in the Cañada Larga syncline east of the section, and this contact is projected westward into the air in this section. The minimum amount of movement that is post-Saugus is interpreted to be that amount that would move the synclinal hinge that projects up from the blind thrust fault tip far enough north to allow the Saugus Formation to wedge out on the homocline (Figure 3-3a, 3-3b). This yields 3.0 km of shortening along the upper flat of the blind thrust. An additional 1.4 km of shortening is taken up by steepening the strata as they pass through the hinge at the top of the ramp.

It is also possible that the Ojai Valley was once overlain by the Miocene-Pleistocene stratigraphy that is presently found in the Upper Ojai Valley. Additional movement on the blind thrust would have to be restored in order to lower the Ojai Valley block so that the top of Saugus would be restored to the same elevation as in the Santa Clara Valley. This is interpreted to be the maximum amount of movement on the blind thrust because it allows for the thickest accumulation of post-Sespe strata that is observed this far north. This increases the movement on the blind thrust to 3.1 km. Flattening of strata in the hanging-wall block of the Oak Ridge fault is 0.3 km. Total shortening on cross section B-B' since the end of Saugus deposition is 6.7-7.3 km, occurring at a rate of 29±7 mm/y. These amounts could be higher if there is more displacement on the Sisar décollement, transferred from the Oak Ridge fault. It is not possible with these data to determine how much more,

but 0.5 km of shortening has been taken into account in addition to the 2.0 km of shortening at the Ventura Avenue anticline so that the total equals the maximum observed shortening, 2.5 km, at the Ventura Avenue anticline at Figure 3-2.

The amount of uplift of the Taylor thrust between 250±50 ka and 975±75 ka is determined to be 71% of the total uplift. This is calculated using Figure 3-5 of Yeats [1983a]. The thickness between horizons 2 and 4 is unchanged across the Taylor thrust, inferring that horizon 4 predates movement on the fault. The thickness between the base of Saugus Formation and horizon 4 is 1.67 km in the footwall block of the fault and 0.83 km in the hanging-wall block. The difference, 0.84 km, is the total uplift. The thickness between horizons 4 and 5 is 0.46 km in the footwall block and 0.22 km in the hanging-wall block. The difference is the uplift prior to 975±75 ka, assuming constant deposition rates. This value is for vertical uplift in the plane of the cross section. Yet, tectonic transport of the Taylor thrust was S45°E based on a piercing point offset of isopachs [Hsü, 1977] and the trend of the Grubb and Taylor 99 tear faults [Yeats, 1983a]. Thus, rocks moved in and out of the plane of the cross section. The minimum displacement within the plane of the cross section is then 0 km. At horizon 5, Yeats [1983a] found 250 m of horizontal shortening in the north-south direction. This is the apparent displacement which only equals the dip-slip displacement in the dip-slip direction and increases to infinity in the strike direction. If 250 m is the

apparent displacement, and the trend of Figure 3-3 is 53° from the direction of dip-slip displacement, then the true displacement is (250 m)cos53° = 150 m. The component of true displacement in the line of Figure 3-3 must be cosine corrected again and is (250 m)$\cos^2$53° = 90 m. Thus, the amount of maximum displacement on the Taylor thrust in the plane of Figure 3-3 is rounded off to 0.1 km. The calculation of dip-slip displacement from apparent displacement in Yeats [1983a] was in error.

The amount of shortening taken up on the blind thrust between 250±50 ka and 1.025±.025 Ma is not well constrained. Fernando Formation with Venturian microfossils (QTf on Figures 3-2 to 3-4) is not observed north of the Lion fault in the Upper Ojai Valley [Huftile, 1991], and the overlying Mudpit Shale is not observed north of Sulphur Mountain (Figure 3-1). The minimum displacement on the blind thrust is considered to be that amount that would not lower the present-day stratigraphy so far that it allows deposition of any of the upper Fernando Formation in Ojai Valley. This value is 3.0 km, the minimum value at 250±50 ka, and, because it infers that thrusting ceased during that time, is probably not correct. The maximum displacement again assumes that the stratigraphy now present in the Upper Ojai Valley once overlay the stratigraphy in Ojai Valley, and the displacement on the blind thrust could be retrodeformed farther without allowing for deposition of the upper Fernando Formation that far north. This adds 2.2 km in displacement on the upper flat and 1.2 km in unfolding the hanging-wall block. The total

shortening since 975±75 ka is then 10.2-10.8 km. The shortening between 975±75 ka and 250±50 ka is then 2.9-4.1 km, and the rate of shortening is 5±2 mm/y (Tables 3-2, 3-3).

Cross section C-C'. This cross section crosses the western end of the San Cayetano fault and the south-dipping homocline, inferring that displacement is partitioned between the surface reverse fault and the blind thrust. The Lion fault set dips south and extends downward in bedding of the Miocene Rincon Formation [Huftile, 1988a, 1991]. At the surface, the Lion fault set is composed of the Lion, Sisar, and Big Canyon faults. Between the south-dipping Lion fault set and the north-dipping San Cayetano fault, the Upper Ojai Valley is underlain by as much as 600 m of Saugus Formation. The Saugus Formation is underlain, with angular unconformity, by strongly folded Pliocene and Miocene sedimentary rocks. The folds, the Lion Mountain anticline and Reeves syncline, are south-vergent and strata as young as early Repettian (early Pliocene) are folded. The age of the folding is between the early Repettian and the onset of Saugus deposition [Huftile, 1988a, 1991]. These folds are inferred to have been caused by a north-dipping fault.

The San Cayetano fault dips approximately 50°N west of Figure 3-4 to the base of well control [Huftile 1988a, 1991]. A focal mechanism solution was calculated for the 12 June 1984 earthquake focus, about 11 km to the east of this cross section, by Simila et al. [1987] and G. Simila [written communication, 1988]. The earthquakes show a dip of 50°N on the San Cayetano fault to a

depth of 16 km. Rockwell [1988] calculated slip rates for the western San Cayetano fault near Figure 3-4 using ^{14}C dating and correlation of soils on alluvial fans displaced by the fault as 1.05±0.2 mm/y. The rate of displacement decreases to zero to the west in the Ojai Valley, and it increases to the east. Folding of the hanging-wall block is not occurring, except at Bear Canyon [Rockwell, 1988], where the San Cayetano fault splits into a shallow-dipping lobate strand, and an active northern strand [Huftile, 1988a, 1991]. This is consistent with the observation that rocks in the hanging-wall block are overturned and have normal stratigraphic separation across the north strand of the San Cayetano fault, inferring that the overturning occurred prior to the faulting.

East of Figure 3-4, the San Cayetano fault has overridden both the nonmarine Saugus Formation in the Upper Ojai Valley and the south-dipping Lion fault set [Huftile, 1988a, 1991; Figure 3-1]. It is interpreted that all movement on the surface trace of the San Cayetano fault is post-Saugus because of the lack of sedimentary breccia in the Saugus near the San Cayetano fault. Gentle folds within the Saugus Formation at the Modelo lobe segment of the San Cayetano fault farther east are truncated by the fault [Yeats, 1983a; Huftile and Yeats, in prep.], and a nearly complete section of Saugus is entirely overthrust just east of Figure 3-4 [Huftile, 1988a, 1991]. The amount of displacement varies between 1.8 and 2.9 km based on how far the overturned limb in the hanging-wall block of the fault is projected into the

subsurface. If the strata pass through a hinge, becoming south-dipping, as high as well control allows, then displacement is maximized (as drawn in Figure 3-4a). If the overturned limb is allowed to project downward to the fault, displacement is minimized.

Timing of folding and faulting of the Sulphur Mountain anticlinorium is not well constrained. The Sulphur Mountain anticlinorium began moving later than 2.0-2.2 Ma according to Lagoe and Thompson [1988] and G. H. Blake [personal communication, 1987], because Venturian-age Pico member (QTf on Figures 3-2, 3-3, 3-4, 3-5, 3-7) of the Fernando Formation is the youngest formation folded in the Big Canyon syncline, within the Lion fault set. Yet, if the anticlinorium began forming prior to the onset of "Mudpit Shale" deposition, ~1.2 Ma, the "Mudpit Shale" would thin towards and onlap onto the south flank of the fold. The "Mudpit Shale" shows no such thinning; rather, it thickens slightly northward between well control at the Ventura Avenue anticline and its northernmost surface exposure. The Pliocene Fernando Formation in the Big Canyon syncline contains clasts derived from Miocene strata, and the Pleistocene Saugus Formation contains clasts derived from Eocene and Oligocene strata. This is interpreted as evidence of the unroofing of highlands to the north, with successively older source terranes providing clasts for progressively younger formations. Overlying the Saugus Formation is an alluvial-fan debris that is dominated by clasts derived from Eocene strata north in the Upper Ojai Valley, and dominated by clasts of Miocene strata to

the south in the Upper Ojai Valley [Figure 3-8 of Huftile, 1991; Schlueter, 1976; Rockwell, 1983, 1988] inferring the erosion of Miocene strata from Sulphur Mountain to the south. The Lion fault cuts the Saugus Formation and forms its southern boundary in the Upper Ojai Valley. Certainly some of the folding of the Sulphur Mountain anticlinorium and faulting of the Lion fault set is post-Saugus, but the timing of the onset of movement is uncertain.

The displacement on the Lion fault set and folding of the Sulphur Mountain anticlinorium is the result of passive backthrusting from the fault-bend fold and possibly some amount of deformation transferred from the Oak Ridge fault, but not taken up in folding of the Ventura Avenue anticline. In Figure 3-4, the Ventura Avenue anticline is plunging east, and dying out. In the plane of the cross section, there is only 0.7 km of shortening taken up in the fold. It is unlikely that the 2.5 km of vertical displacement on the Oak Ridge fault at South Mountain decreases to 0.7 km of folding at Figure 3-4 and increases farther east to 2.5 km of folding at Figure 3-2. Instead, the additional shortening not taken up in folding at the east end of the Ventura Avenue anticline is probably taken up at the Sulphur Mountain anticlinorium. The folding and the fault displacements at the Sulphur Mountain anticlinorium are drawn to show the minimum displacement. Yet, there is more displacement on the passive backthrust and associated folding than required by the fault-bend fold, implying that additional displacement could be transferred from the Oak

Ridge fault. Shortening at the Ventura Avenue anticline is 0.7 km with an additional 1.8 km at the Sulphur Mountain anticlinorium.

There is 0.4 km of shortening taken up by folding in the hanging-wall block of the Oak Ridge fault.

The top of the Saugus Formation in the Upper Ojai Valley must be lowered in elevation to that of the Saugus Formation in the Santa Clara Valley by removing displacement that has occurred on the ramp of the fault-bend fold. If the top of the Saugus Formation in the Upper Ojai Valley is the same age as that in the Santa Clara Valley to the south, as implied by Figure 3-4b, then flattening the Saugus requires that some of the Sulphur Mountain structure predates Saugus. If the top of the Saugus in the Upper Ojai Valley is older than that in the Santa Clara Valley, inferring a greater thickness partially removed by erosion, its elevation would have to be reduced more, decreasing the amount of folding at Sulphur Mountain and increasing the amount of displacement on the fault-bend fold. This requires 1.3 km of displacement along the upper flat of the fault-bend fold and an additional 0.5 km of shortening taken up by folding the rocks as they pass through the hinge at the top of the ramp.

The total horizontal shortening is 4.7-7.6 km. The shortening rate along Figure 3-4 is 2.5±1.3 cm/y.

Between 250±50 ka and 975±75 ka there was additional unfolding of rocks in the hanging-wall block of the Oak Ridge fault and movement along the blind thrust. Folding at the Oak Ridge fault is minimal, 0.1 km.

Folding at the Sulphur Mountain anticlinorium is constrained by the deposition of some Venturian-age Fernando Formation within the Big Canyon syncline, in a fault block bordered by faults of the Lion fault set. North of the Lion fault set, there is no deposition between Repettian-age Fernando Formation, which is strongly folded, and Pleistocene Saugus Formation, which is not. The Lion Mountain anticline, Reeves syncline, and the Matilija overturn are interpreted to entirely precede 975±75 ka because the overturned limb in Carpinteria basin is overlain by the Santa Barbara Formation, approximately age equivalent to the Mudpit Shale. Figure 3-4c is drawn with the minimum displacement that would allow deposition of the 0.3 km [Huftile, 1988a, 1991] of Venturian-age Fernando in the Big Canyon syncline. The geometry of the Lion Mountain anticline infers that no Venturian age Fernando Formation was deposited north of the Lion fault set. This requires 2.9 km of displacement on the blind thrust plus 0.5 km of folding at the hinge above the ramp. An additional 0.2 km of shortening is possible if all displacement on the blind thrust is restored, and the Venturian in the Big Canyon syncline was originally thicker than 0.3 km.

Total shortening at 975±75 ka along Figure 3-4 is 8.2-11.3 km. The shortening between 250±50 ka and 975±75 ka was 0.6-6.6 km and the shortening rate was 6±5 mm/y (Tables 3-2, 3-3).

RESIDUAL GRAVITY MODELING

Figures 3-9 and 3-10a-f are the residual gravity verification of the balanced structural cross sections in which structural methods have been used to predict the locations of structures beneath the data set. The balanced cross sections are checked for agreement with an independent data set. The verification does not prove the structural interpretation, but either allows the interpretation or denies it.

The isostatic residual gravity (Figure 3-9) is from A. Griscom [written communication, 1991; see Jachens and Griscom, 1985 and Griscom and Sauer, 1991]. The isostatic residual removes the effects of topography and the Moho so that the residual, high-frequency gravity anomaly is the gravitational expression of shallow crustal structure.

Figure 3-10a is the first pass at gravity modeling Figure 3-2a. Densities are from neutron density logs of oil wells listed in Table 3-4. Table 3-4 also shows the range of measured densities for various formations. A density of 2.60 was determined for Eocene and older formations, not penetrated by nearby wells, using the method of Nettleton [1971] for determining near-surface density over topographic relief. The calculated curve for Figure 3-10a-f is pinned to the observed curve many km to the north. To the north in Figure 3-10a, mostly Cretaceous sedimentary rocks are at the surface. These rocks have probably been buried deeply, and the density is near that of average crust, 2.67 g/cm^3. Thus, the anomaly at the north is approximately horizontal and is about

Figure 3-9: Map showing residual gravity over the study area from A. Griscom [written communication, 1991] that was used to model the structural cross sections. The locations of Figures 2-4 are shown in heavy dashed lines. The coastlines are shown is a diagonal dashed pattern. Fault traces have a shaded pattern. SCF is the San Cayeatno fault. The contour interval is 10 mgal.

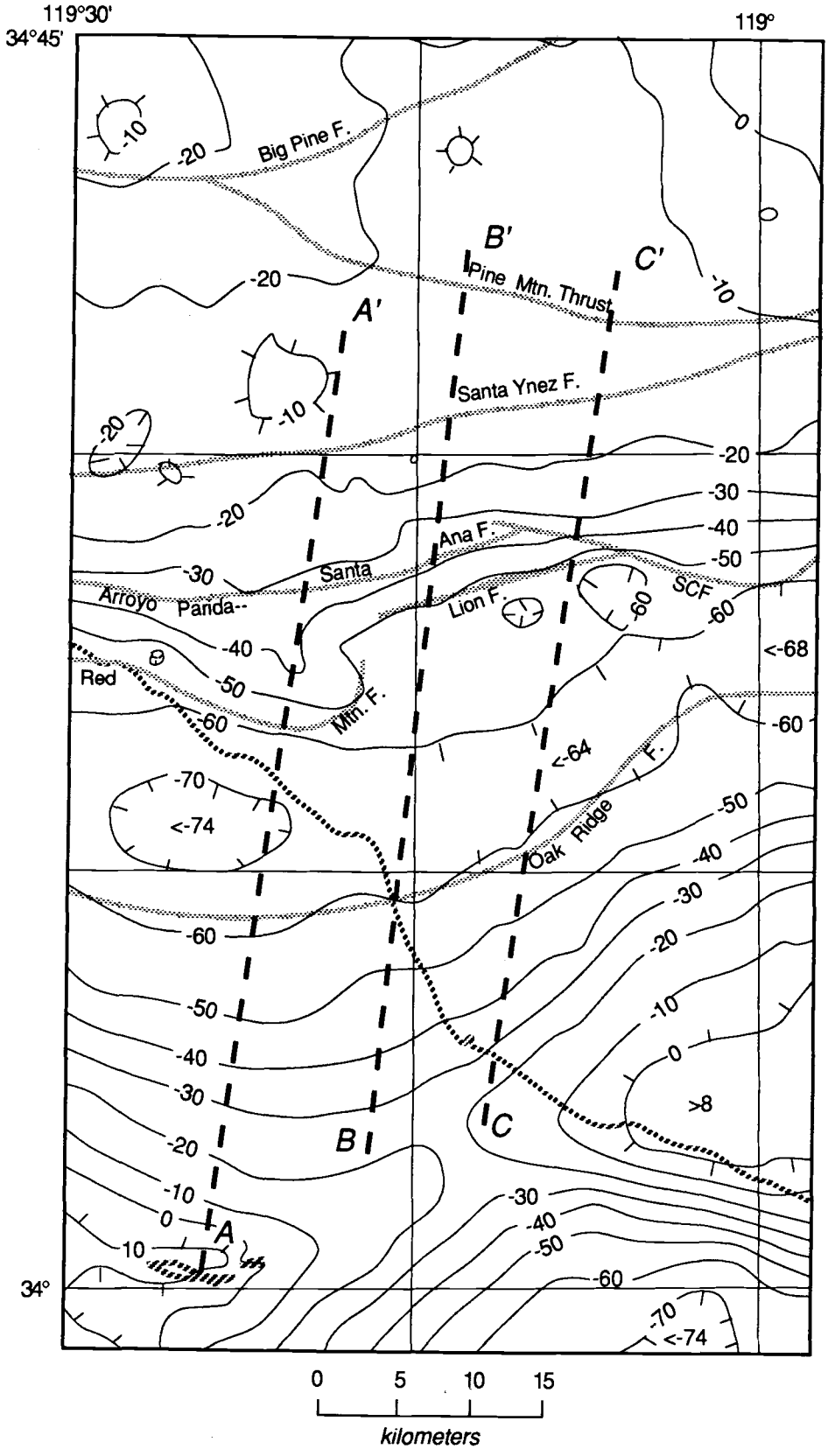
119°30'
119°
34°45'
34°
Big Pine F.
Pine Mtn. Thrust
Santa Ynez F.
Santa Ana F.
Arroyo Parida--Santa Ana F.
Red Mtn. F.
Lion F.
SCF
Oak Ridge F.
A
A'
B
B'
C
C'
-10
-20
-30
-40
-50
-60
-70
<-74
<-68
<-64
0
>8
0
5
10
15
kilometers

Figure 3-9

Figure 3-10: Residual gravity models of structural cross sections, Figures 3-2, 3-3, 3-4. **(a)** first pass model along Figure 3-2 using densities from neutron density logs from oil wells (Table 3-4). **(b)** altered model of Figure 3-2 showing that adjusted densities is sufficient to match the observed residual gravity, and that no adjustment of the structural interpretation is needed. **(c)** and **(d)** first pass and altered models of Figure 3-3. **(e)** and **(f)** first pass and altered models of Figure 3-4.

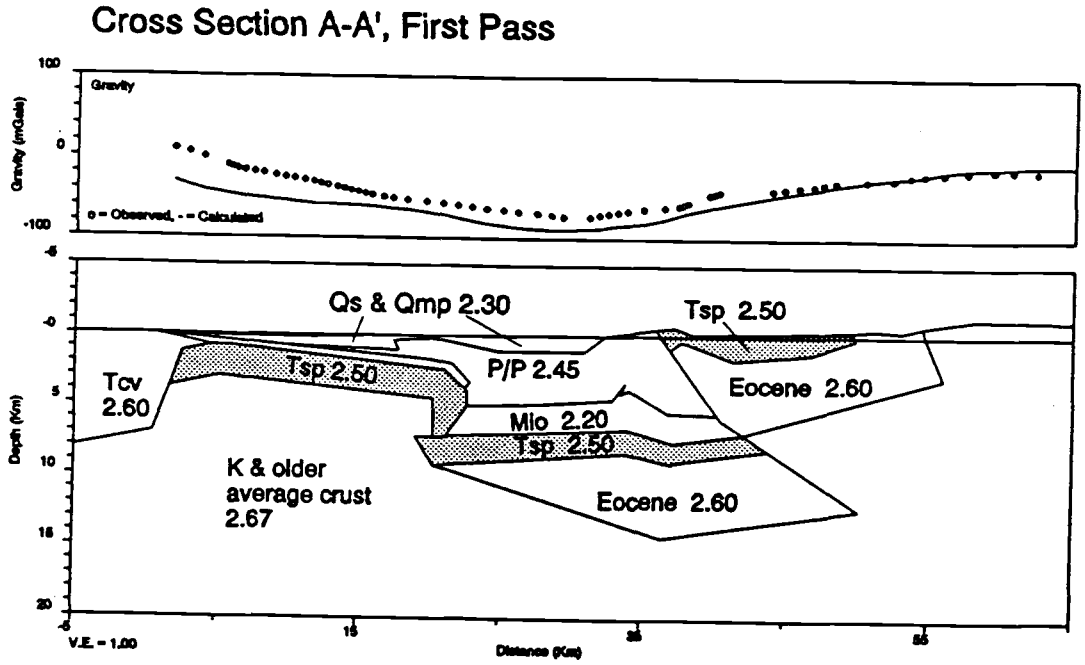

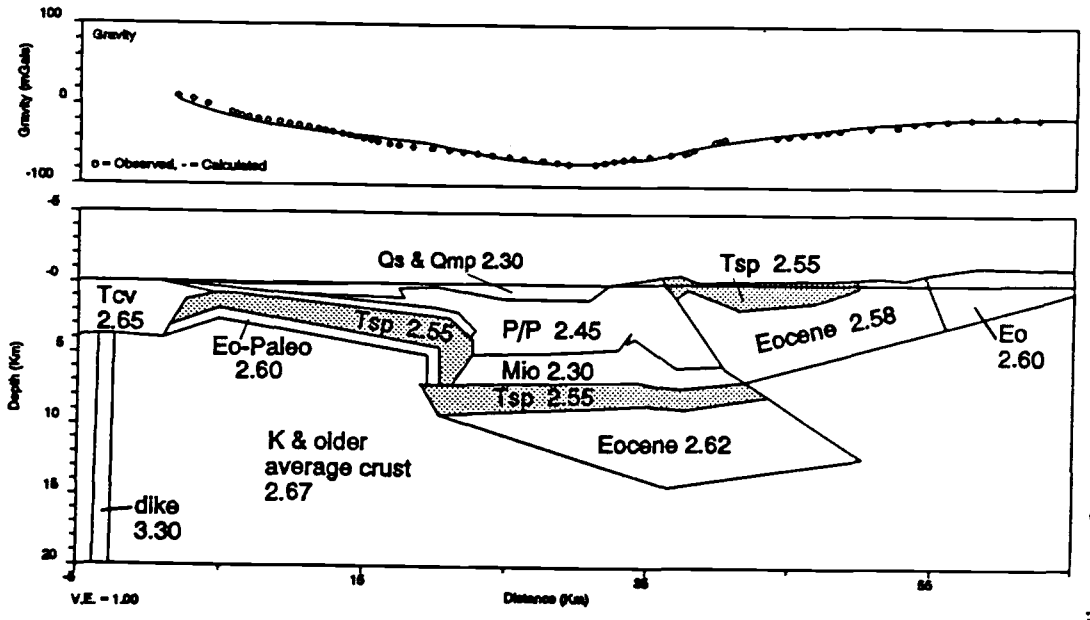

Figures 3-10a and 3-10b

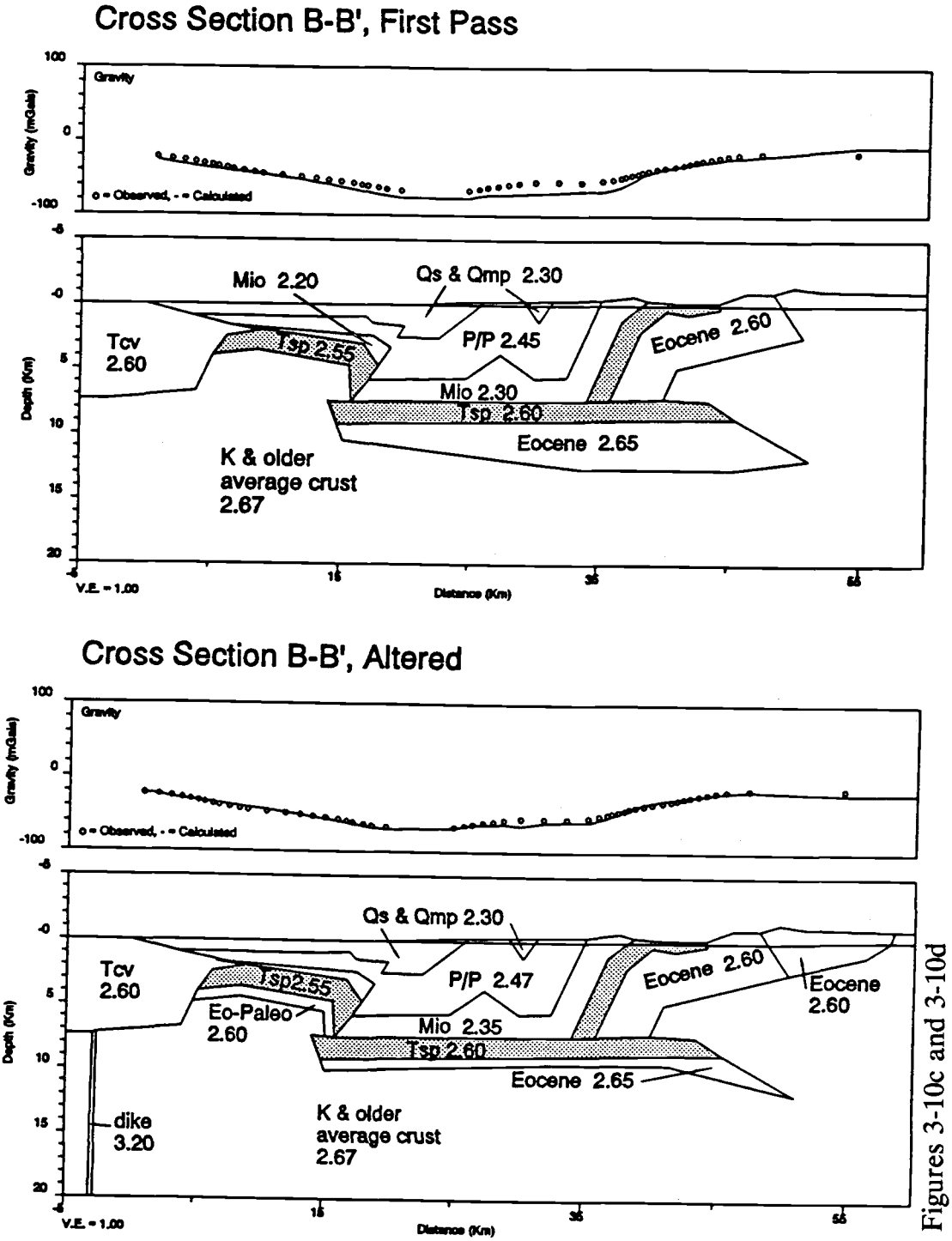

Figures 3-10c and 3-10d

Cross Section C-C', First Pass

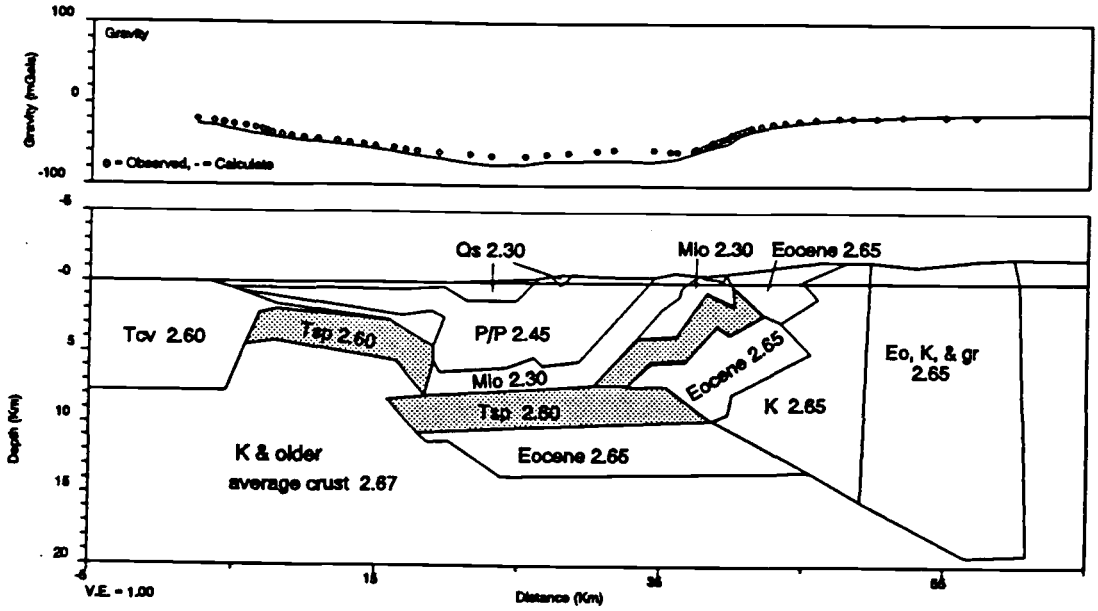

Cross Section C-C', Altered

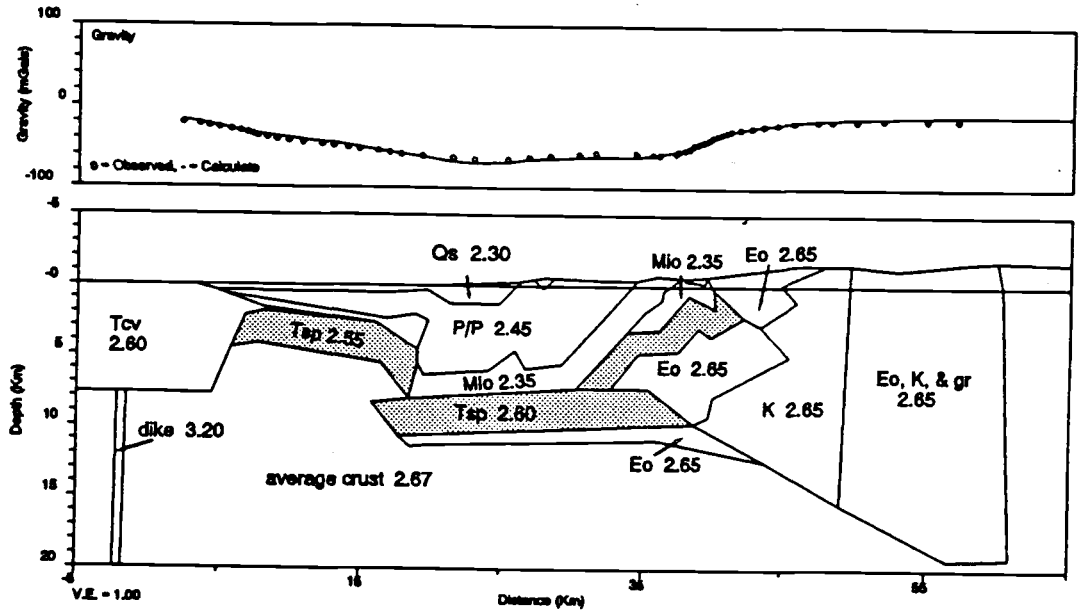

Figures 3-10e and 3-10f

Table 3-4

Densities used in Modeling of Residual Gravity Anomalies

Symbol	Formation(s)	Well Density Range(g/cc)	Wells
Pleis	Saugus Fm. & Mudpit Shale	2.22-2.40	Laura Lawton 1, Ojai 404
Plio	Fernando Fm.	2.34-2.45	Laura Lawton 1, NLF 1, Utsuki-Burns 1, Barker-Ferndale 3 & 6, [*McCulloh*, 1960]
Mio	Sisquoc, Monterey, Rincon	1.98-2.45	Utsuki-Burns 1, Ex-Mission 4, Ojai 404, Sakioka 1, Nesbitt 2, Barker-Ferndale 3 & 6, Sulphur Crest 8
Tcv	Conejo Volcanics	2.3-2.65	Sakioka 1
Tsp	Vaqueros & Sespe Fms.	2.43-2.50	Hoffman 1-10, Ojai 404, Sakioka 1, Anderson 1
Eo	Coldwater & Cozy Dell Fms.	2.43-2.51	Newton 1, Anderson 1, Nesbitt 2

0 mgal. The calculated Ventura basin anomaly is lower than the observed anomaly, implying that the structure is incorrect or that the densities used are too low. To the south, an arbitrary base of the Conejo Volcanics is inferred. The anomaly to the south is quite a bit lower than the observed, implying a smaller volcanic pile or possibly a high-density root beneath it. Neither of these possibilities affects the calculation of shortening.

Figure 3-10b shows that by altering the densities within the ranges on Table 3-4, plus the addition of a high-density dike to the south, the calculated curve closely approximates the observed. Some additional formations have been separated from other blocks in order to better match the anomalies. The residual gravity models predict the thickness of the Pliocene-Pleistocene basin, honoring the observed density ranges, and changes in the slope of the observed anomaly may indicate bedding and fault dips at depth.

Figures 3-10c and 3-10d show the first pass and the altered residual gravity models along Figure 3-3. The densities in Figure 10b are used in the first pass (Figure 3-10c). The basin anomaly is too large, implying that densities must still be higher or the sedimentary basin thinner. Figure 3-10d shows both of these alternatives provides a good fit. Neither of these alternatives affects the estimate of shortening. A thin, high density dike to the south is a possibility.

Figures 3-10e and 3-10f show the first pass and the altered residual gravity models along Figure 3-4. The slope of the observed curve above the

Upper Ojai Valley is modeled fairly well, but again the basin anomaly is not. Higher densities and a thinner Eocene sequence in the center of the basin is sufficient to match the observed anomaly. As for the previous figures, these alternatives have no effect on shortening estimates.

In this case, residual gravity modeling forced no changes in the cross sections that would alter estimates of shortening. Yet, this method of modeling residual gravity over near-surface structures, and over cross sections constructed using structural methods remains a valuable one. In particular, it constrains the thicknesses of basins, shows low density rocks that have been overthrust, and it may confirm or deny dips of strata and faults. All of these corrections may greatly affect calculations of shortening.

DISCUSSION

Donnellan et al. [in prep.] determined the rate of crustal convergence using Global Positioning System measurements for several Ventura basin sites over a time span of 2.7 years. They determined a crustal shortening rate of 7±2 mm/y, much slower than the rates determined here by the offset of bedrock horizons. This suggests that strain is accumulating and will be released by earthquakes. The cycle of seismic activity must be longer than the 200-year historical record. Some of the strain may be taken up by creep on the Oak Ridge, Red Mountain, and San Cayetano faults beneath a locked zone near the surface, but there is no evidence of creep at the surface.

The three cross sections in this paper are too close together, and the rates of shortening could be the same, allowing for the error bars. Thus, these cross sections cannot alone address the tectonic models of southern California [Weldon and Humphreys, 1986; Bird and Rosenstock, 1984; Chen and Minster, 1991]. Future work in the east Ventura basin (Figure 3-1) will address this using the same methods as in this paper. The east Ventura basin is far enough away from the cross sections shown in this paper to determine if there is a change in shortening rates laterally along the basin. Then any difference in the shortening rates between the east and west Ventura basin can be compared to the crustal models.

CONCLUSIONS

In the central Ventura basin, south-vergent shortening in the central Ventura basin is taken up on surface reverse faults, blind thrusts, and by a combination of the two. North-vergent shortening is transferred from the Oak Ridge surface reverse fault, with 2.5 km of vertical displacement at South Mountain, to the Ventura Avenue-Rincon anticline in the west. Yet, horizontal shortening and shortening rates are fairly consistent. Tables 3-2 and 3-3 summarize the horizontal shortening and shortening rates on the three cross sections. This may imply an increase in convergence from west to east, although, within the error bars, the shortening and shortening rates could be equal along all three cross sections. The convergence rates are somewhat consistent with earlier estimates by Yeats [1981, 1983a] of 2.0 cm/y and Rockwell [1983] of 1.7±0.4 cm/y.

APPENDIX

Constraints on the method of using balanced cross sections in determining crustal convergence rates. The use of balanced cross sections in calculating crustal convergence rates is based on the structural techniques of Woodward et al. [1989] which predict the location of folds and faults beneath the data set. The use of the kink method of modeling the structures with straight limbs and abrupt hinges fits the data well in most places, with the exception of the Sulphur Mountain anticlinorium and the Ventura Avenue anticline. There, bed length is preserved in the models, but no effort is made to model the folds as kinks.

In using these techniques to calculate crustal convergence rates, we adhere to several conditions which serve to ensure the accuracy of the cross sections and address the way in which the data should be presented. We construct a series of cross sections in the study area. This allows a regional consistency in the geologic interpretation that is not afforded by a single cross section. In this study, three structural segments of south-verging structures of the central Ventura basin are represented. The western segment has a surface reverse fault, the Red Mountain fault. Across a transfer zone at the east end of the Red Mountain fault, south-verging displacement is taken up on a blind thrust. The eastern segment has both a surface reverse fault, the western San Cayetano, and the blind thrust. Cross sections across each segment, each constructed with an independent data set, should have similar estimates of

shortening and convergence rates or those estimates should vary smoothly along strike.

Mapped structures should be projected down plunge or up plunge into the section. Offhand, this seems obvious. However, there are geologic indications that can be far away from the cross section that could illustrate how a cross section should be drawn. Within the study area, the only indication of the age of the Matilija overturn depends on the interpretation of the north limb of the Reeves syncline being part of the Matilija overturn. The Matilija overturn strikes west between the Santa Ynez fault on the north and the Arroyo Parida fault on the south. North of Santa Barbara, the overturn occurs south of the Arroyo Parida fault and is overlain with angular unconformity by the Pleistocene Santa Barbara Formation [Jackson and Yeats, 1982] which is approximately age-equivalent to the Mudpit Shale in this study area. Thus, the Matilija overturn is older than 1 Ma and should remain after retrodeformation to that time. Another example is the dip of bedding south of the Matilija overturn, in Ojai Valley. This limb is covered by alluvium where cross section B-B' (Figure 3-3) and sections by Namson [1987], Namson and Davis [1989], and Laird [1988] cross the valley. All the previously published sections assume that the limb dips are roughly parallel to the ramp of the blind thrust (~30°N) that is interpreted to lie beneath the Ojai Valley. Structurally, in drawing a balanced cross section, this may be the expedient interpretation. This interpretation results a tightly-folded syncline to a depth of several km, with

both limbs of the fold dipping north. However, several km to the west, where these rocks are exposed, Dibblee [1987a, 1987b] shows that the limb immediately south of the overturned limb dips ~30°S. Projecting this geometry into cross section B-B' greatly alters the interpretation and the total bed length of the strata.

We have routinely become involved in detailed interpretation of relatively small areas in order to construct a cross section through that area. Huftile [1991] is such a study, covering the Upper Ojai Valley area. A reprocessed and recorrelated seismic-reflection profile verifies the interpretation of a blind thrust at depth and locates the base of the sedimentary section.

Cross sections should be drawn in the direction of tectonic transport so that the displacement of structural elements remains in the two-dimensional section. In this study, we use a piercing-point offset across a fault, earthquake focal mechanisms, and borehole breakouts to determine that this direction is NNE.

Cross sections should be retrodeformed in steps, flattening well-dated horizons. This allows for the calculation of convergence rates since the deposition of the youngest, well-dated deformed beds. Retrodeformation that removes all displacement over a longer period of time has little relation to current crustal convergence rates. Retrodeformation to a horizon beneath the present surface, removing the overlying strata, requires that the remaining

strata be decompacted using backstripping techniques. Thus, the retrodeformed cross sections remain geologic in nature, apt to allow for the deposition that is now known to have occurred. For this study, decompaction curves were calculated using the Subside software of Hsui [1989]. Several one-dimensional backstripping operations were calculated for each cross section.

Alternate interpretations that would affect convergence rates should be reported along with the possible affects on convergence rates. The modeling of residual gravity over the cross sections can validate or deny the structural interpretation with an independent data set.

Chapter 4:

Crustal Convergence Across the Modelo Lobe Segment of the San Cayetano Fault: Implications for Crustal Kinematic Models of Southern California

ABSTRACT

The central Ventura basin contains a thick accumulation of Plio-Pleistocene sedimentary rocks bordered by opposing reverse faults, on the north by the north-dipping San Cayetano fault and on the south by the south-dipping Oak Ridge fault. Deformation can be separated into three phases: (1) pre-Vaqueros (late Oligocene-early Miocene) tilting in the hanging-wall block of the Oak Ridge fault that is coincident with normal faulting farther south at Big Mountain and to the east in the east Ventura basin, (2) pre-Pleistocene reverse faulting and folding, and (3) Quaternary deformation. Strands of the San Cayetano and Oak Ridge faults offset late Quaternary surfaces. East of Sespe Creek, the San Cayetano fault has a lobate surface trace, called here the Modelo lobe segment. The Oak Ridge fault is steeply dipping, but it has low dips in its upper 2.5 km. The Simi fault was, in part, a normal fault during the middle Miocene deposition of the Conejo Volcanics and has been reactivated as a reverse fault in the Quaternary. A balanced and retrodeformed cross section constrains shortening in this segment of the Ventura basin. Post-Saugus Formation shortening is 4.1-7.1 km in the last 250±50 ka, occuring at a rate of 25±11 mm/y. Post-Fernando Formation shortening is 14.4-16.2 km in the last

975±75 ka. Displacement rates between 250±50 ka and 975±75 ka is 14±6 mm/y.

INTRODUCTION

The Red Mountain, San Cayetano, and Santa Susana faults are part of a south-verging zone of reverse faults extending from the western Santa Barbara Channel to the San Andreas fault near San Bernardino (Figure 4-1). In the central Ventura basin, this Quaternary fault system coincides with the northern edge of the thick Pliocene-Pleistocene trough. However, in the east Ventura basin, the south-verging Santa Susana fault is south of the trough, not north of it, and this fault marks a zone in which the trough sequence is thrust southward over its own structural shelf (Yeats, 1979). The trough sequence and its northern structural shelf are deformed in a fold belt. Young reverse faults cut these folds, but except for two, the Holser and Del Valle faults, displacements are relatively small. A geologic map of the east Ventura basin and surrounding area (after Yeats et al., submitted) is shown in Figure 4-2.

On the south side of the Santa Clara Valley, the hanging-wall block of the Oak Ridge fault contains strata as old as Oligocene at the surface. Farther east, the Oak Ridge fault divides into three strands (Figure 4-1), and only the northern strand at the edge of the Santa Clara Valley appears to be active. In the subsurface of the hanging-wall block of the Oak Ridge fault, wells penetrate strata as old as Paleocene (Seedorf, 1983). On the north side of the Santa Clara Valley, the Modelo lobe of the San Cayetano fault consists of a fold belt of Miocene strata with fold axes roughly parallel to the southward-convex surface trace of the fault.

Figure 4-1: Index map showing the locations of folds and faults in the study area, cross section A-A' (Figure 4-3), areas of Figures 4-2 and 4-4a. The large arrow points to the downdip compression direction of a focal mechanism solution of Yerkes and Lee (1979). SC is Sespe Creek, and WF is the Whitaker fault.

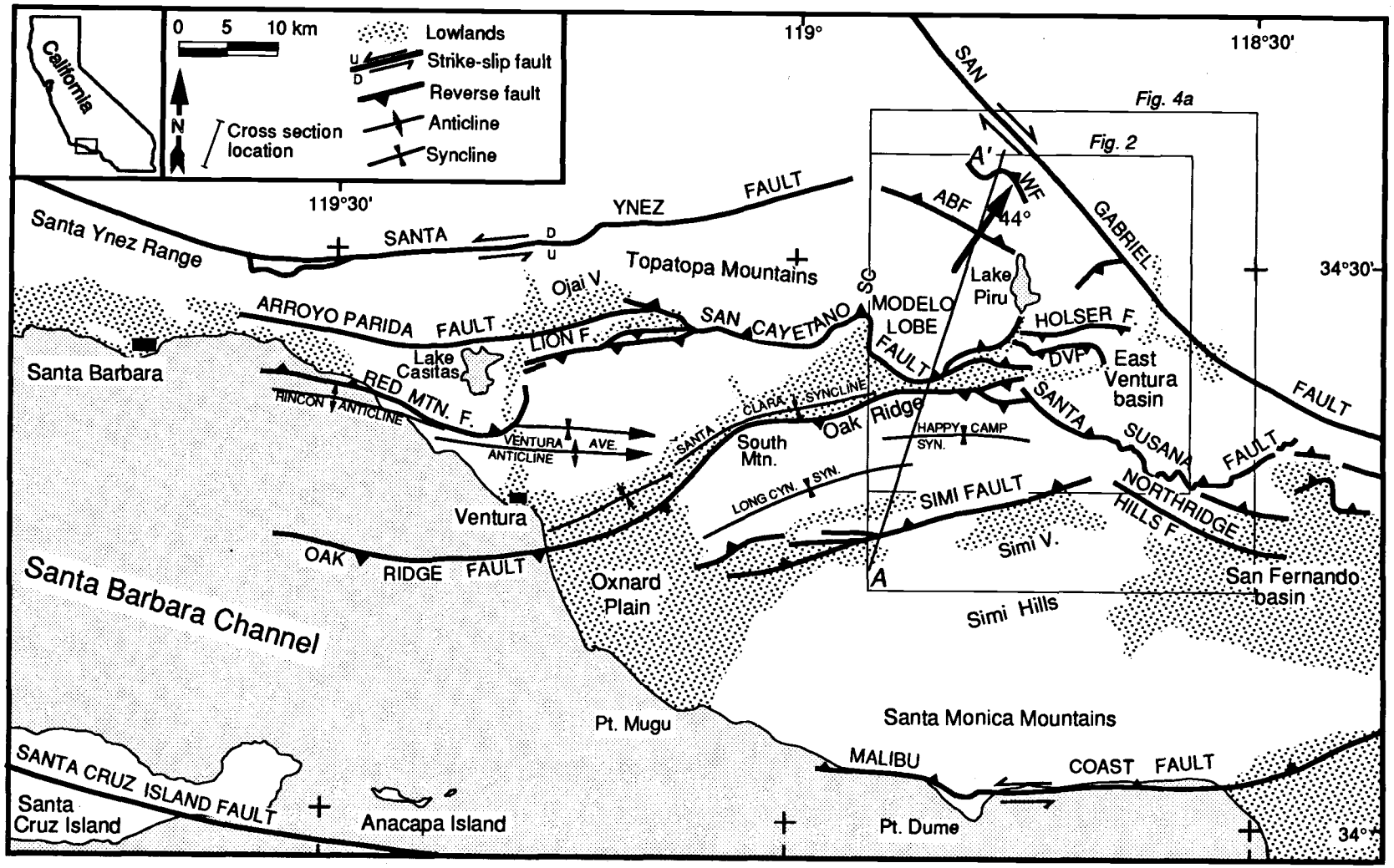
California
0 5 10 km
N
Cross section location
Lowlands
Strike-slip fault
Reverse fault
Anticline
Syncline
119°
118°30'
119°30'
34°30'
34°
44°
Fig. 4a
Fig. 2
SAN GABRIEL FAULT
A'
A
WF
ABF
SCC
Lake Piru
Santa Ynez Range
SANTA YNEZ FAULT
Topatopa Mountains
Ojai V.
ARROYO PARIDA FAULT
LION F.
SAN CAYETANO FAULT
MODELO LOBE
HOLSER F.
DVF
East Ventura basin
Lake Casitas
Santa Barbara
RED MTN. F.
RINCON ANTICLINE
VENTURA AVE. ANTICLINE
SANTA CLARA SYNCLINE
Oak Ridge
HAPPY CAMP SYN.
SANTA SUSANA FAULT
South Mtn.
LONG CYN. SYN.
SIMI FAULT
NORTHRIDGE HILLS F.
Ventura
OAK RIDGE FAULT
Simi V.
Oxnard Plain
San Fernando basin
Simi Hills
Santa Barbara Channel
Pt. Mugu
Santa Monica Mountains
MALIBU COAST FAULT
SANTA CRUZ ISLAND FAULT
Santa Cruz Island
Anacapa Island
Pt. Dume

Figure 4-1

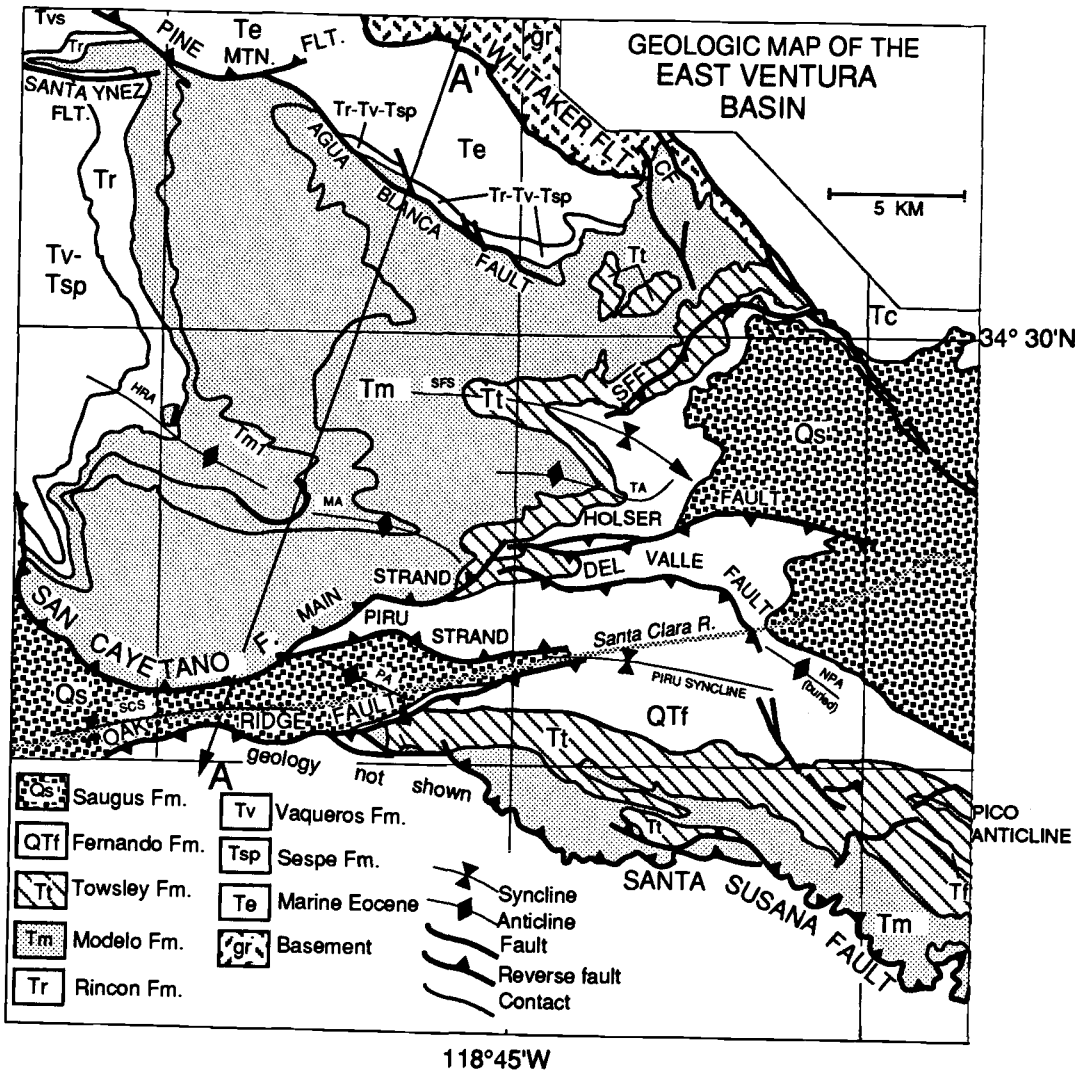

Figure 4-2: Geologic map of the east Ventura basin and the Modelo lobe area. Abbreviations: HRA- Hopper Ranch anticline, MA- Modelo anticline, SFS- Santa Felicia syncline, TA- Temescal anticline, SCS- Santa Clara syncline, PA- Piru anticline, NPA- Newhall-Potrero anticline.

Shortening in the western Transverse Ranges is taken up on both north- and south-verging structures, including outcropping reverse faults, blind thrusts, and folds. This paper addresses crustal shortening and shorteningrates across the Modelo lobe segment of the San Cayetano fault and the Oak Ridge fault.

A model of the structural geology is presented in a balanced cross section (Figure 4-3). The cross section is drawn in the direction of tectonic transport shown by the large arrow on Figure 4-1 which points down dip at 44°N based on a focal mechanism solution of Yerkes and Lee (1979). The tectonic transport diection is also discussed by Yeats et al. (1988) and Huftile and Yeats (submitted).

Hadley and Kanamori (1977) suggested that the surface trace of the San Andreas fault in the big bend area does not correspond with the plate boundary between the Pacific and North American plates, based on the identification of anomalous, high-velocity mantle that spans the fault. This interpretation implies that the plate boundary between the San Andreas fault and the eastern edge of the mantle anomaly must be a horizontal thrust. Hadley and Kanamori (1978) subsequently found some earthquakes at mid-crustal depths beneath the central Transverse Ranges with horizontal nodal planes. Webb and Kanamori (1985) found additional occurrences of near-horizontal nodal planes at mid-crustal depths beneath the Transverse Ranges and the San Emigdio Mountains. They argued that a regional, mid-crustal décollement lies beneath the Transverse Ranges. Yeats (1981a) suggested that

Figure 4-3: (a) Present-day structure of the Modelo lobe segment of the San Cayetano fault and Oak Ridge fault. Abbreviations: BA- Buckhorn anticline, HRA- Hopper Ranch anticline, SCS- Santa Clara syncline, PA- Piru anticline, PS- Piru syncline, 1- Arco Laura Lawton 1 well, 2- Texas Lawton 1 well, 3- Union Moran 1 well, Qs- Saugus Formation, QTf- Fernando Formation, Tfr- Repettian age Fernando Formation, Tt- Towsley Formation, Tm- Modelo Formation, Tm1- lower shale member of the Modelo Formation, Tm2- lower sandstone member of the Modelo Formation, Tm3- middle shale member of the Modelo Formation, Tm4- upper sandstone member of the Modelo Formation, Tr- Rincon Formation, Tcv- Conejo Volcanics, Ttp- Topanga Formation, Tv- Vaqueros Formation, Tsp- Sespe Formation, Te- unnamed Eocene strata, Tll- Llajas Formation, Tpl- Paleocene strata, K- Cretaceous strata.

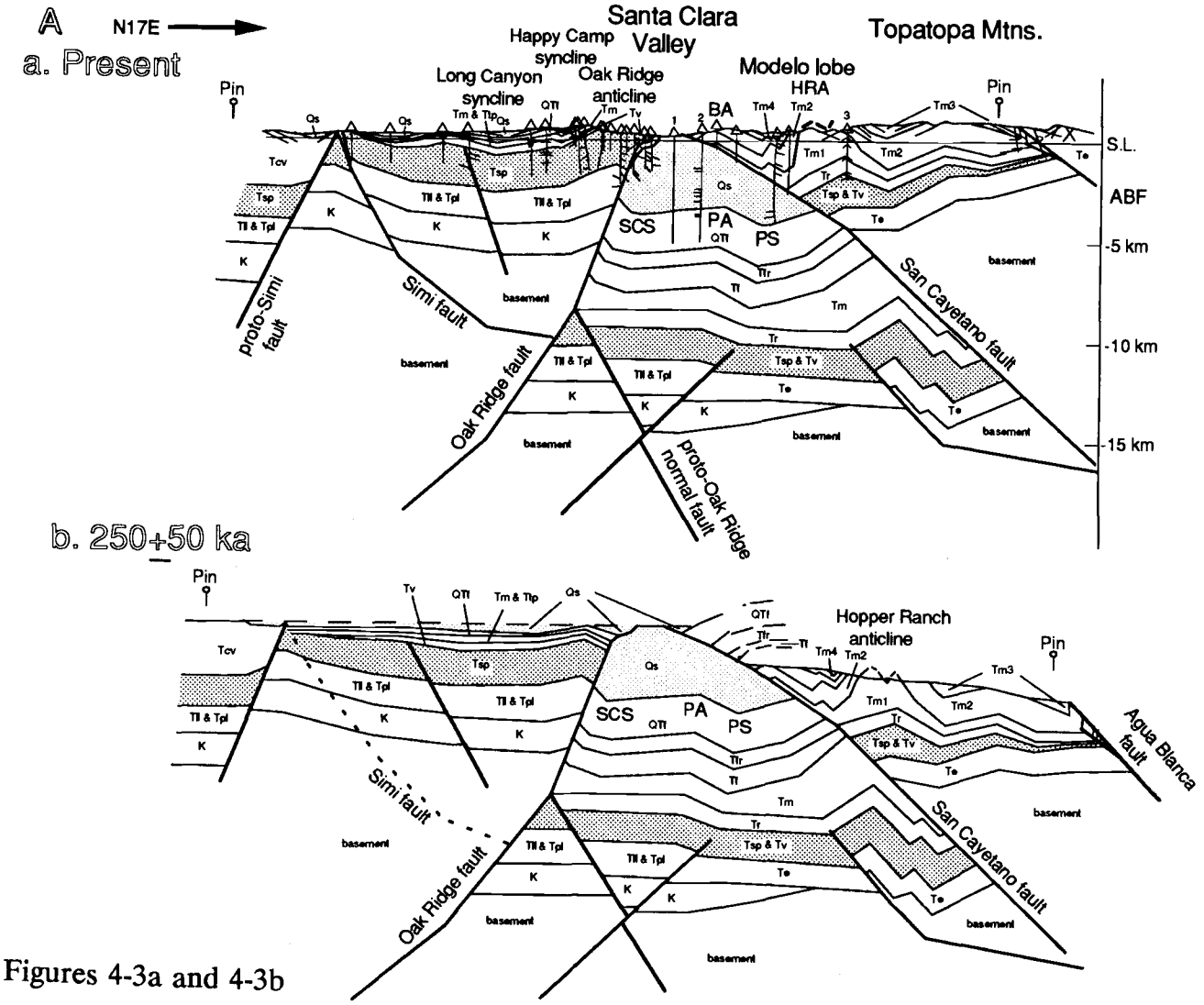

Figures 4-3a and 4-3b

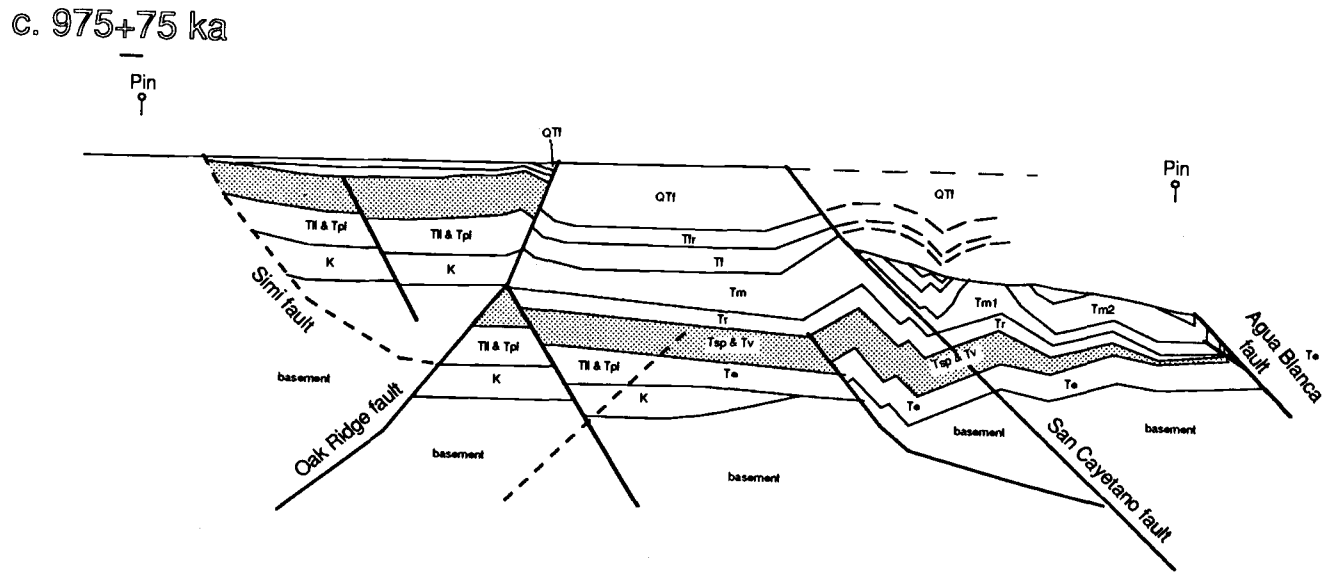
c. 975+75 ka
Pin
QTl
Tll & Tpl
K
Tlr
Tl
Tm
Tr
Tsp & Tv
Te
Tm1
Tm2
basement
Simi fault
Oak Ridge fault
San Cayetano fault
Agua Blanca fault

Figure 4-3c

the central Transverse Ranges are a "tectonic flake," using the terminology of Oxburgh (1972). Later, Yeats (1983a) noted that the mid-crustal décollement coincides with the base of earthquakes and concluded that the décollement marked the rheological change between high-strength, brittle rocks and underlying ductile rocks. Shortening occurring at the horizontal brittle-plastic transition is equal to the dip-slip displacement of an associated surface reverse fault plus the shortening taken up in folding.

The cross section in Figure 4-3 is retrodeformed back to the top of the Pleistocene Saugus Formation, estimated to be 250±50 ka (Lajoie et al., 1982; Yerkes et al., 1987; Lajoie et al., 1991) in the central Ventura basin and estimated to be 400 ka (Levi et al., 1986 and in press) in the east Ventura basin in order to determine the amount of structural shortening and rate of deformation since Saugus deposition ended. This allows the determination of convergence rates for only the youngest structures formed after the end of Saugus deposition. The cross sections are then retrodeformed to horizon 5 of Yeats (1981b) which is at the base of the Saugus Formation near the Modelo lobe, estimated to be 975±75 ka (Blackie and Yeats, 1976). This was done to document the increase in convergence rates over the last few hundred thousand years. Emphasis is placed on putting upper and lower bounds on the deformation, rather than defending a favorite interpretation.

STRATIGRAPHY

Overview of stratigraphy. West of the Canton fault (CF on Figure 4-2), a splay of the San Gabriel fault, the basement consists of the Whitaker granodiorite of Shepherd (1960) which is thrust over Paleogene strata along the Whitaker fault (Figures 4-1, 4-2, 4-3). In the Piru Creek area, north of Lake Piru (Figure 4-1), basement is composed of Precambrian gneiss and Mesozoic granodiorite (Yeats et al., 1985). There, upper Paleocene to upper Eocene conglomerate, sandstone, and shale rest unconformably on granitic basement (Nilsen and Clarke, 1975; Kriz, 1947). At the east end of the outcrop belt, middle and upper Eocene strata (Shepherd, 1960; Squires, 1977) are in fault contact with granitic basement along the Whitaker fault (Figure 4-2), which Shepherd (1960) regarded as an overturned, sheared unconformity.

South of the Oak Ridge fault, the well-known sedimentary section of the Simi Hills and Simi Valley has been traced to the footwall of the Santa Susana fault (Yeats, 1979; Seedorf, 1983). At least 2000 m of Upper Cretaceous deep-water strata (base not exposed), largely turbidites, are found in the Simi Hills, with the base not exposed. The nonmarine Paleocene Calabasas Formation of the western Simi Valley is overlapped eastward by Paleocene-Eocene Santa Susana Formation, which is predominantly deep-water mudstone with a basal conglomerate (Yeats, 1987; Zinsmeister, 1974). Paleocene strata are 500 m thick in the Union Torrey 92 well, ~2.7 km east of Figure 4-3 (Seedorf, 1983).

The Eocene Llajas Formation is composed of sandstone, siltstone, and shale. It is 1500 m thick in the Shell Dryden 2 well ~7 km west of Figure 4-3, and it is 900 m thick in the Union Torrey 92 well (Seedorf, 1983).

Late Eocene to early Miocene nonmarine Sespe Formation and the lower Miocene shallow marine Vaqueros Formation form the top of a sandstone-rich, competent sequence. To the north, the Sespe Formation is composed of well-indurated maroon sandstone which thins to the north. In the south, it is thicker, varigated, and much less indurated, though it is nevertheless sandstone rich. In the type section along lower Sespe Creek (Figure 4-1), Eschner (1957) reported 853 m of exposed section. Downplunge, the Union Moran 1 (well 3 on Figure 4-3a) well is the easternmost well north of the San Cayetano fault to reach the Sespe Formation. To the north, J. C. Crowell (1953, unpublished mapping) shows approximately 150 m of the sandstone. The Vaqueros Formation is composed of transgressive marine sandstone and siltstone deposited in shallow water (Edwards, 1971; Jestes, 1957). The Vaqueros is exposed south of the Oak Ridge fault where it was shown by Jestes (1957) to be 472 m thick. The formation thins to the east because of pre-middle Miocene erosion (Huftile, 1988b). It is composed of sandstone interbedded with siltstone (Ricketts and Whaley, 1975). Hall et al. (1967) and Canter (1974) show that the contact with the underlying Sespe Formation is unconformable at Big Mountain (Figure 4-1) as does Huftile (1988a, b) at Wiley Canyon, just east of Figure 4-3. North of the San Cayetano fault, the

Vaqueros Formation is exposed in the northwest corner of Figure 4-2 (Huftile and Yeats, submitted; Dibblee, 1990; Eschner, 1957; Edwards, 1971; Çemen, 1977, 1989; Argo Petroleum, 1982) and in the hanging-wall block of the Agua Blanca fault (J. C. Crowell, 1953, unpublished mapping; Yeats et al., 1985). Edwards measured 165 m of Vaqueros along Little Sespe Creek (Figure 4-1). North of the Agua Blanca fault, Crowell (1953, unpublished mapping) mapped a 110 m thick section, and Edwards (1971) measured an 80 m section along Piru Creek, The Union Moran 1 well penetrated 83 m of greenish gray, massive, medium- to fine-grained sandstone.

The early Miocene Rincon Formation is composed of deep-water mudstone and siltstone that are less competent than the underlying strata. The Rincon Formation is not found south of the Oak Ridge fault, though it is found in the fault zone of the Oak Ridge fault (Rieser, 1976), implying that it was deposited that far south in the footwall block. To the west, the Rincon is composed of ductile, deepwater mudstone and is inferred to be a décollement horizon. However, as far east as the Modelo lobe, the Rincon Formation is composed of enough siltstone that it is not weak enough to act as a décollement. North of the San Cayetano fault, the overlying Miocene Modelo Formation is composed of a lower shale, lower sandstone, middle shale, upper sandstone, and upper shale members. Figure 4-2 shows that in the northwest corner of the Piru quadrangle, the Rincon Formation is gently folded in the Hopper Ranch anticline and the lower shale member of the Modelo Formation

(Tm_1 of Figures 4-2 and 4-3) is intensely folded, implying that the lower shale member is acting a décollement layer in the Modelo lobe area. The depocenter for the lower members is north of the Ventura basin in the Modelo lobe area (Figure 4-2). South of the Oak Ridge fault, the Modelo Formation is exposed between the north and south strands of the Oak Ridge fault. There the Modelo ranges in age from Luisian to Mohnian (Ricketts and Whaley, 1975), and is composed of friable sandstone, shale, and siltstone. It unconformably overlies the Vaqueros Formation. A sliver of Modelo Formation wedged into the fault zone of the Oak Ridge fault (Figure 4-3).

Isopachs of the Mohnian part of the Modelo Formation outline a linear, northwest-deepening depocenter beneath the Pico anticline (Figure 4-2) south of the Santa Clara River (Yeats et al., submitted).

Farther south, the middle Miocene Conejo Volcanics was deposited in a normal faulted basin. Some basalt flows topped the normal faults and extended as far north as South Mountain in the west (Yeats, 1986) and into the hanging-wall block of the younger Santa Susana fault in the east. The basalt in the Topanga Formation is radiometrically dated as 14.1 ± 1 Ma (Turner, 1970).

A sequence of sandstone, conglomerate, and mudstone on the north slope of the Santa Susana Mountains (Figure 4-2), previously mapped as Modelo by Kew (1924) was named the Towsley Formation by Winterer and Durham (1954 and 1962). The age of the local "Delmontian" stage of southern California is estimated as 4.98 ± 0.15 to 6.5 ± 0.3 Ma (Blake, 1991).

In the western part of the east Ventura basin, the Fernando Formation consists of a lower member with Repettian microfossils and an upper member with shallower-water "upper Pliocene" or "Pico" microfossils not easily correlated to the Venturian or Wheelerian stages of Natland (1952) in the west Ventura basin. The top of the Fernando Formation near Newhall is about 2 Ma based on magnetic stratigraphy (Levi et al., 1986 and in prep.), but the top is younger westward and older eastward due to a facies change to Saugus Formation from west to east. Repetto age Fernando Formation is composed of siltstone, sandstone, and conglomerate (Winterer and Durham, 1962; Yeats et al., 1985). In the east Ventura basin, the thickness increases from 900 to 2500 meters due to coeval development of a southwest-verging monocline or fault-propagation fold at the site of the younger Newhall-Potrero anticline (Figure 4-2). Fernando thickness is also 2500 m in the Santa Clara Valley where it is preserved between the San Cayetano and Oak Ridge faults (Figure 4-3).

The Fernando Formation grades upward and laterally to shallow-marine to nonmarine strata which comprise the uppermost major formation of the east Ventura basin. The Saugus Formation is composed of sandstone and siltstone (Winterer and Durham, 1962). In many areas, the base of the Saugus is placed at the top of the fossiliferous sequence, but in the Santa Clara Valley between the Oak Ridge and San Cayetano faults, the contact is placed between fine-grained Fernando strata and fossiliferous sandstone and conglomerate of the Saugus Formation. The Saugus Formation is 3.7 km thick in the Arco Laura

Lawton 1 well (well 1 on Figure 4-3) in the footwall block of the San Cayetano and Oak Ridge faults. In the hanging-wall block of the Oak Ridge fault, the top of the Saugus can be correlated with e-log markers from the Oxnard Plain (Figure 4-1), where it is not displaced vertically by the Oak Ridge fault, east along the Long Canyon syncline where it maintains its thickness as far east as South Mountain (Yeats, 1988a). The Saugus in Figure 4-3 is not as thick. There, it is interpreted that the top of Saugus has been eroded away, and that it was originally as thick as it is to the west, 400 m. Yeats (1988a) observed that the dips across the basal contact of Saugus do not change and he concluded that the Saugus maintained a constant thickness from the Long Canyon syncline in the south, to the Oak Ridge anticline in the north (his Figure 5). Our view here differs with that interpretation in that the Oak Ridge fault is a growth structure that moved during the deposition of Saugus. Rocks south of the Long Canyon syncline (or the Happy Camp syncline on Figure 4-3) would have been deposited conformably on the underlying strata. Strata deposited north of the syncline would onlap onto the substrate. As conformable strata move through the hinge, accompanying movement on the Oak Ridge fault, they would have the same dip as the underlying strata, although coeval strata to the north would not (Suppe and Medwedeff, 1990).

Age of top of Saugus. The top of the Saugus Formation was defined just east of Ventura as the uppermost strongly deformed sedimentary rock (Lajoie et al., 1982). The age of the top of the Saugus Formation was

estimated to be 250±50 ka on the basis of amino-acid racemization of marine shells at the top of the formation (Lajoie et al., 1982; Yerkes et al., 1987; Lajoie et al., 1991). In the east Ventura basin, the top of the Saugus was estimated to be about 400 ka by paleomagnetic stratigraphy (Levi et al., 1986). The top of the Saugus in Figure 4-3 is not likely to be older than 250±50 ka because Saugus thickens in the direction of Figure 4-3.

Age of horizon 5. Horizon 5 was defined by Yeats (1976) and labeled the 1 Ma datum by Yeats (1981b). The age of horizon 5 is determined using the Edwards 11 oil well in West Saticoy oil field (see Huftile and Yeats, submitted). In the Edwards 11 well, horizon 5 is within 3 measured meters of the base of the Jaramillo normal magnetic event (Blackie and Yeats, 1976; Yeats and Taylor, 1989). The date of this event is determined by K-Ar dating of volcanic rocks from various places in the world (Mankinen and Dalrymple, 1979) to be 975±75 ka.

To the west, near Ventura, horizon 5 occurs between the Bishop ash and the Bailey ash (Sarna-Wojcicki et al., 1987; Sarna-Wojcicki et al., 1991; Yeats, 1988), which are dated as 738±3 ka (Izett et al., 1988) and 1.2±0.2 (Izett et al., 1974) respectively. A date for horizon 5 can be estimated using its position between two ash beds and assuming constant deposition rates. But constant deposition rate is not a valid assumption because a plot of stratigraphic position in Sexton Canyon versus age of the Lava Creek B (0.62 Ma; Christiansen and Blank,, 1972; Sarna-Wojcicki et al., 1984, 1987, 1991) Bishop,

and Bailey ash beds does not lie on a straight line (Sarna-Wojcicki et al., 1987, their Figure 5). The range of values estimated by assuming constant deposition rates includes the range of the base of the Jaramillo. Thus, the estimated age for horizon 5 used in this report is 975±75 ka.

Geologic mapping of the hanging-wall block Oak Ridge fault by Yeats (1967, 1988a) shows horizon 5 just north of the Long Canyon syncline. The horizon can be traced eastward from Oxnard Plain to just west of Figure 4-3 where it onlaps onto the underlying Modelo Formation. Sandstone beds within the formation continue eastward to the cross section, implying that very little strata overlying horizon 5 was lost. It is interpreted that no more than 100 m of additional strata was lost, adding to the error in the estimate of displacement.

STRUCTURE

The structure of the east Ventura basin is discussed in three parts: (1) deposition of a rifted basin in middle and late Miocene time, (2) faulting and folding during deposition of the Pliocene-Pleistocene sequence, and (3) post-Saugus deformation which, for the most part, still continues today.

Miocene rifting. Crowell (1973) pointed out that the Ventura basin may have had a Miocene normal-faulted precursor, and Yeats (1987b; 1989) showed that Oak Ridge was a positive feature controlled by normal faults, inferring that the Oak Ridge fault bounding Oak Ridge on the north could also have a normal-fault precursor.

The thick Miocene sequence exposed south of the Agua Blanca fault (ABF, Figure 4-2) is not obviously bounded by faults on the south and north, although the fault zone may be the northern boundary of the trough. The Agua Blanca fault and associated folded beds as young as early Miocene Rincon Shale to the north of this fault are covered unconformably by Mohnian Modelo Formation (Yeats et al., 1985), indicating strong deformation along this zone in middle Miocene time.

In the east Ventura basin, deep-test wells penetrated a much greater thickness of Modelo Formation than that exposed to the southwest and documented in the subsurface to the northeast. Yeats et al. (submitted) show that the boundary between thin Modelo underlain by Sespe(?) Formation and thick Modelo beneath Pico anticline (Figure 4-2) is so abrupt that it must be a

fault. On the footwall side of the Santa Susana fault, Modelo Formation of middle and late Miocene age (Luisian and Mohnian stages) is much thinner than coeval strata cropping out on the hanging-wall side, and no gradation between these two sequences is seen in the direction of the fault. This relation leads to the suggestion that the Santa Susana fault reactivated an old normal fault that marked the northeast margin of the Oak Ridge-Simi Hills structural block. East of Figure 4-3, the south strand of the Oak Ridge fault (Yeats, 1979; 1987) is a north-dipping normal fault that can be traced in the subsurface as far east as Oakridge oil field, where the normal fault is overridden by the Santa Susana fault. The normal fault probably continues southeast, deeper than well control, where it may have served as the zone of weakness for the Santa Susana fault.

North of the Santa Clara River, the Towsley Formation shows no evidence of the rifted trough, indicating that rifting ended there prior to 6.5 Ma. However, south of the river, the Towsley thickens to the southwest across the axis of the older rift and is thickest in the outcrop section in the Santa Susana Mountains (Yeats et al., submitted). There is no Towsley in the footwall block of the Santa Susana fault, indicating that the thick Towsley ended at a fault near the younger Santa Susana fault (Yeats, 1979), about the same place as the Modelo rift boundary. Thus the rift influenced Towsley thicknesses, but it was much more restricted areally, and its axis shifted

southwest. The Miocene rifting was coincident with most of the strike-slip movement on the San Gabriel fault (Yeats et al., submitted).

In Figure 4-3, the Oak Ridge fault is modeled with a normal-fault precursor that has been folded along with strata in the footwall and hanging-wall blocks of the fault, following the model of Namson (1987). The normal faulting affected rocks as young as Towsley Formation.

Pliocene convergence. The Towsley Formation of latest Miocene-early Pliocene age (~6.5-5 Ma) increases in thickness southwestward toward the Santa Susana fault, yet there is no Towsley farther southwest in the footwall block of the Santa Susana fault. The Towsley was probably terminated southwestward by a normal fault that may have been used later as a zone of weakness by the Santa Susana fault.

The Fernando thickens southwestward from about 1400 m northeast of the Newhall-Potrero anticline (Figure 4-2) to 2500 m southwest of this anticline so that the anticline does not continue upward to the surface except locally (Winterer and Durham, 1962). The anticline is interpreted as a southwest-verging fault-propagation fold (cf. Suppe and Medwedeff, 1990) in which the fault tip has not continued upward into strata younger than Modelo Formation.

North of the Santa Clara River, the Santa Felicia syncline (SFS on Figure 4-2) folds conformable Modelo and Towsley formations. The overlying Fernando Formation greatly thickens southward across the fold. Yet, the Santa Felicia syncline does not fold the base of the Saugus Formation, dated at ~2

Ma (Levi et al., 1986), inferring that this compressional structure entirely preceded the two horizons, 250±50 ka and 975±75 ka, that will be flattened in the retrodeformations in Figure 4-3. By analogy to the Newhall-Potrero anticline, we speculate that the Temescal anticline and the Hopper Ranch-Modelo anticline in the Modelo lobe of the San Cayetano fault are also fault-propagation folds formed as the Fernando was deposited. A sharp isopach gradient at Newhall-Potrero anticline continues west-northwest to the vicinity of the Del Valle fault where this gradient projects west to a position immediately south of the Hopper Ranch-Modelo anticline (Yeats et al., submitted). To the north, a gradient of 500 to 800 m projects west toward the Temescal anticline. There are two extreme possibilities (cf. Yeats, 1983). (1) The Fernando and Saugus were never deposited on the Modelo lobe, implying that the lobe was positive throughout that time. This extreme case is unlikely because, in contrast to the Red Mountain fault in the western Ventura basin (Yeats et al., 1987), the Fernando Formation in the footwall block shows no northward change in grain size, and no sediments locally derived from the north, which could be considered as evidence for a positive Modelo lobe. (2) The Fernando and Saugus were as thick atop the Modelo lobe as they are in the Santa Clara syncline in the footwall of the San Cayetano fault. This is also unlikely because it would require that the Modelo still preserved would have been overlain by up to 7 km of Towsley, Fernando, and Saugus formations. The porosity of Modelo sandstone, which comprises the reservoir for several small oil fields in

the Modelo lobe, indicates much less overburden than the full thickness of post-Modelo strata in the Santa Clara syncline. Furthermore, the thickness of Fernando in the Santa Clara syncline is 2500 m, thicker than in any section measured northeast of the San Cayetano fault.

The first extreme maximizes the displacement on the San Cayetano fault prior to the end of Saugus deposition and minimizes post-Saugus displacement. The second extreme requires all displacement on the San Cayetano to be post Saugus. We favor an intermediate explanation that calls for displacement on fault-propagation-fold (Temescal and Hopper Ranch-Modelo anticlines), across which Fernando thicknesses increase from 900 to 2500 m. We project the thickness measured in the east Ventura basin westward 10-12 km to the Modelo lobe, although it is likely that some westward thinning occurs, and strata younger than Towsley may never have been deposited west of, say, Sespe Creek. In the hanging-wall block of the San Cayetano fault is the Buckhorn and Hopper Ranch anticlines (Figure 4-3). These folds are well constrained in the subsurface. The San Cayetano fault ramps across Paleogene strata, forms a décollement within the lower shale member of the Modelo Formation, and ramps across overlying strata. This ramp-flat-ramp geometry must be the result of (1) a change in the dip of the San Cayetano fault as it propagated toward the surface, or (2) the result of the San Cayetano cutting a preexisting structure. Because there is no evidence of dip changes on the San Cayetano fault, other than a gentle shallowing of dips toward the surface, the

latter possibility is more plausible. Thus, an extension of the Buckhorn anticline is modeled in the footwall block of the San Cayetano fault.

Contemporary structures. The present-day structures began to form near the end of Saugus deposition. In the central Ventura basin, late Quaternary displacement on the San Cayetano fault was described by Yeats (1983) and Çemen (1989), and on the Oak Ridge fault by Yeats (1988a; 1989). Whereas the pre-Saugus trace of the Oak Ridge fault turns east-southeast beneath the Santa Susana fault, the post-Saugus trace continues east-northeast along the southern margin of Santa Clara Valley and dies out. Stream terraces of the Santa Clara River apparently have been cut by the fault. Just east of Figure 4-3, the San Cayetano fault bifurcates into two strands (Figures 4-1 and 4-2). The San Cayetano fault appears to become a blind thrust to the east. North of the Santa Susana fault and southeast of Lake Piru, the sequence, including the Saugus Formation, is deformed into a fold belt cut by several south-dipping reverse faults. The southernmost two faults, the Del Valle and Holser faults, have relatively large separations, and the faults may be backthrusts rising from the blind thrust.

Both strands of the San Cayetano fault have evidence of late Quaternary displacement. The fan at the mouth of Modelo Canyon, just south of Lake Piru, appears to be cut by the Main strand. Aerial photographs show that drainages are more incised west of the fault than they are east of the fault, suggesting uplift west of the Main strand. Offset of the drainages increases to

the south where dip-slip offset should be greater. Some drainages appear to be offset left-laterally, implying oblique offset for this part of the fault as would be expected for a reverse fault that turns in the direction of stress shown by Mount and Suppe (1987) and dies out.

The southern, Piru strand of Çemen (1977) extends to the east through Piru and north of Camulos. The surface trace can be followed by a warp in alluvium that extends through the town of Piru.

The central Ventura basin forms a zig-zag synclinorium with the Santa Clara syncline (SCS on Figure 4-3) separated from the Piru syncline (PS) by the Piru anticline (PA, Figure 4-2). The Piru syncline appears to be north-vergent at Figure 4-3. The south limb of the fold is steeper than the dips observed in the Texas Lawton 1 well (well 2, Figure 4-3a) which penetrates the north limb. Farther east, in the footwall block of the Piru strand of the San Cayetano fault, dips range from 53-68°N on the south limb, and range from less to equal that amount on the north limb implying that the Piru syncline is at least partially north-vergent. Although, in the hanging-wall block of the Piru strand, dips on the north limb are overturned (Huftile and Yeats, submitted), implying that the syncline is also partially south-vergent. In Figure 4-3, where dips on the north limb are shallow, the youngest folding of the Piru syncline, contemporary with deposition of the Saugus Formation, is modeled as entirely north-vergent.

BALANCED CROSS SECTION

The lobate part of the San Cayetano fault has a dip of 22-34°N at the western edge of the Piru quadrangle. The Main strand dips 40°N just east of the intersection between the Main and Piru strands and as much as 66°NW at its eastern end; the Piru strand has a low dip at its western end and steepens to 54°N at its eastern terminus. Çemen (1977, 1989) estimated 5.2-7.3 km stratigraphic separation at Hopper Canyon, and 4.6-5.3 km at Edwards Canyon.

The Hopper Ranch fault (Figure 4-3; Çemen, 1977, 1989) does not connect with the western San Cayetano fault north of Fillmore as mapped by Jennings and Strand (1969), rather it is likely a flexural-slip fault between the competent lower sandstone and incompetent lower shale members of the Modelo Formation (Çemen, 1977; Yeats, 1983a). Its age is uncertain, but is assumed to be coincident with folding.

Figure 4-3 extends across the Oak Ridge fault where the fault surface dips 64-77°S at depth but much shallower in the upper 2.5 km. Through the Pliocene and early Pleistocene, the Oak Ridge fault had no topographic expression, but both sides of the fault subsided and received sediments, with the north side subsiding more (Yeats, 1965; 1988b). Yeats (1988a) calculated a slip rate of 5.9-12.5 mm/y since the end of Saugus deposition at 250±50 ka. Yeats assumed that the Saugus does not onlap onto the Oak Ridge anticline, maintaining its thickness over the crest of the structure. This is based on the observation that dips do not change across the basal contact between Saugus

and underlying strata. However, the Oak Ridge fault was active through deposition of Fernando and Saugus formations. The Oak Ridge anticline, north of the Happy Camp syncline, should be a topographic feature and sediment would onlap on the north limb of the Happy Camp syncline. The apparent contradiction is best explained by the model of Suppe and Medwedeff (1990) for growth structures. In that model, strata would be conformable south of the Happy Camp syncline and unconformable north of it. With continued movement on the Oak Ridge fault, conformable strata would pass northward through the hinge of the Happy Camp syncline. If the onlapping part of the Saugus was eroded away, the remaining strata on the north limb of the Happy Camp syncline would appear conformable as it does at the present time. Figures 4-3b and 4-3c allow for the onlapping of Fernando and Saugus formations on to the Oak Ridge anticline, which results in less displacement on the Oak Ridge fault than was reported by Yeats (1988a).

The Oak Ridge fault zone is composed of fractured Modelo Formation (Huftile, 1988a, b). To the west, the fault zone contains Rincon Formation, implying that the formation was deposited as far south as the Oak Ridge fault (Rieser, 1976).

Suppe and Medwedeff (1990) and Namson (1987) both modeled cross sections across the active part of the Oak Ridge fault. These models shallow the Oak Ridge fault at ~3 km depth. Beneath the fault is a normal-fault precursor to the Oak Ridge fault. Yet, the shallowing of the the Oak Ridge

fault at 3 km depth would cause a strongly folded synclinal hinge in the hanging-wall block of the fault. No such synclinal hinge is observed. The Oak Ridge fault as modeled would have to be a normal fault into the time of deposition of the Saugus Formation, be folded by very young compression with the Santa Clara syncline in the footwall block and it would have no compressional movement on the Oak Ridge fault. This is implausible because (1) The North strand of the Oak Ridge fault has significant movement on it, without the Santa Clara syncline in the footwall block, implying that it cannot be a folded normal fault, and (2) Modelo and Rincon formations occur within horses in the Oak Ridge fault zone, juxtaposed against Saugus Formation in the footwall block and Sespe Formation in the hanging-wall block. This could not occur if the Oak Ridge fault was normal during deposition of the Saugus Formation. The Miocene strata would have to have been dragged up from the footwall block of the fault along with compressional movement on the fault. Two gently folded synclines, the Happy Camp syncline and the Long Canyon syncline, occur in the hanging-wall block of the Oak Ridge fault. Since the geometry of the hanging-wall block reflects uunderlying fault geomtry, a more likely construction would have the Oak Ridge fault gently shallowing at its intersection with the axial surfaces of these synclines. The degree of folding of the synclines precludes a sharp bend in the Oak Ridge fault based on the model of Woodward et al. (1989). In Figure 4-3, the Oak Ridge fault shallows

from 69°S dip to 56°S dip across the axial plane of the Happy Camp syncline, and shallows to 46°S dip across the axial plane of the Long Canyon syncline.

Retrodeformation to 250±50 ka. Post-Saugus defomation includes some displacement on the Oak Ridge fault, some displacement on the San Cayetano fault, and all of the compressional displacement on the Simi fault. Dip-slip displacement on the Oak Ridge fault is determined by restoring movement on the Oak Ridge fault so that the top of the Saugus Formation in the hanging-wall block onlaps onto the south limb of the Oak Ridge anticline. This requires the restoration of 1.7 km of dip-slip displacement on the Oak Ridge fault.

Displacement on the Simi fault is measured by projecting the top of the Saugus into the air, at its observed surface dip, to its intersection with the fault, then restoring the displacement necessary to lower it to the Saugus in the footwall block. This amount is 0.2 km.

The Piru syncline folds strata within the Saugus Formation. Yet it is overthrust by 4.4 km of dip-slip displacement on the San Cayetano fault. It does not fold the top of the Saugus anywhere from Figure 4-3 to the east (Huftile and Yeats, submitted; Yeats, et al., 1985; Yeats et al., submitted). Thus, it is presumed to be older than the top of Saugus.

Only the lowermost, marine Saugus Formation occurs in the hanging-wall block of the San Cayetano fault; the upper 2.4 km of Saugus does not (Huftile and Yeats, submitted). Maximum post-Saugus displacement is that

amount that would restore marine Saugus in the hanging-wall to the present level of the top of the Saugus in the footwall block, assuming the maximum thickness of Fernando Formation in the hanging-wall block. This maximizes the post-Saugus estimate of displacement and minimizes the displacement during Saugus deposition. Isopachs of the Fernando Formation (Yeats et al., submitted) show an increase of thickness from 900-2000 m southward south of the Del Valle fault (Figure 4-2). The trend of the isopach contours indicates that this increase may have occurred at the Hopper Ranch-Modelo anticline. The maximum post-Saugus displacement on the San Cayetano fault is 5.2 km, slightly more than is restored in Figure 4-3b. The minimum displacement on the San Cayetano fault is that in which the marine Saugus is deposited on the minimum estimated thickness of Fernando Formation, 900 m, in the hanging-wall block. This amount of displacement is 2.2 km. Displacements are summarized in Table 4-1. Total displacement is between 4.1-7.1 km. The displacement rate since 250±50 ka is 25±11 mm/y.

Retrodeformation to 975±75 ka. Post-horizon 5 displacement includes north-vergent folding of the Piru syncline and additional movement on the Oak Ridge and San Cayetano faults. Dip-slip displacement on the fault that forms the Piru syncline is 0.2 km.

Displacement on the Oak Ridge fault is determined by flattening horizon 5 which is at the base of the Fernando Formation in the hanging-wall block and at the base of Saugus Formation in the footwall block. Figure 4-3c

shows decompacted Fernando Formation resulting from the removal of 3.7 km of Saugus Formation. The upper Fernando Formation (QTf on Figures 4-2 and 4-3) is 1.0 km thicker in Figure 4-3c than is Figures 4-3a and 4-3b. However, this amount cannot be included in shortening because it was not caused by horizontal stresses but rather by vertical compaction. Dip-slip displacement on the Oak Ridge fault since 975±75 ka is 4.0 km.

Displacement on the San Cayetano fault is constrained by how much Fernando Formation once overlayed the Modelo lobe. Isopachs of the Fernando Formation show a sharp gradient from 900 m to 2000 m east of, but on trend with the Hopper Ranch anticline. The maximum displacement on the San Cayetano fault allows for 2000 m of Fernando in the hanging-wall block of the fault. This restores all movement on the San Cayetano fault and is as shown on Figure 4-3c. The maximum dip-slip displacement on the San Cayetano fault sine 975±75 ka is 11.8 km; again this is not influenced by the decompaction of Fernando Formation in Figure 4-3c.

The minimum displacement on the San Cayetano fault is determined by allowing for only 900 m of Fernando to have been deposited on the Modelo lobe. This reduces the dip-slip displacement on the fault to 10.1 km.

Total displacement ranges between 14.5-16.2 km. The deformation rate between 250±50 ka and 975±75 ka is 14±6 mm/y.

Table 4-1:

Ranges of Shortening on Cross Section A-A'

Simi fault	Oak Ridge fault	Piru syncline	San Cayetano fault	Total (km)
250±50 ka to present				
0.2	1.7	0	2.2-5.2	4.1-7.1
975±75 ka to present				
0.2	3.9-4.0	0.2	10.1-11.8	14.4-16.2

RESIDUAL GRAVITY MODELING

Figures 4-4a and 4-4b are the residual gravity verification of the balanced structural cross section in which structural methods have been used to predict the locations of structures beneath the data set. The balanced cross sections are checked for agreement with an independent data set. The verification does not prove the structural interpretation, but either allows the interpretation or denies it.

The isostatic residual gravity (Figure 4-4a) is from A. Griscom (written communication, 1991; see Jachens and Griscom, 1985 and Griscom and Sauer, 1991). The isostatic residual removes the effects of topography and the Moho so that the residual, high-frequency gravity anomaly is the gravitational expression of shallow crustal structure.

Densities are from neutron density logs of oil wells, from McCulloh (1967), and are estimated from density-depth curves for rock type and rock age (Woollard, 1962). The calculated curve for Figure 4-4b is pinned to the observed curve many km to the north. To the north in Figure 4-4a, Mesozoic granite is at the surface. Thus, the anomaly at the north is approximately horizontal and is about 0 mgal.

A high-density root to the Conejo Volcanics to the south of Figure 4-4b is necessary. The residual gravity models predict the thickness of the Pliocene-Pleistocene basin, honoring the observed density ranges, and changes in the slope of the observed anomaly may indicate bedding and fault dips at depth.

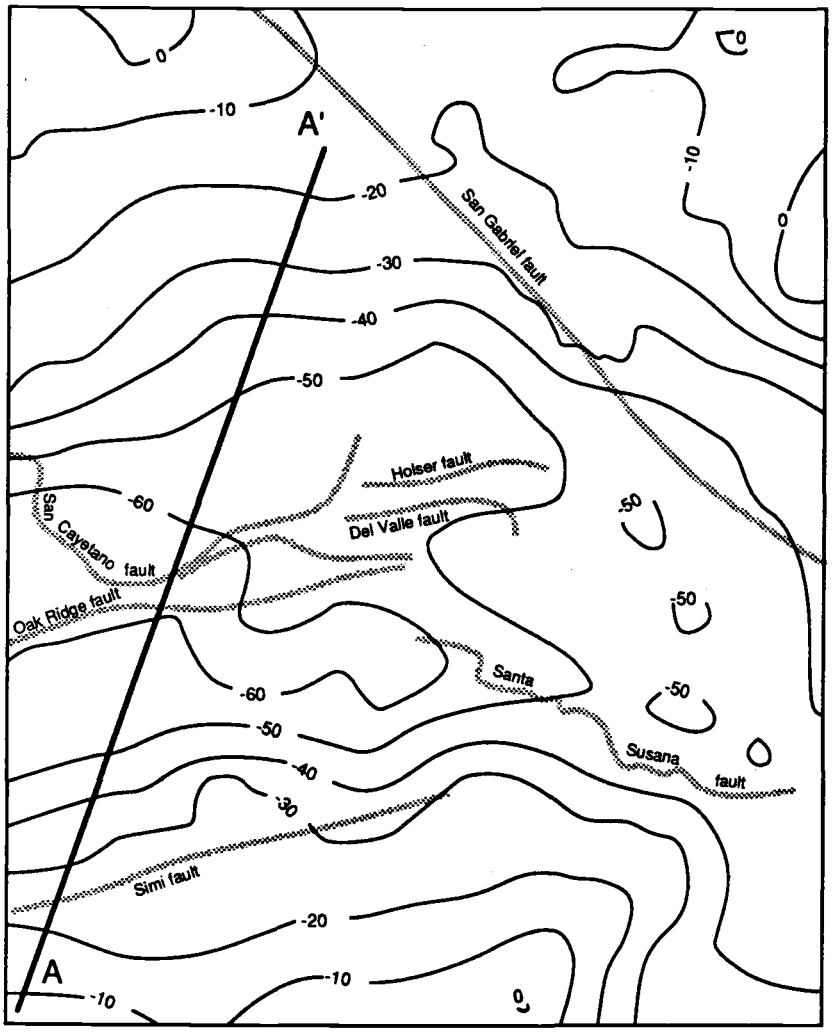

Figure 4-4a: Residual gravity map over the study area, located on Figure 4-1 (A. Griscom, written communication).

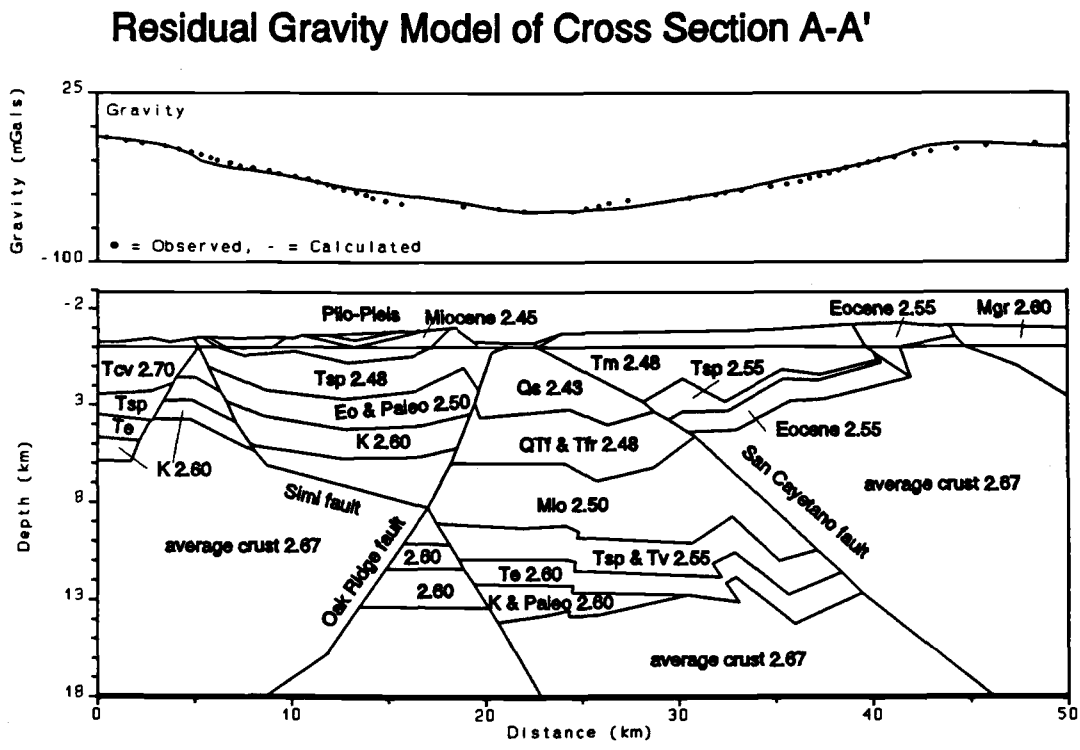

Figure 4-4b: Residual gravity model over Figure 4-3 showing agreement of an independent data set, residual gravity, with the structural model.

The residual gravity map (Figure 4-4a) shows low residual gravity values over Oak Ridge, implying that there are low-density strata overthrust by the Oak Ridge fault. The model preferred here, shallowingthe Oak Ridge fault at its intersection with the axial surface of the Happy Camp syncline, is allowed by the gravity modeling. However, the models of Suppe and Medwedeff (1990) and Namson (1987), which shallow the dip on the Oak Ridge fault more drastically at about 3 km depth, are also not denied by the gravity modeling.

The residual gravity modeling forced no changes in the cross section that would alter estimates of shortening.

CONCLUSIONS

The east Ventura basin originated as a rift basin in middle Miocene time extending from the outcrop north of the Modelo lobe of the San Cayetano fault southeast to the subsurface north of the Santa Susana Mountains. This rift contains a great thickness of middle and late Miocene strata dominated by sandstone.

The Fernando Formation rests on the contrasting Miocene sequence of the east Ventura basin and it was deposited during a compressional regime. The Newhall-Potrero anticline developed as a growth fault-propagation fold during Fernando deposition, and the Pico anticline to the southeast and the Temescal anticline, Hopper Ranch-Modelo anticline, and Santa Felicia syncline to the northwest may have formed in the same way at the same time.

Post-Saugus structures include some of the movement on the Oak Ridge fault, some or all of the movement on the San Cayetano fault, and all of the reverse displacement on the Simi fault. Post-Saugus shortening is 4.1-7.1 km in the last 250±50 ka, occurring at a rate of 25±11 mm/y. This rate is very close to those rates determined as far west as Ventura (Huftile and Yeats, submitted). Post-Fernando shortening is 14.4-16.2 km, occurring at a rate of 14±6 mm/y. This rate is considerably higher than those for the same interval to the west.

BIBLIOGRAPHY

Argo Petroleum, 1982, Geologic map of the Sespe field area, in Nulty, G. E., ed., Geologic guide of the Central Santa Clara Valley Sespe and Oak Ridge trend oil fields, Ventura County, California: Coast Geol. Soc.-Pacific Sect. Am. Assoc. Petrol. Geol. Spring Field Trip, Guidebook Number 53, Plate IV, Scale 1:12,000.

Bailey, T. L., 1951, Geology of a portion of Ventura Basin, Los Angeles and Ventura Counties, California: unpub. map, Scale 1:24,000.

Bain, R. J., 1954, Geology of the Eureka Canyon area, Ventura County, California: unpub. M.A. thesis, University of California, Los Angeles, 39p.

Berger, R. A., ed., 1977, Deep water oil sand reservoirs of the Monterey Formation, Fillmore-Piru area, Ventura County, California, guidebook: Coast Geological Society, 35 p.

Berggren, W. A., and Van Couvering, John, 1973, Late Neogene chronostratigraphy, biostratigraphy, biochronology, and paleoclimatology: unpub. technical report Nat. Sci. Foun., Woods Hole Oc. Inst., 334p.

Bird, P., and R. W. Rosenstock, 1984, Kinematics of present crust and mantle flow in southern California: Geol. Soc. Am. Bull., v. 95, p. 946-957.

Blackie, G. W., and Yeats, R. S., 1976, Magnetic-reversal stratigraphy of Pliocene-Pleistocene producing section of Saticoy oil field, Ventura basin, California: Am. Assoc. Petrol. Geol. Bull., v. 60, p. 1985-1992.

Blake, G. H., 1983, Benthic foraminiferal paleoecology and biostratigraphy of the Vaqueros Formation, Big Mountain area, Ventura County, California, *in* Squires, R. L., and Filewicz, M. V., eds., Cenozoic geology of the Simi Valley area, southern California: Pacific Section, Soc. Econ. Paleon. and Mineralogists, volume and guidebook, p. 173-181.

Blake, G. H., 1991, Review of the Neogene biostratigraphy and stratigraphy of the Los Angeles basin and implications for basin evolution, in Biddle, K. T., ed., Active Margin basins: AAPG Memoir 52, p. 135-184.

Bohannon, R. G., 1975, Mid-Tertiary conglomerates and their bearing on Transverse Range tectonics, southern California: Calif. Div. Mines Geol. Spec. Rep. 118, p. 75-82.

Bohannon, R. G., 1976, Mid-Tertiary nonmarine rocks along the San Andreas fault in southern California: unpub. Ph. D. dissertation, Univ. California, Santa Barbara, 327p.

Bush, G. L., 1956, Geology of the Upper Ojai Valley, Ventura County, California: unpub. M. A. thesis, University of California, Los Angeles, 60 p.

California Division of Mines and Geology, 1972, Geologic map of southern Ventura County, California: California Division of Mines and Geol., Open-File Report 72-26, Scale 1:48,000.

Canter, N. W., 1974, Paleogeology and paleogeography of the Big Mountain area, Santa Susana, Moorpark, and Simi quadrangles, Ventura County, California: unpub. M. S. thesis, Ohio University, Athens, 58p.

Çemen, I., 1977, Geology of the Sespe-Piru Creek area, Ventura County, California: unpub. M. S. thesis, Ohio University, Athens, 69 p.

Çemen, I., 1989, Near-surface expression of the eastern part of the San Cayetano fault: A potentially active thrust fault in the California Transverse Ranges: Jour. Geophys. Res., v. 94-B7, p. 9665-9677.

Chen, Y., and J. B. Minster, 1991, Slip line model for southern California crustal kinematics: Tectonics, v. 10, p. 577-586.

Christiansen, R. L., and H. R. Blank Jr., 1972, Volcanic stratigraphy of the Quaternary rhyolite plateau in Yellowstone National Park: U. S. Geol. Surv. Prof. Pap. 729-B, p. B1-B18.

Cordova, S., 1956, Geology of the Piru area, Ventura County, California: unpub. M. S. thesis, Univ. California, Los Angeles, 58p.

Crowell, J. C., 1973, Problems concerning the San Andreas fault system in southern California, in Kovach, R. L., and Nur, A., eds., Proceedings of the Conference on Tectonic Problems of the San Andreas Fault System: Stanford Univ. Publ. Geol,. Sci., v. 13, p. 125-135.

Crowell, J. C., Hope, R. A., Kahle, J. E., Ovenshine, A. T., and Sams, R. H., 1966, Deepwater sedimentary structures, Pliocene Pico Formation, Santa Paula Creek, Ventura basin, California: California Division of Mines and Geology Special Report 89, San Francisco, 40p.

Dibblee, T. W, Jr., 1950, Geology of southwestern Santa Barbara County: Point Arguello, Lompoc, Point Conception, Los Olives, and Gaviota quadrangles: Calif. Div. Mines Geol. Bull. 150, 95p.

Dibblee, T. W., Jr., 1979, Geologic map of the Lockwood Valley quadrangle, California: USGS Open File Report 79-1464, scale 1:24,000.

Dibblee, T. W., Jr., 1982, Geologic map of the Santa Paula Peak quadrangle, California: USGS Open File Report 82-73, scale 1:24,000.

Dibblee, T. W., Jr., 1985, Geologic map of the Wheeler Springs quadrangle, California: Thomas Wilson Dibblee, Jr. Geological Foundation, Santa Barbara, California, scale 1:24,000.

Dibblee, T. W., Jr., 1987a, Geologic map of the Ojai quadrangle, California: Thomas Wilson Dibblee, Jr. Geological Foundation, Santa Barbara, California, scale 1:24,000.

Dibblee, T. W., Jr., 1987b, Geologic map of the Lion Canyon quadrangle, California: Thomas Wilson Dibblee, Jr. Geological Foundation, Santa Barbara, California, scale 1:24,000.

Dibblee, T. W., Jr., 1987c, Geologic map of the Matilija quadrangle, California: Thomas Wilson Dibblee, Jr. Geological Foundation, Santa Barbara, California, scale 1:24,000.

Dibblee, T. W, Jr., 1987d, Geologic map of the White Ledge Peak quadrangle, California: Thomas Wilson Dibblee, Jr. Geol. Foun., Santa Barbara, California, scale 1:24,000.

Dibblee, T. W, Jr., 1988, Geologic map of the Pitas Point and Ventura quadrangles, California: Thomas Wilson Dibblee, Jr. Geol. Foun., Santa Barbara, California, scale 1:24,000.

Dibblee, T. W., Jr., 1990, Geologic map of the Fillmore quadrangle, Ventura County, California: Dibblee Geological Foundation, Map #DF-27, Santa Barbara, California, Scale 1:24,000.

Dibblee, T. W., Jr., 1991, Geologic map of the Piru quadrangle, Ventura County, California: Dibblee Geological Foundation, Map #DF-34, Santa Barbara, California, Scale 1:24,000.

Donnellan, A., B. H. Hager, and R. W. King, Rapid north-south shortening of the Ventura basin, southern California, preprint.

Durham, J. W., Jahns, R. H., and Savage, D. E., 1954, Marine-nonmarine relationships in the Cenozoic section of California: California Div. Mines Bull. 170, ch. III, p. 59-71.

Edwards, L. N., 1971, Geology of the Vaqueros and Rincon formations, Santa Barbara embayment, California: unpub. Ph. D. dissertation, University of California, Santa Barbara, 240p.

Eldridge, G. H., and Arnold, Ralph, 1907, The Santa Clara Valley, Puente Hills and Los Angeles oil districts, southern California: U. S. Geol. Survey Bulletin 309, 266p.

Eschner, S., 1957, Geology of the central part of the Fillmore quadrangle, Ventura County, California: unpub. M. A. thesis, University of California, Los Angeles, 58p.

Fine, S. F., 1954, Geology and occurrences of oil in the Ojai-Santa Paula area, Ventura County: California Division of Mines Bulletin 170, Map Sheet 28.

Gordon, S. A., 1978, Relations among the Santa Ynez, Pine Mountain, Agua Blanca, and Cobblestone Mountain faults, Transverse Ranges, California, M. A. thesis, University of California, Santa Barbara, 77 p.

Grigsby, B. F., 1986, Quaternary tectonics of the Rincon and San Miguelito oil fields area, western Ventura basin, California, M. S. thesis, Oregon State University, Corvallis, 110 p.

Griscom, A., and P. E. Sauer, 1991, Gravity and magnetic maps of the Santa Maria province, California (abstract): Am. Assoc. Petrol. Geol. Bull., v. 75, p. 366.

Hadley, D., and H. Kanamori, 1977, Seismic structure of the Transverse Ranges, California: Geol. Soc. Am. Bull., 88, p. 1469-1478.

Hadley, D., and H. Kanamori, 1978, Recent seismicity in the San Fernando region and tectonics in the west-central Transverse Ranges, California: Bull. Seismol. Soc. Am., v. 68, p. 1449-1457.

Hall, E. A., Durrie, J., and Saunders, 1967, Field trip morning section, Big Mountain oil field: Am. Assoc. Petrol. Geol., 10p.

Hornafius, J. S., B. P. Luyendyk, R. R. Terres, and M. J. Kamerling, 1986, Timing and extent of Neogene tectonic rotation in the western Transverse Ranges, California: Geol. Soc . Am. Bull., v. 97, p. 1476-148.

Hsü, K. J., 1977, Studies of Ventura field, California I: Facies geometry and genesis of lower Pliocene turbidites: Am. Assoc. Petrol. Geol. Bull., v. 61, p. 137-168.

Hsü, K. J., Kelts, K., and Valentine, J. W., 1980, Resedimented facies in Ventura basin, California, and model of longitudinal transport of turbidity currents: Am. Assoc. Petrol. Geol. Bull., v. 64, p. 1034-1051.

Hsui, A. T., SUBSIDE, A basin subsidence analysis program, Callidus Software, Urbana, Illinois, 9 pp., 1989.

Huftile, G. J., 1987, A retrodeformable cross section across the central Ventura basin, California: Eos Transactions, American Geophysical Union, v. 68, p. 1502.

Huftile, G. J., 1988a, Structural geology of the Upper Ojai Valley and Chaffee Canyon areas Ventura County, California: unpub. M. S. thesis, Oregon State University, Corvallis, 103p.

Huftile, G. J., 1988b, Structural geology of the Chaffee Canyon oil field, Ventura County, California, *in* Sylvester, A. G., and Brown, G. C., Santa Barbara and Ventura basins: Coast Geol. Soc. Guidebook 64, p. 125-132.

Huftile, G. J., 1988c, Subsurface connection between the Red Mountain and San Cayetano faults, Ventura basin, California: EOS Transactions, American Geophysical Union, v. 69, p. 1419.

Huftile, G. J., 1989, Displacement transfer on the Oak Ridge fault, Ventura basin, California: Geol. Soc. America Abs. with Prog., v. 21-5, p. 95.

Huftile, G. J., 1991, Thin-skinned tectonics of the Upper Ojai Valley and Sulphur Mountain area, Ventura basin, California: Am. Assoc. Petrol. Geol. Bull., v. 75, p. 1353-1373.

Huftile, G. J., and R. S. Yeats, Cenozoic structure of the Piru 7½-minute quadrangle: submitted as a U. S. Geol. Surv., Open-File Rep.

Huftile, G. J., and R. S. Yeats, Convergence rates across a displacement transfer zone in the western Transverse Ranges near Ventura, California: submitted to Jour. Geophys. Res.

Izett, G. A., Naeser, C. W., and Obradovich, J. D., 1974, Fission track age of zircon from an ash bed in Pico Formation (Pliocene-Pleistocene) near Ventura, California: GSA Abstracts with Programs, v. 6, p. 197.

Izett, G. A., J. D. Obradovich, and H. H. Mehnert, 1988, The Bishop ash bed (middle Pleistocene) and some older (Pliocene and Pleistocene) chemically similar ash beds in California, Nevada, and Utah: U. S. Geol. Surv. Bull. 1675, 37 p.

Jachens, R. C., and A. Griscom, 1985, An isostatic residual gravity map of California--A residual map for interpretation of anomalies from intracrustal sources, *in* Hinze, W. J., ed., The utility of regional gravity and magnetic anomaly maps, Soc. Expl. Geophys., Tulsa, Oklahoma, p. 347-360.

Jackson, P. A., and R. S. Yeats, 1982, Structural evolution of Carpinteria basin, western Transverse Ranges, California: Am. Assoc. Petrol. Geol. Bull., v. 66, p. 805-829.

Jennings, C. W., and Troxel, B. W., 1954, Geology of southern California, Ventura basin, California: California Division of Mines Bulletin 170, Guide 2, p. 27-29.

Jennings, C. W., and Strand, R. G., 1969, Geologic map of California, Los Angeles sheet: California Division of Mines and Geology, scale 1:250,000.

Jestes, E. C., 1957, Geology of the Wiley Canyon area, Ventura County, California: unpub. M. A. thesis, University of California, Los Angeles, 45p.

Kerr, P. F., and Schenk, H. G., 1928, Significance of the Matilija overturn (Santa Ynez Mountains, California): GSA Bulletin, v. 39-4, p. 1087-1102.

Kew, W. S. W., 1924, Geology and oil resources of Los Angeles and Ventura Counties, California: U. S. Geol. Survey Bulletin 753, 202p.

Kleinpell, R. M., 1938, Miocene stratigraphy of California: Am. Assoc. Petrol. Geol., Tulsa, Oklahoma, 450p.

Kriz, S. J., 1947, Stratigraphy and structure of the Whitaker Peak-Reasoner Canyon area, Ventura and Los Angeles Counties, California: unpublished Ph.D. dissertation, Princeton Univ., Princeton, New Jersey, 68 p.

Lagoe, M. B., and Thompson, P. R., 1988, Chronostratigraphic significance of late Cenozoic planktonic foraminifera from the Ventura basin, California: Potential for improving tectonic and depositional interpretation: Journal of Foraminiferal Research, v. 18, p. 250-266.

Laird, B. A., 1988, Geometry and kinematics of geologic structures, Pine Mountain, Ojai area, western Transverse Ranges, California, M.S. thesis, Univ. of Nevada, Reno, 107 p.

Lajoie, K. R., Sarna-Wojcicki, A. M., and Yerkes, R. F., 1982, Quaternary chronology and rates of crustal deformation in the Ventura area, California: GSA Cordilleran Section Field Trip Guidebook, p. 43-51.

Lajoie, K. R., D. J. Ponti, C. L. Powell, S. A. Mathieson, and A. M. Sarna-Wojcicki, 1991, Emergent marine strandlines and associated sediments, coastal California; a record of Quaternary sea-level fluctuations, vertical tectonic movements, climatic changes, and coastal processes, *in*, Morrison, R. B., ed., Quaternary nonglacial geology; conterminous U. S., v. K-2, Geology of North America series: Geol. Soc. Am., Boulder, Colorado, p. 190-214.

Lander, E. B., 1983, Continental vertebrate faunas from the upper member of the Sespe Formation, Simi Valley, California, and the terminal Eocene event, *in* Squires, R. L., and Filewicz, M. V., eds., Cenozoic geology of the Simi Valley area, southern California: Pacific Section, Soc. Econ. Paleon. and Mineralogists, volume and guidebook, p. 142-153.

Lee, W. H. K., Yerkes, R. F., and Simirenko, M., 1979, Recent earthquake activity and focal mechanisms in the western Transverse Ranges, California: U. S. Geological Survey Circular 799-A, p. 1-26.

Levi, S., Schultz, D. L., Yeats, R. S., Stitt, L. T., and Sarna-Wojcicki, A. M., 1986, Magnetostratigraphy and paleomagnetism of the Saugus Formation near Castaic, Los Angeles County, California: Cordilleran Section, Geol. Soc. America, Neotectonics Field Trip Guide, p.

Liddicoat, J. C., 1990, Tectonic rotation of the Santa Ynez Range, California, recorded in the Sespe Formation: Geophys. J. International, v. 102, p. 739-745.

Liddicoat, J. C., 1992, Paleomagnetism of the Pico Formation (Pliocene), Santa Paula Creek, Ventura basin, California: in press, Geophys. J. International.

Link, M. H., 1971, Sedimentology, petrography, and environmental analysis of the Matilija sandstone north of the Santa Ynez fault, Santa Barbara County, California: unpub. M. A. thesis, Univ. of Calif., Santa Barbara.

Luyendyk, B. P., and J. S. Hornafius, 1987, Neogene crustal rotations, fault slip, and basin development in southern California, *in* Ingersoll, R. V., and Ernst, W. G., eds., Cenozoic basin development of coastal California (Rubey Volume VI): Prentice-Hall, Englewood Cliffs, New Jersey, p. 259-283.

Mallory, V. S., 1959, Lower Tertiary biostratigraphy of the California Coast Ranges: Am. Assoc. Petrol. Geol., Tulsa, Oklahoma, 416p.

Mankinen, E. A., and G. B. Dalrymple, 1979, Revised geomagnetic polarity time scale for the interval 0-5 m.y. B.P.: Jour. Geophys. Res., v. 84, p. 615-626.

Mason, M. A., and Swisher, C. C., 1988, New evidence for the Arikareean age of the South Mountain local fauna, Ventura County, California and its relationship to marine geochronology: Geol. Soc. America Abs. with Prog., v. 20, p. 211.

McCracken, W. A., 1969, Environmental reconstruction-Sespe Formation, Ventura basin, California: Geol. Soc. Am. Abstr. Programs, pt. 7, p. 145-146.

McCulloh, T. H., 1960, Gravity variations and the geology of the Los Angeles basin of California: U. S. Geol. Surv. Prof Pap. 400B, p. B320-B326.

McCulloh, T. H., 1967, Mass properties of sedimentary rocks and gravimetric effects of petroleum and natural-gas reservoirs: U. S. Geol. Survey Prof. Paper 528-A, 50 p.

McCulloh, T. H., 1981, Middle Tertiary Laumonite isograd offset 37 km by left-lateral strike-slip on Santa Ynez fault, California: Am. Assoc. Petrol. Geol. Bull., v. 65, p. 956.

Mitchell, S. W., 1967, North Sulphur Mountain area, Ojai oil field: California Division of Oil and Gas Summary of Operations, v. 52-2, part 2, p. 45- 53.

Mitchell, S. W., 1968, Sisar Creek area, Ojai oil field: California Division of Oil and Gas Summary of Operations, v. 53-2, part 2, p. 35-41.

Mitchell, S. W., 1969, Silverthread area of Ojai oil field: California Division of Oil and Gas Summary of Operations, v. 54-2, part 2, p. 5-13.

Mitra, S., 1990, Fault-propagation folds: geometry, kinematic evolution, and hydrocarbon traps: Am. Assoc. Petrol. Geol. Bull., v. 74, p. 921-945.

Morton, D. M., 1972, Reconnaissance photo-interpretation map of major landslides, southern Ventura County, California: California Div. Mines and Geol., Open-File Report 72-26, Scale 1:48,000.

Mount, V. S., and Suppe, J., 1987, State of stress near the San Andreas fault: Implications for wrench tectonics: Geology, v. 15-12, p. 1143-1146.

Muehlberger, W. R., 1958, Geology of northern Soledad basin, Los Angeles County, California: Am. Assoc. Petrol. Geol. Bull., v. 42, p. 1812-1844.

Nagle, H. E., and Parker, E. S., 1970, Future oil and gas potential of onshore Ventura basin, California, *in* Cram, I. H., ed., Future petroleum provinces of the United States--their geology and potential: Am. Assoc. Petrol. Geol. Memoir 15, p. 254-296.

Namson, J., 1987, Structural transect through the Ventura basin and western Transverse Ranges, *in* Davis, T. L. and Namson, J. S., eds., Structural evolution of the western Transverse Ranges: Society of Economic Paleontologists and Mineralogists, Pacific Section Guidebook 48A, p. 29-41.

Namson, Jay, and Davis, Thom, 1988, Structural transect of the western Transverse Ranges, California: Implications for lithospheric kinematics and seismic risk evaluation: Geology, v. 16, p. 675-679.

Natland, M. L., 1952, Pleistocene and Pliocene stratigraphy of southern California: unpub. PhD. thesis, Univ. California Los Angeles, 165 p.

Natland, M. L., and Kuenen, P. H., 1951, Sedimentary history of the Ventura basin, California, and the action of turbidity currents: Soc. Econ. Paleon. and Mineralogists Special Publication 2, p. 76-107.

Natland, M. L., and Rothwell, W. T., 1954, Fossil foraminifera of the Los Angeles and Ventura regions, California: California Division of Mines and Geology Bulletin 170, p. 33-42.

Nettleton, L. L., 1971, Elementary gravity and magnetics for geologists and seismologists: Soc. Expl. Geophys., Monograph Series, Number 1, 121 p.

Nilsen, T. H., and Clarke, S. H., Jr., 1975, Sedimentation and tectonics in the early Tertiary continental borderland of central California: U. S. Geol. Survey Prof. Paper 925, 64 p.

O'Brien, J., 1973, Narizian-Refugian (Eocene-Oligocene) sedimentation, western Santa Ynez Mountains, Santa Barbara County, California, M. A. thesis, Univ. Calif., Santa Barbara.

Oxburgh, E. R., 1972, Flake tectonics and continental collision: Nature, v. 239, p. 202-204.

Page, B. M., J. G. Marks, and G. W. Walker, 1951, Stratigraphy and structure of the mountains northwest of Santa Barbara, California: Am. Assoc. Petrol. Geol. Bull., v. 35, p. 1727-1780.

Putnam, W. C., 1942, Geomorphology of the Ventura region, California: GSA Bulletin, v. 53, p. 691-754.

Ricketts, E. W., and Whaley, K. R., 1975, STructure and stratigraphy of the Oak Ridge-Santa Susana fault intersection, Ventura basin, California: unpub. M. S. thesis, Ohio University, Athens, 81p.

Rieser, R. B., 1976, Structural study of the Oak Ridge fault between South Mountain and Wiley Canyon, Ventura County, California: unpub. M. S. thesis, Ohio University, Athens, 93p.

Robinson, B. B., 1956, Geology of the Holser Canyon area, Ventura County, California: unpub. M. A. thesis, Univ. California, Los Angeles, 61p.

Rockwell, T. K., 1983, Soil chronology, geology, and neotectonics of the north central Ventura basin, California: unpub. Ph. D. dissertation, University of California, Santa Barbara, 424p.

Rockwell, T. K., 1988, Neotectonics of the San Cayetano fault, Transverse Ranges, California: GSA Bulletin, v. 100, p. 500-513.

Roubanis, A. S., 1963, Geology of the Santa Ynez fault, Gaviota Pass-Point Conception area, Santa Barbara County, California, M. A. thesis, Univ. Calif., Los Angeles.

Sarna-Wojcicki, A. M, Bowman, H. R., Meyer, C. E., Russell, P. C., Woodward, M. J., McCoy, G., Rowe Jr., J. J., Baedecker, P. A., Asaro. F., and Michael, H., 1984, Chemical analyses, correlations, and ages of upper Pliocene and Pleistocene ash layers of east-central and southern California: U. S. Geol. Survey Professional Paper 1293, 38p.

Sarna-Wojcicki, A. M., S. D. Morrison, C. E. Meyer, and J. W. Hillhouse, 1987, Correlation of upper Cenozoic tephra layers between sediments of the western United States and eastern Pacific Ocean and comparison with biostratigraphic and magnetostratigraphic age data: Geol. Soc. Am. Bull., v. 98, p. 207-223.

Sarna-Wojcicki, A. M., K. R. Lajoie, C. E. Meyer, D. P. Adam, and H. J. Rieck, 1991, Tephrochronologic correlation of upper Neogene sediments along the Pacific margin, conterminous United States, *in* Morrison, R. B., ed., Quaternary nonglacial geology; conterminous U. S.: Geology of North America series, Geol. Soc. Am., Boulder, Colorado, v. K-2, p. 117-140.

Savage, D. E., Downs, T., and Poe, O. J., 1954, Cenozoic land life of southern California: California Div. Mines Bull. 170, ch. III, p. 43-58.

Schlueter, J. C., 1976, Geology of the Upper Ojai-Timber Canyon area, Ventura County, California: unpub. M. S. thesis, Ohio University, Athens, 67p.

Schmidt, R. R., 1970, Planktonic foraminifera from the lower Tertiary of California: unpub. Ph. D. dissertation, Univ. California, Los Angeles, 338p.

Schmitka, R. O., 1973, Evidence for major right-lateral separation of Eocene rocks along the Santa Ynez fault, Santa Barbara and Ventura Counties, California: Geol. Soc. Am. Abstr. Programs, v. 5, p. 104.

Schroeter, C. E., 1972, Stratigraphy and structure of the Juncal Camp-Santa Ynez fault slice, southeastern Santa Barbara County, California: unpub. M. A. thesis, Univ. Calif., Santa Barbara, 89 p.

Seedorf, D. C., 1983, Upper Cretaceous through Eocene subsurface stratigraphy, Simi Valley, and adjacent regions, California, *in* Squires, R. L., and Filewicz, M. V., eds., Cenozoic geology of the Simi Valley area, southern California: Pacific Section, Soc. Econ. Paleon. and Mineralogists, volume and guidebook, p. 109-128.

Shepherd,, G. L., 1960, Geology of the Whitaker Peak-Canton Canyon area, southern California: unpublished M. A. thesis, Univ. of California, Los Angeles, 64 p.

Simila, G. W., Armand., P., and Van Waggoner, B., 1987, Seismicity of the San Cayetano fault, western Transverse Ranges: Seismological Research Letters, v. 58, p. 28.

Slade, R. C., 1975, Hydrogeologic investigation of Carpinteria groundwater basin, Santa Barbara County, California: unpub. M.S. thesis, Univ. Southern Calif., Los Angeles, 141 p.

Squires, R. L., 1977, Middle Eocene molluscan assemblage and stratigraphy, lower Piru Creek, Transverse Ranges, California: California Division of Mines and Geology Special Report 129, p. 81-86.

Squires, R. L., 1981, A transitional alluvial to marine sequence: The Eocene Llajas Formation, southern California: Jour. Sed. Pet., v. 51, p. 923-938.

Stitt, L. T., and Yeats, R. S., 1983, Geology, seismic hazard, and ground-rupture hazard of the San Gabriel and Holser faults, Eastern Ventura and western Soledad basins, California: U. S. Geol. Survey, Final Technical Report, Contract Number 14-08-0001-19138, 26p.

Stock, C., 1932, Eocene land mammals of the Pacific coast: Proclamation of Nat. Acad. Sci., v. 18, p. 518-523.

Suppe, John, 1985, Principles of structural geology: Prentice-Hall, Englewood Cliffs, New Jersey, 535p.

Suppe J., and Medwedeff, D. A., 1990, Geometry and kinematics of fault-propagation folding: Eclogae Geol. Helv., v. 83, p. 409-454.

Suppe, J., G. T. Chou, and S. C. Hook, 1992, Rates of folding and faulting determined from growth strata, *in* McKlay, K. R., ed., Thrust tectonics: Unwin Hyman, London.

Truex, J. N., 1977, The Modelo lobe area, *in* Truex, J. N., ed., The San Cayetano fault field trip: Pacific Section, Am. Assoc. Petrol. Geol., p. 8-11.

Turner, D. L., 1970, Potassium-argon dating of Pacific Coast Miocene foraminiferal stages: Geol. Soc. America, Spec. Paper 124, p. 91-129.

Vedder, J. G., 1972, Revision of stratigraphic names for some Eocene formations in Santa Barbara and Ventura Counties, California: USGS Bulletin 1354-D, p. D1-D12.

Webb, T. H., and Kanamori, Hiroo, 1985, Earthquake focal mechanisms in the eastern Transverse Ranges and San Emigdio Mountains, southern California, and evidence for a regional decollement: Bulletin Seismological Society of America, v. 75-3, p. 737-757.

Weber, F. H., Jr., et al., 1973, Geology and mineral resources study of southern Ventura County, California: Calif. Div. Mines Geol. Prelim. Rep. 14, 102 p.

Weber, F. H., Jr., 1982, Geology and geomorphology along the San Gabriel fault zone, Los Angeles and Ventura Counties, California: Final Tech. Rep. to U. S. Geol. Survey, Contract 14-08-0001-16600, Modification 1, 78p.

Weldon, R., and Humphreys, E., 1986, A kinematic model of southern California: Tectonics, v. 5, p. 33-48.

Welsh, G. J., 1954, Geologic Map of the Ventura District: unpub. map, Scale 1:64,000.

Wilson, R. W., 1949, Rodents and logomorphs of the upper Sespe: Carnegie Inst. of Washington, Pub. 584, p. 51-65.

Winterer, E. L., and Durham, D. L., 1954, Geology of part of the east Ventura basin, Los Angeles County: California Div. Mines, Bulletin 170, map sheet 5.

Winterer, E. L., and Durham, D. L., 1962, Geology of part of the southeastern Ventura basin, Los Angeles County, California: U. S. Geol. Survey, Prof. Paper 334-H, p. 275-366.

Woodward, N. B., S. E. Boyer, and J. Suppe, 1989, Balanced geological cross-sections: An essential technique in geological research and exploration, AGU, Short Course in Geology, v. 6, 132 p.

Woollard, G. P., 1962, Geologic effects in gravity values, part 3, *of* The relation of gravity anomalies to surface elevation, crustal structure, adn geology: Wisconsin Univ., Geophys. and Polar Res. Center, Res. Rep. Ser. 62-9, p. 1-78.

Yeats, R. S., 1965, Pliocene seaknoll at South Mountain, Ventura basin, California: Am. Assoc. Petrol. Geol. Bull., v. 49, p. 526-546.

Yeats, R. S., 1967, South Mountain area, Ventura County, California: Geol. Soc. America Guidebook, 63rd Annual Meeting, 10 p.

Yeats, R. S., 1976, Neogene tectonics of the central Ventura basin, California, in The Neogene Symposium: Pacific Sect., Soc. Econ. Paleon. Min., p. 19-32.

Yeats, R. S., 1977, High rates of vertical crustal movement near Ventura, Calif ornia: Science, v. 196, p. 295-298.

Yeats, R. S., 1979, Stratigraphy and paleogeography of the Santa Susana fault zone, Transverse Ranges, California, in Armentrout, J. M., Cole, M. R., and Ter Best, H., eds., Cenozoic paleogeography of the western United States: Pacific Coast Paleogeography Symposium 3: Los Angeles, Calif., Pacific Sec., Soc. Econ. Paleontologists and Mineralogists, p. 191-204.

Yeats, R. S., 1981a, Quaternary flake tectonics of the California Transverse Ranges: Geology, v. 9, p. 16-20.

Yeats, R. S., 1981b, Deformation of a 1 Ma datum, Ventura basin, California: final report, U. S. Geol. Survey Contract 14-08-0001-17730, Mod. 3, Menlo Park, 26 p.

Yeats, R. S., 1983a, Large-scale Quaternary detachments in the Ventura basin, southern California: Jour. of Geophys. Res., v. 88-B1, p. 569-583.

Yeats, R. S., 1983b, Heavy oil accumulations in the Oxnard field, Ventura basin, California, in, Isaacs C. M. , and Garrison R. E., eds., Petroleum generation and occurrence in the Miocene Monterey Formation, California, Pacific Sect., Soc. Econ. Paleon. Min., Los Angeles, California, p. 85-98.

Yeats, R. S., 1987, Changing tectonic styles in Cenozoic basins of southern California *in* Ingersoll, R. V., and Ernst, W. G., eds., Cenozoic basin development of coastal California, Rubey Volume VI: Prentice-Hall, Englewood Cliffs, New Jersey, p. 284-298.

Yeats, R. S., 1988a, Late Quaternary slip rate on the Oak Ridge fault, Transverse Ranges, California: Implications for seismic risk: Jour. Geophys. Res., v. 93, p. 12,137-12,149.

Yeats, R. S., 1988b, Oak Ridge fault, Ventura basin, California: Slip rates and late Quaternary history: U. S. Geol. Survey, Final Technical Report, Contract 14-08-0001-G1194, 33p.

Yeats, R. S., 1989, Oak Ridge fault, Ventura basin, California: Slip rates and late Quaternary history: U. S. Geol. Surv. Open-File Rep. 89-343, 30 p.

Yeats, R. S., McDougall, J. W., and Stitt, L. T., 1985, Cenozoic structure of the Val Verde 7 ½-minute Quadrangle and south half of the Whitaker Peak 7 ½-minute Quadrangle, California: U. S. Geol. Survey Open-File Report 85-587, 23p., map scale 1:24,000.

Yeats, R. S., Lee, W. H. K., and Yerkes, R. F., 1987, Geology and seismicity of the eastern Red Mountain fault, Ventura County, California, *in* Morton, D. M., and Yerkes, R. F., eds., Recent reverse faulting in the Transverse Ranges, California: USGS Professional Paper 1339, p. 161-167.

Yeats, R. S., Huftile, G. J., and Grigsby, B. F., 1988, Oak Ridge fault, Ventura fold belt, and the Sisar decollement, Ventura basin, California: Geology, v. 16, p. 1112-1116.

Yeats, R. S., and Huftile, G. J., 1989, Comment on "Structural transect of the western Transverse Ranges, California: Implications for lithospheric

kinematics and seismic risk evaluation" by Jay Namson and Thom Davis: Geology, v. 17, p. 771-772.

Yeats, R. S., and Taylor, J. C., 1989, Saticoy oil field--U.S.A., Ventura basin, California, *in* Beaumont, E. A., and Foster, N. H., eds., Structural Traps III, tectonic fold and fault traps, Treatise of petroleum geology, atlas of oil and gas fields: Am. Assoc. Petrol. Geol., Tulsa, Oklahoma, p. 199-215.

Yeats, R. S., and Huftile, G. J., 1991, Transfer of displacement from surface faulting at South Mountain to folding and blind thrusting at Ventura Avenue anticline, *in* Keller, E., ed., Active folding and reverse faulting in the western Transverse Ranges, southern California: Geol. Soc. Am. guidebook, Annual Convention, p. 27-28.

Yeats, R. S., Huftile, G. J., and Stitt, L. T., Late Cenozoic tectonics of the east Ventura basin, Transverse Ranges, California: submitted to Am. Assoc. Petrol. Geol. Bull.

Yerkes, R. F., and Lee, W. H. K., 1979, Late Quaternary deformation in the western Transverse Ranges, California: USGS Circular 799-B, p. 26-37.

Yerkes, R. F., A. M. Sarna-Wojcicki, and K. R. Lajoie, 1987, Geology and Quaternary deformation of the Ventura area, in Morton, D. M., and Yerkes, R. F., eds., Recent reverse faulting in the Transverse Ranges, California, edited by D. M. Morton, and R. F. Yerkes: U. S. Geol. Surv. Prof. Pap. 1339, p. 169-178.

Zinsmeister, W. J., 1974, Paleocene biostratigraphy of the Simi Hills, Ventura County, California: unpub. Ph.D. dissertation, Univ. of California, Riverside, 236 p.

Zoback, M. D., et al., 1987, New evidence on the state of stress of the San Andreas fault system: Science, v. 238, p. 1105-1111.